



**UNIVERSIDADE ESTADUAL DE CAMPINAS  
FACULDADE DE ENGENHARIA DE ALIMENTOS**

**RENATO CRUZ NEVES**

**TECHNO-ECONOMIC INVESTIGATION OF FIRST-GENERATION SUGARCANE  
BIOREFINERY INTEGRATED WITH SECOND-GENERATION  
THERMOCHEMICAL ROUTE TO PRODUCE BIOJET FUEL**

**INVESTIGAÇÃO TÉCNICO-ECONÔMICA DA BIORREFINARIA DE CANA-DE-  
AÇÚCAR DE PRIMEIRA GERAÇÃO INTEGRADA COM ROTA TERMOQUÍMICA  
DE SEGUNDA GERAÇÃO PARA PRODUIR COMBUSTÍVEL DE AVIAÇÃO**

**CAMPINAS**

**2019**

**RENATO CRUZ NEVES**

**TECHNO-ECONOMIC INVESTIGATION OF FIRST-GENERATION SUGARCANE  
BIOREFINERY INTEGRATED WITH SECOND-GENERATION  
THERMOCHEMICAL ROUTE TO PRODUCE BIOJET FUEL**

**INVESTIGAÇÃO TÉCNICO-ECONÔMICA DA BIORREFINARIA DE CANA-DE-  
AÇÚCAR DE PRIMEIRA GERAÇÃO INTEGRADA COM ROTA TERMOQUÍMICA  
DE SEGUNDA GERAÇÃO PARA PRODUZIR COMBUSTÍVEL DE AVIAÇÃO**

*Thesis presented to the Faculty of Food Engineering of the University of Campinas in partial fulfillment of the requirements for the degree of Doctor in Science.*

Tese apresentada à Faculdade de Engenharia de Alimento da Universidade Estadual de Campinas como parte dos requisitos exigidos para a obtenção do título de Doutor em Ciências.

Orientador: Rubens Maciel Filho

Co-orientador: Edgardo Olivares Gómez

Este exemplar corresponde à versão final de tese defendida pelo aluno Renato Cruz Neves e orientado pelo professor Doutor Rubens Maciel Filho e co-orientado pelo Doutor Edgardo Olivares Gómez.

**CAMPINAS**

**2019**

Ficha catalográfica  
Universidade Estadual de Campinas  
Biblioteca da Faculdade de Engenharia de Alimentos  
Márcia Regina Garbelini Sevillano - CRB 8/3647

N414t Neves, Renato Cruz, 1987-  
Techno-economic investigation of first-generation sugarcane biorefinery integrated with second-generation thermochemical route to produce biojet fuel / Renato Cruz Neves. – Campinas, SP : [s.n.], 2019.

Orientador: Rubens Maciel Filho.  
Coorientador: Edgardo Olivares Gómez.  
Tese (doutorado) – Universidade Estadual de Campinas, Faculdade de Engenharia de Alimentos.

1. Biomassa - Aproveitamento Energético. 2. Pirólise. 3. Gaseificação. 4. Fischer-Tropsch, Processo de. 5. Biorrefinaria. I. Maciel Filho, Rubens. II. Olivares Gómez, Edgardo. III. Universidade Estadual de Campinas. Faculdade de Engenharia de Alimentos. IV. Título.

Informações para Biblioteca Digital

**Título em outro idioma:** Investigação técnico-econômica da biorrefinaria de cana-de-açúcar de primeira geração integrada com rota termoquímica de segunda geração para produzir combustível de aviação

**Palavras-chave em inglês:**

Biomass - Utilization energetic

Pyrolysis

Gasification

Fischer-Tropsch process

Biorefinery

**Área de concentração:** Bioenergia

**Titulação:** Doutor em Ciências

**Banca examinadora:**

Rubens Maciel Filho [Orientador]

Daniel Ibram Pires Atala

Manoel Regis Lima Verde Leal

Tânia Forster Carneiro

Bruna de Souza Moraes

**Data de defesa:** 14-06-2019

**Programa de Pós-Graduação:** Bioenergia

**Identificação e informações acadêmicas do(a) aluno(a)**

- ORCID do autor: <https://orcid.org/0000-0002-0412-0857>

- Currículo Lattes do autor: <http://lattes.cnpq.br/3314436176621762>

EXAMINATION COMMITTEE

Dr. Rubens Maciel Filho – President  
University of Campinas

Dr. Daniel Ibraim Pires Atala  
Bioprocess Improvement Consultoria e Pesquisas em Bioprocessos

Dr. Manoel Regis Lima Verde Leal  
National Center for Research in Energy and Materials

Dra. Tânia Forster Carneiro  
University of Campinas

Dra. Bruna de Souza Moraes  
University of Campinas

Ata da defesa com as respectivas assinaturas dos membros encontra-se no SIGA/Sistema de Fluxo de Dissertação/Tese e na Secretaria do Programa da Unidade.

## Dedication

To my family

&

To those people who are here among us...

*and also those who are not*

## ACKNOWLEDGMENTS

To my beloved Carina, for her help, love, and immeasurable strength immeasurable patience. She makes me see the world through different perspectives. My eternal love.

To my parents and family, Joana and Leonardo, for encouraging me to seek my dreams even do not understand a unique word what I am writing here, but even so, encourage me to seek my dreams. To my brother, Gabriel, who left the world behind to fly over a new one. To my sister in law, Arieli, for her support.

To my second family, Eva, Luiz, Renata and Guto, for the whole support and their teaching: the world is very different, and happiness is all that matters.

To my Vó, Madrinhas, Padrinhos, for praying and cheering for me in a way that I cannot measure. To my uncles, aunts and cousins.

To my advisor, Rubens Maciel Filho, for his support to develop this thesis.

To my co-advisor, Edgardo Olivares Gómez, for his friendship and teaching me that the world is not so simple like we wish, his fulfillment with the science and his simplicity over the past years.

To Mylene Rezende, who has left a great impact throughout this thesis.

To Bruno Klein, Edvaldo Moraes, Bonomi and other colleagues from CTBE for their support.

To my colleagues that taught me that the world is huge: Axel Funke, Nicolaus Dahmen, Felipe, Tomohiro, Renata, Michelly, and the two Carols.

To those who have participated, motivated me and made this life lighter to keep walking: Barbs, Sato, Pablo, Melina, Merighi, Ricardo Silva, Adriano Siqueira, Caio Soares, and GDM&GDMas.

To those who have impacted a lot my path and I cannot remember right now.

This study was financed in part by BE MUNDUS (Brazil-Europe: 3rd Call for Applications for sandwich PHDs) - BM15DM0953.

This study was financed in part by the Coordenação de Aperfeiçoamento de Pessoal de Nível Superior – Brasil (CAPES) – Finance code 001. CAPES number 23038.006737/2012-56.

Thanks all...

## RESUMO

A partir da cana-de-açúcar e seus resíduos podem ser produzidos açúcar, produtos químicos, energia elétrica e etanol de Primeira Geração (1G), além de etanol e produtos químicos da Segunda Geração (2G). No entanto, ainda é necessário estudar possíveis rotas para o uso de bagaço e palha de cana-de-açúcar para a produção de combustíveis líquidos, nesse caso via rota termoquímica para produção de gás de síntese e sua conversão em combustível líquido por processos químicos. Dentro deste propósito, o objetivo principal desta tese foi realizar a investigação técnico-econômica da Biorrefinaria 1G de Cana-de-Açúcar integrada à rota 2G Termoquímica para produzir biocombustível de aviação. Uma revisão abrangente da rota termoquímica serviu de base para o desenvolvimento deste trabalho. Após isso, a simulação e os dados experimentais do processo de pirólise rápida da biomassa lignocelulósica, mistura de bagaço de cana e palha de cana-de-açúcar, da biorrefinaria de cana-de-açúcar 1G permitiram entender o comportamento do processo e a compreensão geral da integração 1G2G fornecida. Além disso, a investigação técnico-econômica foi realizada considerando conceitos de cenários centralizados e descentralizados de pirólise rápida. Esta investigação foi realizada no ambiente de simulação de Aspen Plus® e parte do trabalho da Biorrefinaria Virtual de Cana-de-açúcar do Laboratório Nacional de Ciência e Tecnologia do Bioetanol (CTBE) do Centro Nacional de Pesquisa em Energia e Materiais (CNPEM). O balanço de massa do biocombustível de aviação considerando o bagaço e a palha da cana-de-açúcar entrando na hierarquia da pirólise rápida foi de cerca de 1,64% para ambos os cenários, valor similar se comparado com os dados da literatura, além de estar de acordo com requisitos aprovados pelas agências reguladoras. Essa quantidade de biocombustível de aviação aliada aos outros materiais produzidos a partir da integração 1G2G, a saber, açúcar, etanol anidro, nafta verde e eletricidade, apresentou Taxa Interna de Retorno de 6,80% no caso do cenário centralizado. Para atingir a Taxa Mínima de Retorno Aceitável igual a 12%, o preço de venda do biocombustível de aviação deve ser multiplicado por um fator de 4,2 para o cenário centralizado, e por um fator de 16,0 no cenário descentralizado. A avaliação completa da integração de 1G2G é discutida nesta tese. Com os resultados obtidos neste trabalho, espera-se que esta investigação possa contribuir para a avaliação das rotas termoquímicas BTL para a produção de biocombustível de aviação com operação de cogeração de energia elétrica em um ambiente de integração com a Biorrefinaria 1G de cana-de-açúcar.

## ABSTRACT

From the sugarcane and its residues can be produced sugar, chemical products, electrical energy and ethanol from First-Generation (1G), besides ethanol and chemical products from Second-Generation (2G). Nevertheless, it is still a need to perform possible routes for the use of sugarcane bagasse and straw to produce liquid fuels via thermochemical production of syngas and its conversion into liquid fuel through chemical process. Within this purpose, the main goal of this thesis was to perform the techno-economic investigation of 1G Sugarcane Biorefinery integrated with the 2G Thermochemical route to produce biojet fuel. A comprehensive review covering thermochemical route served as basis for the development of this work where experimental data of fast pyrolysis process and the complete simulation of 1G2G integration were investigated. The simulation and experimental data of fast pyrolysis process of lignocellulosic biomass, a mixture of sugarcane bagasse and sugarcane straw, from 1G sugarcane biorefinery allowed the understanding of the process behavior and the overall understanding of 1G2G integration provided. Also, the techno-economic investigation was carried out considering different centralized and decentralized pyrolysis scenarios. This investigation was held in the Aspen Plus® simulation environment and some work from the Virtual Sugarcane Biorefinery from Brazilian Bioethanol Science and Technology Laboratory (CTBE) of the National Center for Research in Energy and Materials (CNPq). The biojet fuel mass conversion considering sugarcane bagasse and straw entering the fast pyrolysis hierarchy was around 1.64% for both scenarios, good agreement with literature data, besides being in accordance with regulatory agencies. This amount of biojet fuel allied with other materials produced from the 1G2G integration, namely sugar, anhydrous ethanol, green naphtha and electricity, showed Internal Rate of Return of 6.80% in the case of centralized scenario. In order to achieve the Minimum Acceptable Rate of Return equal to 12%, the selling biojet fuel price should be raised by a factor of 4.2 for centralized scenario, and by a factor of 16.0 in decentralized scenario. The complete evaluation of 1G2G integration is discussed in this thesis. With the results from this work, it is expected that this investigation can contribute to evaluate the BTL thermochemical routes to produce biojet fuel with electricity cogeneration operation in an integration environment with First Generation Sugarcane Biorefinery.

## CONTENTS

<b>1</b>	<b>Introduction .....</b>	<b>10</b>
<b>2</b>	<b>Chapter I.....</b>	<b>15</b>
<b>3</b>	<b>Chapter II.....</b>	<b>52</b>
<b>4</b>	<b>Chapter III.....</b>	<b>92</b>
<b>5</b>	<b>Discussion.....</b>	<b>109</b>
<b>6</b>	<b>General conclusion .....</b>	<b>126</b>
<b>7</b>	<b>Memorial .....</b>	<b>130</b>
	<b>References.....</b>	<b>132</b>
	<b>Appendix – CAPEX and OPEX .....</b>	<b>153</b>
	<b>Appendix – Fischer-Tropsch hierarchy.....</b>	<b>167</b>

## 1 Introduction

The humanity has faced climate change risks due to the increasing consumption of fossil fuel resources. Nowadays, crude oil price volatility has been affecting the fuel market, i.e. energy sector, along with the very well-established Global Warming Potential because of the Greenhouse Gas emissions. These factors have motivated the search for alternative fuels and energy. Therefore, an urgent global decision should be taken to slow down all these risks around the world.

Many efforts to overcome these risks are being shared by public and private institutions from different countries. Brazil is focused on reducing these risks by creating a more sustainable country where a variety of industries uses biomass to produce bioenergy. Within this context, Brazil is considered the main producer of ethanol and sugar in sugarcane biorefineries where its residues, sugarcane bagasse and straw, are used to produce electricity.

Brazilian sugarcane biorefineries have arisen since the 1970s as a sustainable solution to ensure the demand for ethanol, sugar and electricity across the country. Recently, efforts to create a wide range of portfolio products via green alternative has pointed out the biojet fuel to replace part of the old conventional jet fuel, based on oil. Taking advantage of this portfolio aiming the integration of different biorefineries and the well-established sugarcane biorefineries in Brazil, biojet fuel has highlighted as one the most important biofuels in the near future.

Among the pathways to produce biojet fuel, Biomass to Liquid (BTL) via thermochemical route is a high potential candidate to produce a flexible range of green hydrocarbons. Moreover, this thermochemical route can be named as Second Generation (2G) thermochemical route which can be integrated with the well-established First Generation (1G) sugarcane biorefinery, resulting in some integrated product portfolios such as fuels, chemical, electrical energy and edible food. This extensive portfolio results in more flexibility to the bioeconomy sector.

Thermochemical processes have been studied to supply more products to bioenergy sector, especially when considering pyrolysis and gasification process. The integration of these two important processes may result in synergy for attending expectations for a great variety of products through different 1G2G integrations. This synergy may also result in different configurations regarding centralized and decentralized scenarios.

Considering the integration between biorefineries, the blend of sugarcane bagasse and sugarcane straw from 1G sugarcane biorefinery is the raw material for 2G thermochemical

route. This blend can be fed into the pyrolysis reactor to produce bioslurry, and this material can be gasified in the gasification reactor to produce syngas. Ultimately, this syngas can be converted into biojet fuel by Fischer-Tropsch synthesis. This biojet fuel is a drop-in green hydrocarbon, i.e. it can directly substitute the conventional aviation fuel. This complete integrated biorefineries can be ensured by mass and energy balance and it is extremely beneficial for sugarcane chain once the portfolio items may increase covering a wide range of products with fewer residues disposed on the environment and larger economical flexibility.

This thesis details the study of these topics providing a deeper knowledge as presented by chapters I, II and III.

Chapter I is considered the introduction and the motivation for the overall understanding of this thesis. This chapter shows a comprehensive review of Biomass-to-Liquid (BTL) thermochemical routes in integrated sugarcane biorefineries for biojet fuel production. Moreover, it describes the importance of using biomass from sugarcane biorefinery in order to create synergy ensuring the integration of sugarcane biorefinery with thermochemical biorefineries.

Chapter II approaches the experimental and simulation processes regarding fast pyrolysis technology for bioslurry production. This chapter presents hundreds of bioslurry components from experimental data and two simulations models through kinetic and yield reactors to represent the fast pyrolysis process. Ultimately, energy and exergy efficiencies were also carried out.

The investigation presented in Chapter III ensures mass and energy balance of the integration between the First Generation (1G) sugarcane biorefinery and the Second Generation (2G) thermochemical route. This chapter uses previous information depicted in chapter I and II to show the complete 1G2G integration evaluation regarding the simulation process and economic assessment.

All chapters and annexes are linked directly to the general objectives of this thesis. The general objective of this work is to investigate the BTL thermochemical route to produce renewable jet fuel (biojet fuel) in an integrated environment of the First Generation (1G) sugarcane biorefinery and the Second Generation (2G) thermochemical route. Therefore, an overall discussion issue within a thermochemical route concept is needed.

## 1.1 Objectives

With this purpose, the primary goals of this thesis can be divided into simulation and experimental scopes:

- Simulation scope. Investigate and present the BTL (Biomass-to-Liquid) thermochemical route to produce biojet fuel with electricity cogeneration, considering its integration with the First Generation (1G) sugarcane biorefinery using the Aspen Plus® software to simulate the proposed processes within the scope of the Virtual Sugarcane Biorefinery (VSB) from Brazilian Bioethanol Science and Technology Laboratory (CTBE) of the National Center for Research in Energy and Materials (CNPEM). Additionally, carry out the economic investigation regarding the main financial indicators as a way of providing the information to build a 1G2G biorefinery.
- Experimental scope. Use specific ratio of sugarcane bagasse and sugarcane straw, namely lignocellulosic biomass (LCB) from a First-Generation (1G) sugarcane biorefinery, to produce fast pyrolysis products (Non-condensable gas, biochar and bio-oil) into the Python Process Development Unit (Python-PDU) at Institut für Katalyseforschung und –technologie (IKFT) from Karlsruhe Institut für Technologie (KIT), Karlsruhe, Germany.

The secondary goals are related to:

- Perform, present and discuss the current state of the art of the main alternatives of thermochemical routes from biomass into energy conversion, waste and use of renewable sources which concern the production of liquid biofuels focusing on the production of biojet fuel with the electricity cogeneration operation. *Results*: review criticality of the state of art in pyrolysis, gasification and cleaning and conditioning the producer gas into syngas to the production of biojet fuel. This review will also regard to issues not reported in the literature aiming to be an original contribution to the scientific community and also as a basis for the development of future works.
- Process integration from pretreatment of biomass to final production of biojet fuel with cogeneration. *Results*: integration of all steps necessary for the conversion of sugarcane bagasse and sugarcane straw into biofuels,

mainly biojet fuel through the BTL thermochemical route. The integration of all stages is essential in order to provide, through a techno-economic feasibility investigation, parameters that allow assessing the overall performance of the process.

- Simulate in Aspen Plus® BTL thermochemical route using the Virtual Sugarcane Biorefinery (VSB) at Brazilian Bioethanol Science and Technology Laboratory (CTBE) for the production of biojet fuel. *Results:* Integrate the 1G biochemical into the 2G thermochemical process, i.e. 1G2G thermochemical.
- Present different scenarios configuration of 1G2G biorefinery for biojet fuel production considering centralized and decentralized concepts. *Results:* identify the importance of centralized and decentralized concepts and how the integration can be carried out.
- Perform the economic investigation of the BTL thermochemical route for the production of biojet fuel with cogeneration operation integrated into a 1G sugarcane biorefinery according to the VSB framework. *Results:* present the economic indicator to build a 1G2G biorefinery for biojet fuel production.

## 1.2 *Main contributions of this work*

A comprehensive review showed that BTL thermochemical routes encompass promising pathways to produce biojet fuel in world scale. While biomass corresponds to a very significant cost component in any conversion process, the logistics for transportation and technology for energy densification must also be tackled to improve the feasibility of the complete process. Within thermochemical technologies, fast pyrolysis has become a mature technology that is applied industrially for the conversion of woody biomasses. In spite of this, further research, especially at relevant technical scales, are required to better assess the potential of applying this conversion technology as a pretreatment method prior to gasification. Besides, although the gasification of biomass is considered more mature than fast pyrolysis, more analyses regarding the integration of thermochemical routes in 1G sugarcane biorefineries are required for the development of the centralized and decentralized concepts. This includes better

quantification of the benefits and disadvantages of including the cost and inefficiencies of the overall BTL concept.

Experimental results of biomass characterization and fast pyrolysis process showed great complexity of fast pyrolysis products, especially for aqueous and organic-rich condensates, containing hundreds of components. Allied with experimental data, the integrated process simulation between biomass drying and fast pyrolysis was simulated through yield and kinetic models.

This thesis brings important contributions related to the complete integration of the 1G sugarcane biorefinery with the 2G thermochemical route. With this integration of mass and energy balances through experimental and simulation data alongside with techno-economic indicators, biojet fuel might be considered as an option to replace part of the conventional jet fuel from oil.

## 2 Chapter I

### **A vision on Biomass-to-Liquids (BTL) thermochemical routes in integrated sugarcane biorefineries for biojet fuel production**

Renato Cruz Neves<sup>\*,1</sup>, Bruno Colling Klein<sup>1,3</sup>, Ricardo Justino da Silva<sup>1</sup>, Mylene Cristina Alves Ferreira Rezende<sup>1</sup>, Axel Funke<sup>2</sup>, Edgardo Olivarez-Gómez<sup>4</sup>, Antonio Bonomi<sup>1,3</sup>, Rubens Maciel-Filho<sup>1,3</sup>

<sup>1</sup> Brazilian Bioethanol Science and Technology Laboratory (CTBE), Brazilian Center for Research in Energy and Materials (CNPEM), Zip Code 13083-970, Campinas, Sao Paulo, Brazil.

<sup>2</sup> Institute of Catalysis Research and Technology, Karlsruhe Institute of Technology (KIT), Karlsruhe, Germany

<sup>3</sup> School of Chemical Engineering, University of Campinas, Brazil

<sup>4</sup> Engineering Faculty (FAEN), Federal University of Grande Dourados (UFGD), Brazil

\*Corresponding author: renatocruzneves@gmail.com

Journal name: Renewable and Sustainable Energy Reviews

#### **Abstract**

Crude oil price volatility directly affects the worldwide fuels and chemicals markets, impacts food production costs, as well as it influences investments in alternative energy sources. Global warming is a consequence of greenhouse gases emissions, among which CO<sub>2</sub> plays a crucial role. A circular economy appears to be a global consensus to limit the negative impacts on the environment caused by fossil-based emissions. Transportation of goods and people are responsible for a large fraction of manmade CO<sub>2</sub> vented to the atmosphere. Although alternatives have already been developed and are already in use for Otto and Diesel cycle engines in the form of bioethanol and biodiesel, respectively, the aviation sector is still short of a consolidated solution for biojet fuel procurement. Among the possible pathways, Biomass-to-Liquids (BTL) thermochemical routes are candidates to produce green hydrocarbons in the near future, including biojet fuel. For the deployment of a BTL thermochemical route, a true biorefinery concept can be employed, through which a flexibility in the product portfolio may increase business competitiveness and reduce production costs through heat and mass integration. Bearing this context in mind, this work presents a vision on

BTL thermochemical routes focusing on biojet fuel production through fast pyrolysis, gasification, and Fischer-Tropsch (FT) synthesis in integrated sugarcane biorefineries.

**Keywords:** Biomass-to-Liquid (BTL); pyrolysis; gasification; Fischer-Tropsch; thermochemical processes; biojet fuel.

### **Highlights**

- Biomass-to-Liquid route for biojet fuel production
- Emphasis on fast pyrolysis, gasification and Fischer-Tropsch synthesis
- Integration to a First Generation (1G) sugarcane biorefinery
- Centralized and decentralized concepts in a biorefinery

## **1. Introduction**

Last century, as far as fuel and energy are concerned, was predominantly characterized by technological improvements regarding the production of petroleum-derived fuels and chemicals. Due to imminent effects of human-cause global warming and the reliance of many countries on fossil fuels (CHERUBINI et al., 2014; CHU; MAJUMDAR, 2012), the industry sector and the scientific community alike are increasingly focused on the development of biomass-derived fuels that might replace fossil-based ones (HUANG; YUAN, 2015; KLEIN et al., 2018; MORAIS et al., 2016). Probably, one of the main challenges of the twenty-first century is related to energy security and to how much fuel can be produced to support the demand on Clean, Affordable, Reliable, Sustainable and Renewable (CARSR) liquid fuels in world scale (BAINS; PSARRAS; WILCOX, 2017; CHU; MAJUMDAR, 2012; MENG et al., 2011; SAGAR; KARTHA, 2007). The question that arises is: what sort of biofuel can be produced to fulfill the near future demand regarding CARSR liquid fuels?

In a great effort to solve this issue, the worldwide attention has been recently focused on energy security where biomass can play an important role in the energy matrix, which involves political, economic, technological, food security and environmental aspects (DEMIRBAS, 2009; ESCOBAR et al., 2009). Biomass-to-liquid (BTL) route comprising biochemical and thermochemical technologies is considered as one of the main green alternatives for the production of biobased chemicals, fuels, and energy in the near future (HEIDENREICH; FOSCOLO, 2015; SUNDE; BREKKE; SOLBERG, 2011; SWAIN; DAS; NAIK, 2011). Among such products, one of the liquid fuel that has been receiving much attention is the substitute for the conventional jet fuel, named renewable jet fuel or simply biojet

fuel (ATSONIOS et al., 2015; CORTEZ et al., 2014; GUTIÉRREZ-ANTONIO et al., 2017; KLEIN et al., 2018; WISE; MURATORI; KYLE, 2017).

Biojet fuel usually presents positive sustainability impacts (GOHARDANI et al., 2014; HARI; YAAKOB; BINITHA, 2015; MORAES et al., 2014) while the use of conventional aviation fuel affects atmospheric through a variety of emissions such as CO<sub>2</sub>, NO<sub>x</sub>, aerosols, sulphate, soot and increasing the cloudiness (LEE et al., 2009; ROJO et al., 2015), thus contributing to climate change and to the depletion of the ozone layer (LEE et al., 2010).

Jet fuel can represent up to 40% of the operating costs in an aviation company (FAPESP, 2013) and more than 99% of the produced jet fuel corresponds to conventional jet fuel, i.e. fossil-based fuel (SKYNRG, 2017). The Brazilian jet fuel demand in 2015 was of 5.6 million cubic meters, of which Brazil imported around 1.4 million cubic meters (ANP, 2013, 2016). These numbers reflect the logistic impacts may have on the jet fuel business in the country. Besides, the predicted growth consumption of this fuel in Brazil from 2012 to 2020 is of about 65% (ANP, 2012). On a world scale, the total production of jet fuel in 2012 was of 1.3G of cubic meters (INDEXMUNDI, 2012). The number of global flights is predicted to double in 2035 compared to 2015 and the best option to curb fossil emissions in the aviation sector having CARSR energy is through the production of biojet fuel (ONEFILE, 2015).

Biojet fuel replacing conventional jet fuel should do so without the need for changing the design of the present aircraft engines or fuel distribution systems (HARI; YAAKOB; BINITHA, 2015), thus consisting in a drop-in solution. Biojet fuel differs from conventional jet fuel in some characteristics. Approved routes by American Society for Testing and Materials (ASTM) (ASTM, 2017) are able to produce aromatic-free biojet fuel, whereas conventional jet fuel contains aromatic compounds in its composition. In spite of being responsible for the emissions of particulates during the combustion, aromatic compounds are required to be present in conventional jet fuel in a defined range to avoid engine leakage and guarantee some properties as the density required in the regulation (LIU; YAN; CHEN, 2013). In fact, the biojet fuel must be blended in different amounts with conventional jet fuel so as this specification is achieved. Besides, biojet fuel does not contain sulfur or nitrogen compounds, thus avoiding the production of SO<sub>2</sub> and H<sub>2</sub>SO<sub>4</sub>, for example, during combustion (GUPTA; REHMAN; SARVIYA, 2010).

A promising technology for drop-in biojet fuel production is through thermochemical processing of biomass within BTL routes (GUTIÉRREZ-ANTONIO et al.,

2017; PEREIRA; MACLEAN; SAVILLE, 2017; SANTOS et al., 2017). Among several processes, the conversion of biomass can be carried out either by fast pyrolysis (producing bio-oil, biochar and non-condensable gas) or by gasification (which yields syngas as an intermediate stream).

Syngas is an extremely important industrial raw material. The global production of syngas in 2004 was of 6 EJ, which corresponds to about 2% of the world energy consumption (VAN DER DRIFT; BOERRIGTER; CODA, 2004). The estimated production in 2040 will be of 50 EJ, representing 10% of the world energy consumption in which BTL technologies will reach around 88% of world syngas market (VAN DER DRIFT; BOERRIGTER; CODA, 2004). Syngas may be converted into biojet fuel via Fischer-Tropsch (FT) synthesis. Thus, it is expected that FT will be able to provide a growing and diversified worldwide demand related to liquid biofuels (TAKESHITA; YAMAJI, 2008), including biojet fuel.

To establish a pathway of biojet fuel through the biobased economy, the International Civil Aviation Organization has set a mechanism aiming at the reduction of greenhouse gases, named Carbon Offsetting and Reduction Scheme for International Aviation (CORSIA). This mechanism, which is joined by countries on a voluntary basis, set out the mitigation of emissions in a three-phase plan for international flights: until 2020, improvement of fuel efficiency of the fleet by 1.5% per year; after 2020, stabilization of emissions through carbon-neutral growth; and, in 2050, reduction of 50% of emission levels in comparison to those of 2005 (ATAG, 2010). The use of renewable jet fuel in such cases is imperative. In the CORSIA scope, it is estimated that around 678 thousand tons of renewable jet fuel would be required by 2030 to promote the carbon-neutral expansion of international flights originating in Brazil alone (ICAO, 2017). Besides, as a signatory of the Paris Agreement, Brazil established an aggressive Nationally Determined Contribution towards cutting greenhouse gas emissions. In the aviation sector, the carbon-neutral growth of the entire sector in the country starting in 2020 would demand between 3.75 and 5.6 million tons of renewable jet fuel by 2030 (MME, 2017).

Many efforts and commitments of public and private technological institutions associated with the development of the bioeconomy have been undertaken to increase the efficiency and sustainability of integrated sugarcane biorefineries (BAEYENS et al., 2015; DE SOUZA NOEL SIMAS BARBOSA; HYTÖNEN; VAINIKKA, 2017; KLEIN et al., 2018; MORAIS et al., 2016). With the development and use of computational tools, the sustainability impacts of biomass processing to biofuels and bioproducts can be assessed, since an early stage

of the whole process definitions, considering the three pillars of the sustainability (WATANABE et al., 2016): economic, environmental and social aspects. Within this purpose, Brazilian Bioethanol Science and Technology Laboratory (CTBE) of the National Center for Research in Energy and Materials (CNPEM) has been developing a platform for the integrated assessment of sugarcane (and other feedstocks) named as Virtual Sugarcane Biorefinery (BONOMI et al., 2016a).

Due to the great importance of biojet fuel and the recently the approved route by ASTM (ASTM, 2017), this work presents a vision of thermochemical conversion of biomass through fast pyrolysis and gasification technologies within BTL routes for the production of biojet fuel via Fischer-Tropsch synthesis in an integrated scenario.

This paper is organized as follow: handling and feeding, fast pyrolysis and gasification processes, cleaning and conditioning and Fischer-Tropsch synthesis. Next, biojet fuel regulation and integrated sugarcane biorefineries are also presented.

## 2. Thermochemical routes

A great variety of platform for chemicals, biofuels, and biobased compounds can be produced through BTL routes (BALAN; CHIARAMONTI; KUMAR, 2013; BAO; EL-HALWAGI; ELBASHIR, 2010; HARA; NAKAJIMA; KAMATA, 2015; HARO et al., 2013; LIEW; HASSIM; NG, 2014; NIGAM; SINGH, 2011; SWAIN; DAS; NAIK, 2011): Methane ( $\text{CH}_4$ ), ethylene ( $\text{C}_2\text{H}_4$ ), ethane ( $\text{C}_2\text{H}_6$ ), propane ( $\text{C}_3\text{H}_8$ ), butane ( $\text{C}_4\text{H}_{10}$ ), methanol ( $\text{CH}_3\text{OH}$ ), ethanol ( $\text{C}_2\text{H}_5\text{OH}$ ), dimethyl ether ( $\text{C}_2\text{H}_6\text{O}$ ), ammonia ( $\text{NH}_3$ ), butanol ( $\text{C}_4\text{H}_{10}\text{O}_8$ ), gasoline ( $\text{C}_5\text{-C}_{12}$ ), diesel ( $\text{C}_{13}\text{-C}_{22}$ ), wax and paraffin ( $\text{C}_{20}\text{-C}_{33}$ ), biojet fuel ( $\text{C}_{12}\text{-C}_{14}$ ), among others. Thermochemical processes within BTL routes comprise operations from biomass handling and feeding systems, thermochemical conversion, gas cleaning and conditioning and conversion technologies to energy, biobased chemicals and biofuels (DAMARTZIS; MICHAÏLOS; ZABANIOTOU, 2012; MORAIS et al., 2016).

One of the focuses of thermochemical processes is syngas production. Technologies for syngas production include two different types of processes: direct biomass gasification (LIM; ALIMUDDIN, 2008) and fast pyrolysis followed by catalytic or non-catalytic gasification of bio-oil or bioslurry, which is a mixture of biochar and bio-oil (BULUSHEV; ROSS, 2011; HENRICH; DAHMEN; DINJUS, 2009).

Currently, the main focus of thermochemical processes within BTL routes is biofuels production (HARO et al., 2013; KIM et al., 2013; NOURELDIN et al., 2014;

PANWAR; KOTHARI; TYAGI, 2012). Although thermochemical processes within BTL routes are recognized as one of the most promising technologies for biofuel production, their deployment in large scale still presents several challenges. One of such challenges remains on obtaining tar-free producer gas from biomass gasification, which is an undesirable compound in downstream applications such as internal combustion engines and catalytic synthesis (ASADULLAH, 2014; LIM; ALIMUDDIN, 2008). Another challenge concerns the use of different types of biomass for syngas production, especially agriculture residues, where there are few published works in the literature when compared with wood or coal gasification (AHMED; GUPTA, 2012; AL ARNI; BOSIO; ARATO, 2010). Moreover, hazardous gas compounds (HCl, NH<sub>3</sub>, H<sub>2</sub>S and others) can deactivate the catalysts and inhibit syngas conversion processes, besides fouling and blockage of filter with compounds with heavier hydrocarbons such as aromatics, phenols, and others (ARGYLE; BARTHOLOMEW, 2015; BARTHOLOMEW, 2001; SANCHEZ, 2010). These topics are further addressed over the next sessions.

## **2.1 Biomass handling and feeding systems**

Biomass handling and feeding systems constitute one of the most common bottlenecks in thermochemical routes (BASU, 2010; DAI; CUI; GRACE, 2012). Since biomasses have variable characteristics such as moisture, size, density, thermal energy content (LUQUE et al., 2012), adequate handling and feeding are required to provide a good operation in downstream thermochemical processes. In this step, consisting of receiving, storage and screening, feed preparation, conveying and feeding operations (BASU, 2010) undesired materials are eliminated, the particle size is reduced and moisture content is adjusted. Table 1 summarizes the biomass characteristics and the respective biomass handling operation as well as feeding area employed to prepare the biomass for the downstream operations.

After such operations, the biomass is prepared for the subsequent thermochemical conversion processes. In this work, pyrolysis and gasification are the thermochemical conversion processes to be explored.

## **2.2 Thermochemical conversion processes**

### **2.2.1 Pyrolysis**

Many definitions of pyrolysis and reports of pyrolysis products can be found in the literature. In a classical definition, pyrolysis can be defined as the thermal decomposition of

biomass in the absence of oxygen (BRIDGWATER, 2012a) other than that supplied by the fuel into gas, liquid and solid phases (DHYANI; BHASKAR, 2017).

Pyrolysis processes can be classified according to the operational conditions, mainly temperature, heating rate and residence time. Basu (BASU, 2010), for example, classifies it in three categorizations: torrefaction or mild pyrolysis, slow pyrolysis and fast pyrolysis. Bridgwater (BRIDGWATER, 2012a) presents a similar classification, adding intermediate pyrolysis and gasification. Babu (BABU, 2008) and Dhyani (DHYANI; BHASKAR, 2017) also present hydrolysis as another category of pyrolysis, in which biomass is converted in a hydrogen atmosphere and has the advantage of obtaining a liquid fraction enriched in hydrocarbons. Babu (BABU, 2008) also reports flash pyrolysis as a possible classification, with a higher heating rate and a smaller particle size when compared with fast pyrolysis, leading to a higher fraction of gas products. In the present work. In the present work, the authors opted to focus mostly on the classifications proposed by Bridgwater (BRIDGWATER, 2012a).

The liquid phase from pyrolysis is commonly known as bio-oil, while the solid is named biochar and the gas phase as non-condensable gas (SHEMFE; GU; RANGANATHAN, 2015). The bio-oil can be further divided into heavy and light fractions. The light fraction represents an aqueous condensate resulting from the moisture content in the feeding biomass, the water produced by the pyrolysis reactions and the releasing of volatile organic compounds (TSAI; LEE; CHANG, 2006). The heavy fraction, on the other hand, consists largely of fragments originating from lignin, so-called pyrolytic lignin (SCHOLZE; MEIER, 2001; TSAI; LEE; CHANG, 2006). Within the scope of this review, pyrolysis is discussed as a pretreatment step prior to gasification (DAHMEN et al., 2012, 2017), in which a high yield of bio-oil is desirable to produce a pumpable bioslurry (NICOLEIT; DAHMEN; SAUER, 2016). Therefore, fast pyrolysis will be further discussed in the following.

The pyrolysis reactor type is the core of fast pyrolysis processes (MOHAN; PITTMAN,; STEELE, 2006). Moreover, the system of pyrolysis products recovery also plays an important role in pyrolysis process since the bio-oil yield and quality are dependent on the performance of this system. The ideal design of a pyrolysis reactor realizes high rates of heat transfer through the mixing of biomass with a preheated heat carrier or by contacting the biomass with a hot surface. At the same time, it minimizes the residence time of pyrolysis products at high temperatures (BRIDGWATER, 2012b).

Several reactor types have been developed and tested in pilot scale since the 1980s (VENDERBOSCH; PRINS, 2010). Pyrolysis reactors can be of fixed bed, fluidized bed, ablative, or auger types.

Fluidized bed pyrolysis reactors may operate under bubbling or circulating conditions (HENRICH; WEIRICH, 2004). Nevertheless, differences in bubbling and circulating operation will not further discuss in the scope of this review. The fluidized bed reactor type is used in petroleum processing, being a well-developed technology (ISAHAK et al., 2012).

Auger pyrolysis reactors, also known as moving bed pyrolysis reactors, employ screws to transport the biomass into the reactor along with a heat carrier material such as sand or steel (ARAMIDEH et al., 2015; FUNKE et al., 2016a, 2016b, 2017a; PFITZER et al., 2016). Without heat carrier, it is a common design for continuous operation of slow and intermediate pyrolysis (BHATTACHARYA et al., 2009; FUNKE et al., 2017b; HASSAN et al., 2009; INGRAM et al., 2008; MORGANO et al., 2015; NEUMANN et al., 2015, 2016). The auger reactor requires a circulation system for hot inert material in which the volatiles exit in the upper part of the reactor, while biochar leaves the equipment through the bottom (FUNKE et al., 2016b; ISAHAK et al., 2012). The residence time of biomass is strongly dependent on the screw conveyor design and its rotational speed (ARAMIDEH et al., 2015). If more than one screw is inserted, the pyrolysis reactor is named twin screw mixing reactor or twin-screw pyrolysis reactor (KINGSTON; HEINDEL, 2014; RADLEIN; QUIGNARD, 2013; ROEDIG; KLOSE, 2008). Since auger reactors transport and mix solids by means of mechanical agitation, no fluidizing gas is needed for operation, which is a significant difference compared to fluidized bed technology, ultimately influencing fixed investment and operational cost.

Instead of mixing a preheated heat carrier with the feedstock, ablative pyrolysis reactors achieve high heat transfer rates by mechanically pressing the feedstock against a hot surface (JONES et al., 2009). The surface moves, e.g. as rotating disc, so that liquid and solid pyrolysis products are removed during operation (MOHAN; PITTMAN,; STEELE, 2006). As for mechanically agitated beds, ablative reactors do not require the use of inert fluidizing gas. Another advantage is avoiding extensive grinding of the feedstock to reach an optimum particle size because larger chunks are required to achieve the necessary pressing force on the hot surface (BRIDGWATER, 1999; JONES et al., 2009). On the downside, the building design and the scale-up of the ablative reactors are complex (APFELBACHER; CONRAD; SCHULZKE, 2014; JAHIRUL et al., 2012). In fact, there are several configurations based on

the ablative principle such as the rotating cone pyrolysis reactor, which is basically a combination of ablative and fluidized bed pyrolysis reactor (RADLEIN; QUIGNARD, 2013), the ablative vortex, ablative rotating disk (JAHIRUL et al., 2012), ablative coil, ablative plate (BRIDGWATER, 1999), and cyclone reactor (SANDSTRÖM et al., 2016). However, these reactor types are not on industrial scale yet.

Industrial fast pyrolysis units using the described technologies have seen increased application worldwide during the past years. It is not possible to generally point out the best suitable technology since this analysis depends on the specific application and variables such as feedstock availability and the desirable quality of the final product. Some examples of commercial and operational fast pyrolysis units in pilot scale (> 10 kg/h feed capacity) are summarized in Table 2 to give an overview of feedstocks and technologies.

As the discussion regarding the addition of pyrolysis in the sugar-energy industry is a current subject in the scientific literature (DHYANI; BHASKAR, 2017), a state of the art of experimental results from pyrolysis of sugarcane-related streams is presented in Table 3. It is worth mentioning that the use of sugarcane bagasse is already available in the 1G biorefinery process, thus reducing the logistic costs and other costs by sharing some of the facilities via coupling the thermochemical routes. Moreover, it is observed that sugarcane bagasse shows high organic liquid production potential of up to 57 % if process parameters are carefully chosen (ASADULLAH et al., 2007; CARRIER et al., 2013). This potential is close to the organic liquid yields obtainable from wood (BRIDGWATER, 2012a), which is a common raw material used in industrial fast pyrolysis plants (compare with Table 3). It is also observed that most results are from batch experiments in fixed bed reactors and that the heating rates applied so far are low compared to fast pyrolysis in fluidized beds which may exceed 10.000 K/min (PAPADIKIS; GU; BRIDGWATER, 2009).

The applied temperatures (500-560 °C) are usual in fast pyrolysis process conditions because high organic yields are expected in this temperature range (PAPADIKIS; GU; BRIDGWATER, 2009). This is due to the fact that, with lower temperatures and lower vapors residence time (1-5 s), the secondary pyrolysis reactions are disfavored, thus leading to high bio-oil production (YANIK et al., 2007).

The fast pyrolysis technology is mature enough to represent a feasible alternative for the thermochemical conversion of residues from the sugar-energy industry. Since existing technology is largely designed for woody biomass, further studies are required to better evaluate the organic oil potential of sugarcane bagasse and sugarcane straw. Both laboratory

and pilot scale results would be desirable to build a better basis for the evaluation of the integrated 1G2G BTL process chain.

### 2.2.2 Gasification

Historically, synthetic gas was first produced from coal in 1792 for use in residential lighting purposes (LOWRY, 1945). Since then, the gasification concept and several gasification reactor types were widely disseminated (HEIDENREICH; FOSCOLO, 2015; LAN et al., 2015). Gasification can be defined as the thermal conversion of carbonaceous feedstocks into a fuel gas (SÁNCHEZ, 2010). The exiting gasification gas, named producer gas or raw syngas, is composed mainly of CO, CO<sub>2</sub>, H<sub>2</sub>, CH<sub>4</sub>, O<sub>2</sub>, and other components such as particulate matter and tar. After cleaning and conditioning, the issuing stream is named syngas, being mainly composed of H<sub>2</sub> and CO (GÓMEZ-BAREA; LECKNER, 2010; VAN DER DRIFT et al., 2004) in a specific H<sub>2</sub>/CO molar ratio required for each downstream applications (ROSTRUP-NIELSEN, 2002), such as chemicals and liquid fuels *via* Fischer-Tropsch synthesis (TRIPPE et al., 2011). Table 4 shows a summarized gasification categorization and the respective parameters for the gasification process. Figueroa et al. show that a desired H<sub>2</sub>/CO molar ratio may be achieved by water gas-shift reactions (FIGUEROA et al., 2013).

Many variables related to biomass characteristics directly affect the gasification process such as its size, shape, porosity, density, and composition (hemicellulose, cellulose, lignin, extractives, and ash) (KIRUBAKARAN et al., 2009). Besides the use of *in natura* biomass for gasification processes, another includes the employment of slurries. Slurries can be a mixture of biomass and water (DE SOUZA-SANTOS, 2015), biomass and glycerol (DE SOUZA-SANTOS, 2017) or bio-oil and biochar from biomass fast pyrolysis (DAHMEN et al., 2017; NICOLEIT; DAHMEN; SAUER, 2016; PFITZER et al., 2016).

#### **Gasification reactor types**

Generally, the gasification reactor types are categorized in fixed bed (downdraft and updraft), fluidized bed (bubbling fluidized bed and circulating fluidized bed) and entrained flow (BURAGOHAJN; MAHANTA; MOHOLKAR, 2010; LAN et al., 2015).

In updraft gasifiers, the material is fed at the top of the reactor whereas the gasification agent is injected through the bottom part. In downdraft gasifiers, the material and gasification agent move both from the top to the bottom of the gasification reactor. In bubbling fluidized bed reactors, the material is supported by a distributor plate through which the

gasification agent passes. In circulating fluidized bed, the material is circulated due to a cyclone unit operation placed outside or inside the gasification reactor.

The main point of downdraft gasifiers is that the tar content from the pyrolysis zone passes through the combustion zone, where tar is cracked into light compounds (BRIDGWATER, 1995; BURAGOHAJIN; MAHANTA; MOHOLKAR, 2010). Thus, the tar content in downdraft gasifiers is usually lower when compared with updraft gasifiers (LAN et al., 2015), resulting in a lower number of cleaning steps in downstream processing (BRIDGWATER, 1995), that can be a crucial step in the process cost and application. The main quality for updraft gasifiers is the simple design and construction allied with high thermal efficiency (BRIDGWATER, 1995).

Bubbling fluidized bed is a reactor type in which the producer gas carries elutriated solid whereas in the circulating fluidized bed the elutriated solid is circulated by a cyclone and then returns to the gasification reactor (WARNECKE, 2000).

One intrinsic characteristic of entrained flow gasifiers is the gasification process without inert material where the gasified material (e.g. slurry) is put in contact along with gasification agent inside the gasification reactor. Generally, entrained flow gasification is performed in pressurized systems (> 1 bar) and with high temperature of the burner zone (~2100 K) (HEIDENREICH; FOSCOLO, 2015). Studies report that entrained flow gasifiers are a promising technology due to the production of tar-free producer gas (DAHMEN et al., 2012; RAFFELT et al., 2006; TRIPPE et al., 2011). Currently, in view of the high yield of syngas production, entrained flow gasifier could be employed for the production of high-quality biofuels (TRIPPE et al., 2011). Table 5 presents the state of the art using different conditions for each gasification reactor types and characteristics.

## **2.3 Gas cleaning and conditioning**

### **2.3.1 Gas cleaning**

The gas cleaning step is needed for the removal of impurities to achieve the quality requirements for gas uses such as energy generation and the synthesis of biobased chemical or biofuels (ABDOULMOUMINE et al., 2015). Gas cleaning technologies should remove particulate matter, tar, halogenated, carbon dioxide, alkaline metals and compounds of nitrogen, sulfur (ABDOULMOUMINE et al., 2015; HEIDENREICH; FOSCOLO, 2015) and chlorine, e.g. NH<sub>3</sub>, NO<sub>x</sub>, HCN, H<sub>2</sub>S, COS, SO<sub>2</sub>, HCl, among others. (ABDOULMOUMINE et al., 2015). Basically, gas impurities in producer gas can be classified into three categories

(BASU, 2010): particulate matter (ash and biochar), inorganic impurities (halides, alkali metal, sulfur and nitrogen compounds), and organic impurities (tar, aromatic and organic sulfur compounds).

Particulate matter and tar are usually carried out by the producer gas equipment (SÁNCHEZ, 2010). Although many authors generalize particulate matter as ash, it can also contain macronutrients, unreacted solid (e.g. biochar) and other solid compounds (e.g. silica from feedstock or bed material). Milne et al. (MILNE; EVANS; ABATZOGLOU, 1998) define tar as an organic product obtained from thermal processes or partial oxidation of any carbon-based material. Tar from biomass gasification is a complex mixture of hydrocarbons, oxygenated or not, which composition is dependent on reactor type, feedstock, equivalent ratio, operational temperature, among others (SÁNCHEZ, 2010). Tar is also known as Volatile Organic Compound (VOC) (MILNE; EVANS; ABATZOGLOU, 1998). Therefore, within the scope of many definitions, tar can be defined as a heavy hydrocarbon that can be treated or purified through thermal, catalytic or physical processes (FOURCAULT; MARIAS; MICHON, 2010).

Regarding tar composition, different reports can be found in the literature. Milne et al. (MILNE; EVANS; ABATZOGLOU, 1998) report tar as a hydrocarbon with molecular weight higher than that of benzene. Coll et al. (COLL et al., 2001) report tar as 1 wt.% of hydrocarbons with 4 aromatics rings, 6 wt.% of hydrocarbons with 3 aromatics rings, 13 wt.% of hydrocarbons with 2 aromatics rings, 22 wt.% of hydrocarbons with 1 aromatics ring, 10 wt.% of heterocycles compounds, 7 wt.% of phenolic compounds, 15 wt.% naphthalene, 24 wt.% toluene and 2 wt.% for other compounds.

The removal of impurities from producer gas is highly dependent on upstream characteristics such as biomass composition and reactor type and operational parameters of the gasification process. If the aforementioned impurities are not sufficiently removed, several downstream problems can occur such as corrosion, clogging or blockage of filters, pipes and engines and catalyst deactivation in chemical synthesis (BARTHOLOMEW, 2001; CHIANG et al., 2013; HEIDENREICH; FOSCOLO, 2015).

Two main technological strategies to reduce the amount of or remove impurities in producer gas from biomass gasification are proposed in the literature (RICHARDSON; BLIN; JULBE, 2012): primary and secondary. The former strategy comprises technologies to reduce the formation of impurities (e.g. tar) during the biomass gasification process. The latter

strategy, presented in the next topic, refers to the operations of gas cleaning to provide syngas within specification for downstream processes and gas utilization.

Choosing the best configuration for gas cleaning depends on the desired syngas quality which, in turn, is dependent on the biomass composition and the type of gasifier employed (MORAIS et al., 2016). Typical syngas specifications for different application are presented in Table 6.

The existing technologies for gas cleaning can be categorized according to three temperature ranges (SHARMA et al., 2008): cold ( $< 25\text{ }^{\circ}\text{C}$ ), warm ( $25\text{-}300\text{ }^{\circ}\text{C}$ ) and hot cleaning ( $> 300\text{ }^{\circ}\text{C}$ ). In addition to this categorization, gas cleaning technologies can be classified into five configuration groups (HAN; KIM, 2008): mechanical or physical, modification of operational parameters, catalytic cracking, thermal cracking and plasma cracking. Generally, most gas cleaning configurations use a combination of these five categorizations (ASADULLAH, 2014). Next, these five groups will be briefly presented, except for the modification of operation parameters, which is an upstream modification.

### **Mechanical or physical technologies**

The main target of mechanical or physical technologies is to remove particulate matter. These are simple technologies with relatively low cost, placed immediately after the gasification reactor to avoid erosion and fouling in subsequent downstream units (SIMELL et al., 2014). This categorization can be further classified into two groups: dry and wet gas cleaning. Dry gas cleaning technologies refer to equipment placed to the producer gas cooling step, while wet ones are employed after producer gas cooling to the range of  $20\text{-}60\text{ }^{\circ}\text{C}$  (ANIS; ZAINAL, 2011).

Tar and particulate matter can be separated by tar condensation temperature once temperature for that be identified, which is essential to identify the best removal technology to be used (ANIS; ZAINAL, 2011; SIMELL et al., 2014). However, one issue reported by Zhang et al. (ZHANG et al., 2012) is that the condensation of tar simultaneously with the particulate matter may increase the overall pressure drop of the system, thus leading to a serious operational problem. In addition to the separation of tar and particulate matter using mechanical or physical cleaning, alkali, heavy metals and chlorides can be condensed when producer gas is cooled to less than  $600\text{ }^{\circ}\text{C}$  (ZHANG et al., 2012) and removed using cyclones or filters, e.g. chlorine in HCl can react with calcium or alkali metals and then solid chlorides can be removed

using filters (SIMELL et al., 2014). Table 7 presents a compilation of the main mechanical or physical technologies for tar and particulate matter removal collected from different authors.

### **Catalytic cracking**

Catalytic cracking is considered a feasible option for large-scale plants to reform tar and destroy or adsorb poisonous gases (ASADULLAH, 2014; WOOLCOCK; BROWN, 2013). Catalytic cracking comprises two technological options (ASADULLAH, 2014): primary bed in the gasifier and secondary reformer after gasification. Only the latter is discussed in this session.

Catalytic cracking occurs in the presence of catalysts, such as non-metallic catalysts, e.g. dolomite, zeolite and calcite, and metallic ones, such as nickel compounds (Ni/Mo, Ni/Co/Mo, NiO), Pt, Ru, aluminum oxide, among others (ABDOULMOUMINE et al., 2015; ANIS; ZAINAL, 2011; ZHANG et al., 2012). An extensive review of catalytic cracking was carried out by Anis et al. (ANIS; ZAINAL, 2011) (Anis & Zainal, 2011).

Two approaches were evaluated by Simell et al. (SIMELL et al., 2014) to promote catalytic cracking: scrubbing with organic solvents and catalytic cracking reforming. Catalytic cracking unit operation in gas cleaning projects can be carried out after mechanical or physical separation, being the most used one in commercial scale (SIMELL et al., 2014).

One challenge concerning catalytic cracking is the reactor design: its optimization should consider deactivation of the catalysts, catalyst lifetime, coking problems, maintenance breaks and temperature and pressure operation (SIMELL et al., 2014)

The catalysts allied to the additives, promoters, and supports should guarantee the following requirements (SUTTON; KELLEHER; ROSS, 2001): be capable of removing tar and reforming methane, be resistant to deactivation (carbon fouling and sintering), be easy to regenerate and have a good cost-effectiveness ratio.

### **Thermal cracking**

Thermal cracking comprises hot gas cleaning technologies. The producer gas is heated to a certain temperature and residence time to break up the particulate matter and tar in a gas with smaller particles or a lighter gas, consisting mainly of CO and H<sub>2</sub> (ABDOULMOUMINE et al., 2015). The direct contact of producer gas with a heat source is a way of achieving thermal cracking (BRIDGWATER, 1995). Generally, thermal cracking

occurs in the range of 600-1250 °C (ABU EL-RUB; BRAMER; BREM, 2008; ANIS; ZAINAL, 2011; SIMELL et al., 2014).

### **Plasma cracking**

Plasma cracking can reach temperature up to 20,000 K (SAMAL, 2017), thus providing high conversion of heavy molecules, such as tar, into lighter ones.

For plasma cracking, the plasma torch technology is commonly used. This technology converts electric energy into thermal energy, named plasma, capable to destroy and/or reform the tar and particulate matter (FOURCAULT; MARIAS; MICHON, 2010; HAN; KIM, 2008), besides removing sulfur and nitrogen compounds (ANIS; ZAINAL, 2011). Therefore, plasma technology for producer gas reforming can be defined according to three categorizations (CHANG, 2003). The first group is named remote plasma method in which plasma components at high pressure are used. The second is the indirect radiation method, in which high and low pressures are used to generate ultraviolet radiation, electron beam or gamma radiation to reform the gas. The third one is the corona discharge using alternating current, direct current or pulsating current, which are generated within the gas to be reformed and treated directly by the plasma gas.

Some advantages of using plasma cracking technology have been pointed out in the literature (BOULOS; FAUCHAIS; PFENDER, 1994; CHO et al., 2015; HRYCAK; JASIŃSKI; MIZERACZYK, 2010; NAIR et al., 2004; UHM et al., 2014): i) high temperatures of plasma can destroy VOCs, SO<sub>x</sub> and NO<sub>x</sub> compounds; ii) high density of plasma torch allows a smaller equipment installation when compared to other equipment favoring the design of new reactors; iii) it is an alternative to conventional gas cleaning technologies; iv) thermal plasma provides reactions such as oxidation, cracking and reforming without the need for a catalyst.

Some works covering pyrolysis, combustion and gasification processes using plasma technology were carried out (UHM et al., 2014; VAN OOST et al., 2008; YOON; LEE, 2012). Others studies are focused on the reformation of producer gas or in the development of new types of plasmas allied with simulation data focusing on non-thermal plasma (ELIOTT et al., 2013; FOURCAULT; MARIAS; MICHON, 2010; HRYCAK; JASIŃSKI; MIZERACZYK, 2010; NAIR et al., 2004).

The plasma can be generated by many gases such as inert, oxidant or reducing ones. Bityurin et al. (BITYURIN; FILIMONOVA; NAIDIS, 2009) used N<sub>2</sub> to generate the plasma to reform tar modeled as a naphthalene compound. Neves et al. (NEVES, 2013) reported an

experimental work on the reforming of producer gas from biomass (approximately 22.4 kg/h) in fluidized bed gasification using a commercial plasma torch. A reduction of tar and particulate matter around 23 wt.% was reported when plasma cracking technology was applied.

Plasma cracking technology can also be used to increase the gas cleaning efficiency through hybrid systems, i.e. in which a thermal conversion reactor is coupled with a plasma technology (MATVEEV; SERBIN; LUX, 2008) such as in pyrolysis and gasification processes (SAMAL, 2017). For example, it was developed a gasification-plasma hybrid system assembled by a gasification reactor and a plasma reactor to increase the syngas (H<sub>2</sub> and CO) productivity. In this case, the term hybrid means a gasification reactor coupled with a plasma reactor (CHO et al., 2015; MATVEEV; SERBIN; LUX, 2008; SAMAL, 2017).

Although the advantages of plasma cracking allow this technology to be compared with conventional gas cleaning technologies, there is no techno-economic data on a commercial scale using plasma cracking technology to guarantee that this technology is feasible in integrated processes (ANIS; ZAINAL, 2011; CHANG, 2003; MARIAS et al., 2015), especially, in integrated biorefineries.

### 2.3.2 Gas conditioning

Gas conditioning is performed downstream of gas cleaning technologies. The first step to choose the suitable syngas conditioning option is to know the end-use application of syngas (for example, nitrogen may not be considered an impurity for electricity production purposes, but it must be removed to a certain extent for fuel synthesis). In the case of Fischer-Tropsch synthesis, a high-pressure syngas stream and a specific H<sub>2</sub>/CO molar ratio are required. This ratio can be adjusted using different steps such as Methane Steam Reforming, Methane CO<sub>2</sub> Reforming and Water Gas Shift reaction (RICHARDSON; BLIN; JULBE, 2012), as follows.

#### Methane Steam Reforming and Methane CO<sub>2</sub> Reforming

Methane Steam Reforming (MSR) is used to adjust the H<sub>2</sub>/CO molar ratio of producer gas. Chemically, MSR is set by the chemical reaction (RAMOS et al., 2001) presented in Equation 1 and following the kinetic reaction according to Equation 2.



where the enthalpy of formation is  $\Delta H_{298}^o = 206.6 \text{ kJ/molCH}_4$ .

$$\ln K = -\frac{22,790}{T} + 8.156 \ln T - \frac{4.421}{0.001} T - \frac{4.330}{1,000T^2} - 26.030 \quad (2)$$

where  $K$  is the equilibrium constant in the temperature  $T$  (K).

MSR uses steam as the heat carrier, a utility commonly found in industrial facilities such as biorefineries. Generally, the temperature in the MSR reactor stands between 750 and 900 °C, while the pressure is of 15 to 30 bar (RAMOS et al., 2001). Typically used catalysts for MSR are Ni-based (PALMA et al., 2017), although an improvement in both thermal conductivity and mechanical resistance has been obtained using SiC catalysts (RICCA et al., 2017).

Methane CO<sub>2</sub> reforming (MCR) is considered to have less environmental impacts compared to MSR since this makes use of CO<sub>2</sub> as the reactant (Equation 3). On the other hand, MCR requires more energy to occur than MSR (RAMOS et al., 2001).



where  $\Delta H_{298}^0$  is 247.2 kJ/molCH<sub>4</sub>

### Water Gas Shift reaction

The Water Gas Shift (WGS) reaction can be considered as an alternative to MSR and MCR employed to adjust the H<sub>2</sub>/CO molar ratio (RICCA et al., 2017). Equation 4 presents the WGS reaction while Equation 5 and 6 show its kinetics (CHINCHEN et al., 1988; CHOI; STENGER, 2003). The WGS reaction occurs in the range of temperature from 200 to 300 °C (low temperature) for Fe-based catalyst and from 300 to 500 °C (high temperature) for Cu-based catalysts (LANG et al., 2017).



where  $\Delta H_{298}^0$  is -41.1 kJ/molCO.

$$\ln K = \frac{5693.5}{T} + 1.077 \ln T + \frac{5.44}{0.001} T - 1.125 \times 10^{-7} T^2 - \frac{49,170}{T^2} - 13.148 \quad (5)$$

$$\text{where } K_{equivalent} \cong \frac{P_{CO_2} P_{H_2}}{P_{H_2O} P_{CO}} \quad (6)$$

The endothermic characteristic of MSR and MCR leads to a need for high amounts of water in the processes. On the other hand, due to the exothermic character of the WGS reaction, steam can be generated in a heat integration concept to be used as a utility within biorefineries, such as process steam for the gasification process.

## 2.4 Biojet fuel production via Fischer-Tropsch (FT) synthesis

The main products of FT synthesis are paraffins, iso-paraffins, olefins, aromatics, and naphthalenes (ZHANG et al., 2015), and they are usually categorized into five groups

excluding inert gases (KLERK, 2011): gaseous products (C<sub>3</sub>-C<sub>4</sub>), naphtha (C<sub>5</sub>-C<sub>10</sub>), distillate (C<sub>11</sub>-C<sub>22</sub>), wax (> C<sub>22</sub>) and oxygenated compounds.

In view of FT developments, many researchers have addressed the FT reactions over time (DALAI; DAVIS, 2008). Historically, the FT synthesis was developed by Franz Fischer and Hans Tropsch in 1923 to produce liquid fuels, mainly diesel from coal (ANDERSON; FRIEDEL; STORCH, 1951). The general FT reaction (SCHULZ, 1999; STEYNBERG, 2004) is presented in Equation 7.



where catalysts of Fe, Ni, Co, Ru and Rh can be used. These catalysts can be unsupported and supported (DALAI; DAVIS, 2008). The enthalpy of formation ( $\Delta H^\circ$ ) of the FT reaction is equal to -165 kJ/mol of CO (TIJMENSEN et al., 2002).

FT synthesis can be classified into Low-Temperature FT (LTFT) and High-Temperature FT (HTFT), occurring in the range of 210-260 °C and 310-340 °C, respectively (Leckel, 2009). Studies have pointed out that LTFT is used to produce mainly linear waxes, while HTFT is employed to obtain primary linear olefins (NOURELDIN et al., 2014; STEYNBERG; DRY, 2004). In addition to temperature, parameters such as pressure, H<sub>2</sub>/CO molar ratio, residence time, catalysts and reactor type influence the final product output, i.e. olefins and waxes can be produced in adjustable proportions using either LTFT or HTFT.

The FT products, i.e. liquid hydrocarbon chains, can be predicted according to the Anderson-Schulz-Flory (ASF) distribution (ANDERSON; FRIEDEL; STORCH, 1951; PUSKAS; HURLBUT, 2003; SCHULZ, 1999; SCHULZ; CLAEYS, 1999). ASF is governed by a polymerization kinetic chain model as shown in Equation 8 (BARTHOLOMEW, 1990). The ASF distribution describes the chain growth according to the number of carbon atoms in the reaction medium (BARTHOLOMEW, 1990; DRY, 2002; IGLESIAS GONZALEZ; KRAUSHAAR-CZARNETZKI; SCHAUB, 2011).

$$\ln \frac{z_n}{n_\alpha} = n_\alpha \ln \alpha + \ln \frac{(1-\alpha)^2}{\alpha} \quad (8)$$

where  $z_n$  is the mass fraction (wt.%) of a product which consists of  $n_\alpha$  carbons atoms and  $\alpha$  is the syngas adsorption (growth factor) in the catalysts according to Equation 9 (BARTHOLOMEW, 1990).

$$\alpha = \frac{R_p}{R_p + R_t} = \frac{k_a P_{CO}}{k_a P_{CO} + k_b P_{H_2} + k_c} \quad (9)$$

where  $R_p$  is the rate of propagation,  $R_t$  is the rate of termination,  $k_a$  is the rate constant for CO adsorption on an active site ( $1.22 \times 10^{-5}$  mol/g.s.bar),  $P_{CO}$  is the partial pressure

of CO (bar),  $k_b$  is the rate constant for desorption of paraffins by hydrogenation of active site (mol/g.s.bar),  $P_{H_2}$  is the partial pressure of H<sub>2</sub> (bar) and  $k_c$  is the rate constant for desorption of olefins from active site (mol/g.s).

According to Spath and Dayton (SPATH; DAYTON, 2003), LTFT with Co catalyst, pressure of 7-12 bar and H<sub>2</sub>:CO of 2.15:1 favors high molecules mass linear waxes and HTFT with Fe catalyst, pressure of 10-40 bar and H<sub>2</sub>:CO of 1.7:1 favor low molecular weight olefins. In summary, LTFT is used to produce waxes and diesel fraction while LTFT is used to produce gasoline fraction and light olefins (BOERRIGTER; RACUH, 2005).

#### **2.4.1 Catalysts for Fischer-Tropsch synthesis**

It is estimated that 90% of all products produced in the world employ at least one catalyst at some stage of their production (SAITOVITCH; SILVA, 2005). Since catalysts are extensively modeled, synthesized, characterized, and tested before reaching the optimum point for selectivity towards a specific product, the development of new catalysts to be used in industrial scale can take years of validation (LUQUE et al., 2012). In view of this, traditional metal catalysts, i.e. Fe- and Co-based, remain good choices for using in FT synthesis (SAINNA; MK, 2016). Usually, catalysts for FT synthesis are used supported on alumina, silica and zeolite compounds (FAHIM; AL-SAHHAF; ELKILANI, 2012; IGLESIA, 1997; RAMOS et al., 2001; RIEDEL et al., 1999).

Many compounds can cause catalyst deactivation through either chemical or physical processes (LUQUE et al., 2012). Among the harmful compounds to FT catalysts are sulfur, nitrogen, and chlorine (TIJMENSEN et al., 2002) (see Table 6). Fe-based catalysts are less dependent on the syngas quality and have higher tolerance to high temperatures (HTFT) when compared to the Co-based catalysts (KALTSCHMITT; NEULING, 2018). On the other hand, Co-based catalysts have received attention due to its long life and high catalytic activity (DALAI; DAVIS, 2008).

#### **2.4.2 Upgrading and hydrocracking of Fischer-Tropsch products**

Biojet fuel production can be increased by converting gaseous products, naphtha, and wax into hydrocarbons in the typical jet range in addition to green gasoline and green diesel, besides electricity (KLEIN et al., 2018). Although upgrading and hydrocracking processes are scarce in literature in terms of data, Fischer-Tropsch products need to be upgraded and hydrocracked to meet specifications of biojet fuel (KLERK, 2011). A

combination of the following steps can be performed to obtain biojet fuel (ATSONIOS et al., 2015; ZHANG et al., 2015):

Aromatization process: insert aromatics into the hydrocarbon chains;

Hydrocracking process: break chains, i.e. convert long hydrocarbon chains in biojet fuel range;

Hydrogenation: reduce the olefins and oxygenated compounds in biojet fuel;

Hydroisomerization process: isomerization of linear hydrocarbon chains;

Hydrotreating process: remove heteroatoms and saturated bonds (C-C);

Product separation: water separation and distilling of biojet fuel;

This combination depends on which FT product fraction (gaseous products C<sub>3</sub>-C<sub>4</sub>, naphtha C<sub>5</sub>-C<sub>10</sub>, distillate C<sub>11</sub>-C<sub>22</sub> and wax > C<sub>22</sub>) needs to be prioritized. The process is named upgrading if gaseous products and naphtha will be converted into biojet fuel and named hydrocracking if the conversion is of heavy molecules to lighter ones.

In the case of gaseous products upgrading, biojet fuel can be produced by oligomerization of C<sub>3</sub>-C<sub>4</sub> olefins over a Solid Phosphoric Acid (SPA) oligomerization unit and followed by an aromatic alkylation, producing branched C<sub>8</sub>-C<sub>12</sub> aliphatic biojet fuel (KLERK, 2011).

Naphtha upgrading will convert naphtha to an aromatic hydrocarbon in the biojet fuel range by means of oligomerization and aromatic alkylation (KLERK, 2011). To achieve this goal, naphtha passes through a hydrotreater to remove oxygen and saturate the bonds (BALIBAN et al., 2013). Afterward, naphtha can be isomerized or aromatized (BALIBAN et al., 2013) according to the biojet fuel specification. Naphtha upgrading is performed based on Amorphous Silica-alumina (ASA) and metal promoted zeolite-based (H-ZSM-5) catalysts (KLERK, 2011).

Wax hydrocracking uses H<sub>2</sub> to convert wax to biojet fuel range by means of isomerization and cracking the long chains (BOUCHY et al., 2009). Moreover, hydrocracking of wax adjusts the branched hydrocarbons and reduces olefins and oxygenated compounds to meet the freezing point for biojet fuel (KLERK, 2011). Hydrocracking catalyst is usually composed of noble metal on acidic support, e.g. Pt or Pd on alumina support such as SiO<sub>2</sub>-Al<sub>2</sub>O<sub>3</sub> (CALEMMA et al., 2010). H<sub>2</sub> per wax demand for hydrocracking unit is around 1% wt. (SUDIRO; BERTUCCO, 2009).

One of the key requirements of the upgrading and hydrocracking of FT products is the hydrogen demand that can be produced through different technologies such as biomass

gasification, natural gas steam reforming, steam reforming, water electrolysis, cryogenic separation, Pressure Swing Adsorption (PSA) of off-gas, among others (KLEIN et al., 2018). In addition to H<sub>2</sub> demand, a critical point to increase biojet fuel yields in the final specification of the fuel. This specification is set by regulatory agencies and further discussed in the next session.

Papers involving modeling of FT processes (HALLAC et al., 2015; KLERK, 2011; MOSAYEBI; HAGHTALAB, 2015; SCHULZ; CLAEYS, 1999; WANG et al., 2003) in addition to experimental studies (KIM et al., 2013; ÖZKARA-AYDINOĞLU et al., 2012; YU et al., 2016) have been reported in the literature. However, specific works for biojet fuel production via FT synthesis and upgrading and hydrocracking of FT products are still scarce in the literature, some of which are presented in Table 8.

### **3. Biojet fuel regulations**

Alternative jet fuels, including those produced from biomass (biojet fuels), are currently approved by the American Society for Testing and Materials (ASTM) and other regulatory bodies for use in both civil and military aviation. The certified routes refer to the production of Synthetic Paraffinic Kerosene (SPK), which is exclusively composed of paraffinic compounds. In this way, SPK must be blended with fossil jet fuel (up to a limit of 50%, according to the production route) for utilization in jet engines. Alternative jet fuels with closer composition to conventional jet fuel, i.e. with paraffinic, cyclic, and aromatic molecules, despite having recent approval from ASTM International, is viewed as an option for the long term, since the blend with fossil jet fuel could potentially be dismissed. Commercial flights have successfully demonstrated the technical feasibility of biojet fuel (GUTIÉRREZ-ANTONIO et al., 2017), as shown in Table 9.

The first standard for an alternative jet fuel referred to that produced through FT processes. As previously stated in this work, the production of syngas for FT-SPK synthesis can be performed with the gasification of several types of raw materials, including both fossil (coal, natural gas, and crude oil) and renewable ones (all sorts of biomass). Therefore, the renewable characteristic of the produced jet fuel is ultimately dependent on the input of the gasification section in a thermochemical plant. It is important to note that, besides the FT conversion route, all other three approved pathways are mainly aimed at the processing of biobased raw materials: Hydroprocessing of Esters and Fatty Acids, which transforms vegetable oils and animal fats into hydrocarbons; Direct Sugar to Hydrocarbons, mainly

converting carbohydrates into a molecule in the range of jet fuel (Farnesene); and Alcohol to Jet, which dehydrates isobutanol and combines the resulting isobutylene into hydrocarbons. In all routes, ASTM D1655 regulates the jet fuel according to its performance covering a series of properties such as thermal stability, aromatic contents, viscosity, flash point, among others. Main properties of jet A and A-1, two grades of kerosene fuel that only differ in freezing point, and biojet fuel produced via FT synthesis plus aromatics are presented in Table 10.

For meeting the regulatory requirements of aromatic in the jet fuel, the blend of biojet fuel with conventional jet fuel is necessary (ASTM, 2017; LIU; YAN; CHEN, 2013). Blended jet fuel or fully biojet fuel should provide the following basic extended requirement (ASTM, 2011, 2017): maximum lubricity equal to 0.85 mm according to ASTM D5001 and minimum aromatic equal to 8 or 8.4 vol.% according to ASTM D1319 or D6379, respectively. The major issue concerns the aromatic content in jet fuel is because it produces more smoke in the flame (ASTM, 2011), but it is essential to maintain the aromatic content equal or more than 8 wt.% to avoid engine leakage (BLAKEY; RYE; WILSON, 2011).

#### **4. Thermochemical routes in integrated biorefineries for biojet fuel production**

A biorefinery can be defined as a facility in which processes and equipment are integrated for the conversion of biomass into biofuels, energy and biobased chemicals (DEMIRBAS, 2009). The biorefinery concept is similar to that of existing oil refineries in which a wide variety of fuels is produced from crude oil (MORAIS et al., 2016).

In Brazil, First-Generation sugarcane biorefineries can be divided into three main configurations (BONOMI et al., 2016a): autonomous distilleries in which all sugarcane juice is converted into ethanol; sugar factories in which all sugarcane juice is converted into sugar; and annexed distilleries in which sugarcane juice is converted into both sugar and ethanol. In all configurations, large amounts of sugarcane bagasse are produced and can be used as a fuel in Combined Heat and Power units to supply heat (steam at different pressure levels) and power to the process, as well as exporting surplus electric energy to the grid (MORAIS et al., 2016). Sugarcane bagasse from 1G sugarcane biorefinery and straw (recovered from the field) can be used for the production of advanced biofuels *via* above discussed thermochemical routes, thus resulting in integrated of First- and Second-Generation (1G2G) biochemical sugarcane biorefineries (BONOMI et al., 2016b; JUNQUEIRA et al., 2017; KLEIN et al., 2018).

Such biorefineries can be thought of as centralized or decentralized concepts, mainly differing in terms of pre-treatment and transportation to the conversion facility. In decentralized biorefineries, in view of their low density, polydisperse biomasses are converted in decentralized fast pyrolysis plants to produce a mixture of biochar and bio-oil, named bioslurry, which represents an energetically densified intermediate product: heating value of 11-28 MJ/m<sup>3</sup> with a density of 1,000-1,200 kg/m<sup>3</sup> depending on the condensate fraction (NICOLEIT; DAHMEN; SAUER, 2016). The bioslurry can be further converted into biofuels, biobased chemicals and electricity in centralized gasification facilities (TRIPPE et al., 2011). This decentralized concept is the concept employed by bioliq<sup>®</sup> of Karlsruhe Institute of Technology (KIT) in Germany (DAHMEN et al., 2012, 2017; HENRICH; DAHMEN; DINJUS, 2009; PFITZER et al., 2016; RAFFELT et al., 2006; TRIPPE et al., 2011).

Possible scenarios with centralized and decentralized concepts of integrated 1G2G biochemical-thermochemical biorefineries for biojet fuel production are presented in Figure 1. All hypothetical scenarios produce ethanol and sugar in addition to biojet fuel, green diesel, green gasoline, and electricity.

Centralized concepts of 1G sugarcane biorefinery are shown in Figure 1C1 and C2. Figure 1C1 shows a scenario using gasification of LCB from a 1G sugarcane biorefinery. In this case, LCB to the gasification process is a solid material. Therefore, the employed gasifier should be either a fixed bed or a fluidized bed one. Figure 1C2 presents the same configuration to which a fast pyrolysis step is added. Bioslurry from LCB is produced and used as feedstock in the gasification reactor. Due to the characteristics of bioslurry, an entrained-flow gasifier can be applied, which reduces the problem of tar removal from syngas. In both centralized concepts, the thermochemical plant could be responsible for producing heat (steam) and power (electricity) for the integrated unit.

Decentralized concepts are shown in Figure 1D1 to 1D4. Figure 1D1 presents a scenario in which sugarcane straw recovered from the field and surplus bagasse are gasified in a fixed or fluidized bed reactor. Figure 1D2 presents the same configuration added pyrolysis unit to produce bioslurry from LCB, which is further gasified in an entrained-flow gasifier. Figure 1D3 adds a pyrolysis process into a sugarcane biorefinery to produce bioslurry, further processed in an entrained flow gasifier. Lastly, Figure 1D4 presents two decentralized concepts: standalone pyrolysis and integrated sugarcane biorefinery-pyrolysis. In all decentralized concepts, the sugarcane biorefinery and the thermochemical plant must be independently self-sufficient in terms of heat and power.

## **5. Final remarks**

BTL thermochemical routes encompass promising pathways to produce biojet fuel in world scale. While biomass corresponds to a very significant cost component in any conversion process, the logistics for transportation and technology for energy densification must also be tackled to improve the feasibility of the complete process.

Fast pyrolysis has become a mature technology that is applied industrially for the conversion of woody biomasses. In spite of this, further research, especially at relevant technical scales, are required to better assess the potential of applying this conversion technology as a pretreatment method prior to gasification. Besides, although the gasification of biomass is considered more mature than fast pyrolysis, more analyses regarding the integration of thermochemical routes in 1G sugarcane biorefineries are required for the development of the centralized and decentralized concepts. This includes better quantification of the benefits and disadvantages of including the cost and inefficiencies of the overall BTL concept.

## **Acknowledgment**

The authors acknowledge the Brazilian Bioethanol Science and Technology Laboratory (CTBE) from Brazilian Center for Research in Energy and Materials (CNPEM) for the infrastructure support and CAPES for the scholarship (23038.006737/2012-56).

Table 1. Biomass parameters, implications in the thermochemical processes and biomass handling and feeding technology solution.

Biomass parameters	Biomass value	Implications in the thermochemical processes	Biomass handling and feeding technology solution	Reference
Moisture content	High (40 to 60% - Freshly cut biomass)		Drying process	(BASU, 2010)
		Risk of biological degradation. Cause corrosion (condensation of water in flue gas) Heat value reduction	Drying process	(BACH; SKREIBERG, 2016)
Foreign materials	Stones, ferrous, metals, nonferrous metals	Affect the gasifier operation	De-stoner Nonferrous metals separators Magnetic metal separation	(BASU, 2010)
Particle size	Too large (or uneven in size)		Size-reducing machines	(BASU, 2010)
		Increase grinding energy		(BACH; SKREIBERG, 2016) (BASU, 2010)
Energy density	Low	Require large storage area Increase storage and transportation costs; Require high feeding capacity		(BASU, 2010)
			Optimum design of logistics systems Energy densification (baling, briquetting, palletization, etc.)	(CAI et al., 2017) (GRAMMELIS, 2010)

Table 2. Summary of commercial fast pyrolysis activities with a capacity greater than 10 kg/h and which are reported to be operational (BIOFUELSDIGEST, 2015; BIOWARE, 2015; DEMOPLANTS, 2017; PYNE, 2017).

Technology	Feed Capacity (kg/h)	Feedstock	Product	Company	Country
Fluidized Bed	1,667	Wood	Food additives	Red Arrow	United States
Fluidized Bed	2,500	Wood residues	Heating fuel	Ensyn	Canada
Fluidized Bed	10,000	Pine wood residues	Heating fuel	Fortum	Finland
Fluidized Bed	3,000	Agricultural residues	Heating fuel	Shaanxi Yingjiliang	China
Fluidized Bed	300	Forest residues	Heating fuel	Valmet	Finland
Fluidized Bed	2,000	Unknown	Heating fuel and chemicals	Bioware	Brazil
Rotating Cone	5,000	Wood pellet residues	Heating fuel, transportation fuel	BTG	Netherlands
Auger	40	Various	Unknown	Alternative Energy Solutions Ltd.	New Zealand
Auger	21	Various	Unknown	Renewable Oil International LLC	United States

Table 3. State of the art of experimental results from pyrolysis of sugarcane bagasse and straw.

Reactor	Biomass	Feed	Temperature [°C]	Organic oil yield [%]	Water yield [%]	Biochar yield [%]	Gas yield [%]	Reference
Fixed Bed (50 K/min)	SB AC)	(1.3% 0.2 kg	500	56.8	9.3	24.9	9.0	(ASADULLAH et al., 2007)
Fixed Bed (10 K/min)	SB AC)	(1.7% 0.08 kg	500	43.2 (2.9% AC)	18.8 (2.5% AC)	19.4 (1.2% AC)	17.6 (2.2% AC)	(GARCÍA-PÉREZ; CHAALA; ROY, 2002)
Fixed bed (2.5 K/min)	SB AC)	(1.7% 20 kg	530	31.0	20.3	25.6	22.0	(GARCÍA-PÉREZ; CHAALA; ROY, 2002)
Fixed Bed (30 K/min)	SB AC)	(1.5% 0.04 kg	560	29.8	23.6	25.3	18.3	(VECINO MANTILLA et al., 2014)
Fixed Bed (200 K/min)	SB AC)	(5.2% 0.01 kg	500	~15	~40	~32	n/a	(TSAI; LEE; CHANG, 2006)
Fluidized Bed	SB AC)	(9.6% 0.85 kg/h	400	~52	~13	~9	~25	(CARRIER et al., 2013)
Fluidized Bed	SS AC)	(16.4% ~100 kg/h	470	22.3 <sup>a</sup>	n/a	45.8	n/a	(MESA-PÉREZ et al., 2013)

SB: Sugarcane Bagasse

SS: Sugarcane Straw

AC: Ash content

<sup>a</sup> The authors only reported yields of the organic-condensate with a water content < 3%, which is the value stated here. Additionally, an aqueous condensate of unknown quantity was produced.

Table 4. Categorization of gasifiers – Adapted (SÁNCHEZ, 2010).

Gasification categorization	Parameters
Producer gas heating value	Low (< 5 MJ/Nm <sup>3</sup> ) Medium (5-10 MJ/Nm <sup>3</sup> ) high (> 10 MJ/Nm <sup>3</sup> )
Gasification agent	Air Steam Oxygen Steam and oxygen
Gasifier Bed	Fixed bed Fluidized bed
Gasifier	Direct gasifier - part of biomass is burnt to provide heat for the gasification Indirect heating - heat is provided by indirect ways such as heat exchanger or circulating heat carrier
Pressure operation	Atmospheric Pressurized
Feedstock	Biomasses (wood, wastes, sludge, municipal solid waste, etc.) Fossil fuel derivatives Mixed (cogasification of different materials) Slurries

Table 5. State of the art of gasification reactor types and characteristics.

Reactor	Reference	Biomass	Conditions	Output data
Downdraft	(SHETH; BABU, 2009)	Furniture waste (1.00-3.65 kg/h)	Temperature: 900-1050 °C Air as gasification agent (m <sup>3</sup> /h): 1.85-2.78 Equivalent ratio: 0.16-0.35	Cold gas efficiency: 0.25-0.56 Char produced (kg/h): 0.24-0.32 High heating value (MJ/Nm <sup>3</sup> ): 4.50-6.34
	(KNOEF, 2005)	Wood residues	Temperature: 700 °C	Tar content in producer gas (g/Nm <sup>3</sup> ): 0.01-0.5 Power (MW <sub>th</sub> ): < 5 Lower Heating Value (MJ/Nm <sup>3</sup> ): 4.5-5.0
Updraft	(SEGGIANI et al., 2012)	Sewage sludge mixed with wood pellets (2.87-3.50 kg/h)	Temperature: 700-1150 °C Equivalent ratio: 0.15-0.25	Cold gas efficiency: 0.21-0.59 Lower heating value (MJ/Nm <sup>3</sup> ): 3.32-6.29
	(PLIS; WILK, 2011)	Wood and oats husks pellets (4.1-16.0 kg/h)	Temperature: 800 °C	Lower heating value (MJ/Nm <sup>3</sup> ): 3.84-5.47 Cold gas efficiency: 0.39-0.64 Hot gas efficiency: 0.41-0.68
Fluidized bed	(CAMPOY et al., 2009)	Wood pellet (10-21 kg/h)	Temperature: 755-840 °C Equivalent ratio: 0.24-0.38	Cold gas efficiency: < 0.68 Carbon conversion: 0.97 Lower Heating Value Lower heating value (MJ/m <sup>3</sup> <sub>dry gas</sub> ): < 9.28
Circulating fluidized bed	(VAN DER DRIFT; VAN DOORN; VERMEULEN, 2001)	Biomass residues (50-100 kg/h)	Temperature: 805-855 °C Equivalent ratio: 0.37	Cold gas efficiency: < 0.61 Carbon conversion: 0.92
	(LI et al., 2004)	Biomass sawdust (41 kg/h)	Temperature: 700-850 °C	Tar yield (g/m <sup>3</sup> ): 2.35 Lower Heating Value (MJ/Nm <sup>3</sup> ): 4.6 Cold gas efficiency: 0.60 Carbon conversion: 0.95
Entrained flow	(SENAPATI; BEHERA, 2012)	Coconut doir dust (40 kg/h)	Temperature: 976-1100 Equivalent ratio: < 7.86	Lower heating value (MJ/Nm <sup>3</sup> ): < 7.86

		0.21-0.30 Steam as gasification agent (kg/h): 12 Temperature: 1100-1300 Equivalent ratio: 0.43-0.50 Pressure (bar): ~ 2	Cold gas efficiency: 0.876 Tar content (g/Nm <sup>3</sup> ): < 23.6
(WEILAND et al., 2013)	Stem wood powder (40 kg/h)	Temperature: 1100-1300 °C Equivalent ratio: 0.43-0.50 Pressure (bar): ~ 2	Syngas H <sub>2</sub> /CO ratio: 0.54-0.57 Cold gas efficiency: ~ 0.70
(RAFFELT et al., 2006)	Slurry of cereal straw with 30% solids (350-500 kg/h)	Temperature: 1250-1350 Slurry density (kg/m <sup>3</sup> ): ~ 1300 Slurry viscosity (Pas): < 2 Equivalent ratio: 0.32 Pressure (bar): 26	Cold gas efficiency: 0.50-0.71 Power of produced gas (MW <sub>th</sub> ): 3-5 H <sub>2</sub> /CO ratio: 2.04
(TRIPPE et al., 2011)	Slurry from wheat straw (192 kg/h)	Temperature: 1200 °C Equivalent ratio: 0.38-0.40 Steam: 38 t/h	Cold gas efficiency: ~ 0.77 Power (MW <sub>th</sub> ): ~ 150 H <sub>2</sub> /CO ratio: 1.0-2.0

Table 6. Typical syngas specification for some applications.

	Unit	Internal Combustion Engine	Gas turbine	Methanol synthesis	Fuel cell	FT synthesis
Particle size	$\mu\text{m}$	$< 10^{(i)}$	$< 5^{(ii)}$ ; $0.1^{(iii)}$			
LHV	$\text{MJ}/\text{Nm}^3$		$> 4^{(iii)}$			
Particulate matter	$\text{mg}/\text{Nm}^3$	$< 50^{(i)}$	$< 30^{(ii)}$	$< 0.02^{(iv)}$		$0^{(vi)}$
		$< 50^{(iv)}$	$< 0.03^{(iv)}$			
Alkali metals	$\text{mg}/\text{Nm}^3$	$< 0.25^{(i)}$	$< 0.24^{(ii)}$			
		ppb (wt.%)	$< 50^{(iii)}$			$< 10^{(viii)}$
		ppm (v.%)	$< 0.024^{(iv)}$			$< 0.010^{(vi)}$ , $^{(vii)}$
Tar	$\text{mg}/\text{Nm}^3$	$< 100^{(i)}$ $< 100^{(iv)}$	$< 0.5^{(ii)}$ , *	$< 0.1^{(iv)}$		$0^{(viii)}$
Sulfur	ppm S (wt.%)		$< 1^{(iii)}$ ; $< 20^{(iv)}$	$< 1^{(iv)}$	$< 1^{(v)}$	
		ppb ( $\text{H}_2\text{S} + \text{COS} + \text{CS}_2 +$ organic S) (v.%)				$< 100^{(vi)}$
		ppm ( $\text{H}_2\text{S} + \text{COS} + \text{CS}_2$ ) (v.%)				$< 1^{(vii)}$
Chlorine	ppm HCl (wt.%)		$< 0.5^{(iii)}$		$< 0.1^{(v)}$	$< 0.01^{(viii)}$
			$< 1^{(iv)}$			
Nitrogen	ppm ( $\text{NH}_3 + \text{HCN}$ ) (v.%)		$< 50^{(iv)}$	$< 0.1^{(iv)}$		$< 0.1^{(vi)}$ ; $< 1^{(vii)}$
		ppm ( $\text{NH}_3 + \text{HCN} + \text{NO}_x$ ) (v.%)				
Fluor	ppm HF				$< 0.1^{(v)}$	

(i) (HASLER; NUSSBAUMER, 1999), (ii) (TAO et al., 2013), (iii) (ASADULLAH, 2014), (iv) (WOOLCOCK; BROWN, 2013), (v) (TURK et al., 2001), (vi) (KALTSCHMITT; NEULING, 2018) using Fe-based catalyst, (vii) (BOERRIGTER et al., 2004), (viii) (TIJMENSEN et al., 2002).

\* Vapor phase.

Table 7. Physical and mechanical separation technologies for particulate matter and tar removal.

Dry and wet technologies	Temperature (K)	Pressure (bar)	Particulate matter reduction (wt.%)	Tar reduction (wt.%)
Sand filter	283-293 <sup>(i)</sup>		70-99 <sup>(i)</sup>	50-97 <sup>(i)</sup>
Bag filter	403 9 <sup>(i)</sup>		75-95 <sup>(i)</sup>	< 25 <sup>(i)</sup>
Washing tower	323-333 <sup>(iv)</sup>	20-200 <sup>(v)</sup>	60-98 <sup>(iv)</sup>	10-25 <sup>(i)</sup>
Wet scrubber	< 373 <sup>(i)</sup>	25-250 <sup>(v)</sup>	95-99 <sup>(v)</sup>	< 60
Venturi	283-373 <sup>(viii)</sup>	30-200 <sup>(vii)</sup>	98.8 <sup>(vii)</sup>	50-90 <sup>(vi)</sup>
Atomizer	< 373 <sup>(i)</sup>		95-99 <sup>(i)</sup>	
Electrostatic precipitator			97-99 <sup>(viii)</sup>	
Wet electrostatic precipitator	313-323 <sup>(i)</sup>		> 99 <sup>(i)</sup> > 90 <sup>(viii)</sup>	< 60 <sup>(i)</sup>
Barrier filter	403 <sup>(i)</sup>		70-90 <sup>(i)</sup>	< 50 <sup>(i)</sup>
Rotational separator	403 <sup>(i)</sup>		85-90 <sup>(i)</sup>	30-70 <sup>(i)</sup>
Cyclone	373-1073 <sup>(viii)</sup>	< 10 <sup>(iii)</sup>	> 99 <sup>(i)</sup>	

(i) (HASLER; NUSSBAUMER, 1999), (iii) (REIJNEN; VAN BRAKEL, 1984), (iv) (HASLER; BUEHLER; NUSSBAUMER, 1998), (v) (KUMAR; JONES; HANNA, 2009), (vii) (TEIXEIRA; PRIMO; LORA, 2008), (viii) (ZHANG et al., 2012).

Table 8. Biojet fuel production via FT synthesis.

Parameters	(KLEIN et al., 2018)	(KLEIN et al., 2018)	(HANAOKA et al., 2015)*	(BALIBAN et al., 2013)**	(KUMABE et al., 2010)***
Biomass	Lignocellulosic Biomass (sugarcane bagasse and sugarcane straw)	Eucalyptus	Eucalyptus	Hardwood	Woody biomass
Biojet fuel production	0.053 kg of biojet fuel/kg of LCB in dry basis	0.059 kg of biojet fuel/kg of eucalyptus in dry basis	7.6 wt.% (efficiency of syngas to biojet fuel)	0.026 L of biojet fuel/kg of hardwood in dry basis	0.18 L of biojet fuel/kg of woody in dry basis

\* Biojet fuel range is C<sub>9</sub>-C<sub>15</sub>

\*\* Biojet fuel range is C<sub>11</sub>-C<sub>15</sub>

\*\*\* Biojet fuel range is C<sub>11</sub>-C<sub>14</sub>

Table 9. Commercial flights using biojet fuel blended with jet fuel - Adapted (ICAO, 2017).

Country	Date	Derived from	Route or producer	Blend of biojet fuel (%)	Company
Brazil	June 19 <sup>th</sup> , 2012	Used cooking oil	Produced by SkyNRG		KLM
	June 6 <sup>th</sup> , 2012	Corn oil and used cooking oil	Produced by Honeywell UOP	4	GOL
	June 19 <sup>th</sup> , 2012	Sugarcane	Produced by UOP.	50	The Azul+Verde project is a joint venture including airline constructor Embraer and engine manufacturer GE Aviation
	July 30 <sup>th</sup> , 2016	Sugarcane	Synthetic iso-paraffin from fermented hydroprocessed sugar (Farnesene)	10	Amyris and Tot
Canada	June 18 <sup>th</sup> , 2012				Air Canada
China	April 24 <sup>th</sup> , 2013		Produced by Sinopec		Sinopec
	March 16 <sup>th</sup> , 2015	Used cooking oil	Produced by Fulcrum BioEnergy	50	Dragonair
	March 21 <sup>st</sup> , 2015	Waste cooking oil	Produced by Sinopec	50	Hainan Airlines
Colombia	August 21 <sup>st</sup> , 2013	Camelina based		50	LAN
England	July 24 <sup>th</sup> , 2012	Recycled cooking oil	Produced by SkyNRG	50	Air Canada
Germany	September 16 <sup>th</sup> , 2014		Synthetic iso-paraffin from fermented hydroprocessed sugar (Farnesene)	10	Lufthansa Group
Malaysia	May 3 <sup>rd</sup> , 2017	Used cooking oil	Produced by SkyNRG in cooperation with the North American Fuel Corporation (NAFCO)		Singapore Airlines
Mexico	June 19 <sup>th</sup> , 2012	Cooking oil (88%), camelina oil (10%) and jatropha oil (2%)	Honeywell United Oil Products (UOP) and SkyEnergy	50	Aeromexico, ASA, and Boeing
Norway	November 12 <sup>th</sup> , 2014	Used cooking oil	Produced by SkyNRG	48	SkyNRG and Statoil
South Africa	July 15 <sup>th</sup> , 2016	Nicotine-free tobacco plants	Produced by AltAir		South African Airways in Project Solaris
Sweden	June 26 <sup>th</sup> , 2014		Produced by SkyNRG		SkyNRG and Statoil
United States	June 7 <sup>th</sup> , 2016	Corn	Alcohol to jet	20	Alaska Airlines

	November 14 <sup>th</sup> , 2016	Wood waste	Alcohol to jet	20	Alaska Airlines
Venezuela	May 16th, 2014	Used cooking oil	Produced by SkyNRG	20	KLM

---

Table 10. Main properties of fossil-fuel jet A, jet A-1 and biojet fuel blend with jet fuel (ASTM, 2011, 2017).

Property	Jet A and JetA-1		Biojet fuel (50 %) requirement for blending with jet fuel (50 wt.%)	
	Value	ASTM test	Value	ASTM test
<i>Composition</i>				
Maximum acidity total (mgKOH/g)	0.10	D3242	0.015	D3242
Maximum aromatics content	26.5 %vol.	D6379	20 %wt.	D2425
Maximum cycloparaffins			15 %wt.	D2425
Minimum carbon and hydrogen content			99.5 %wt.	D5291
Maximum sulfur	0.30 %wt.	D1266, D2622, D4294, or D5453	15 mg/kg	D5453, D2622
Maximum nitrogen			2 mg/kg	D4629
Maximum water			75 mg/kg	D6304
Maximum metals			0.1 mg/kg per metal	D7111
Maximum halogens			1 mg/kg	D7359
<i>Volatility</i>				
Minimum flash point (°C)	38	D56 or D3828	38	D56, D3828
Density at 15 °C (kg/m <sup>3</sup> )	775-840	D1298 or D4052	755-800	D1298 or D4052
<i>Fluidity</i>				
Maximum freezing point (°C)	-40 (Jet A); -47 (Jet A-1)	D5972, D7153, D7154, or D2386	-40	D5972, D7153, D7154, or D2386
Maximum viscosity at -20 °C (mm <sup>2</sup> /s)	8.0	D445		
<i>Combustion</i>				
Minimum net heat of combustion (MJ/kg)	42.8	D4529, D3338, or D4809		
One of the following shall be met:	(1) 25 or (2) 25 and 3.0	(1) D1322 or (2) D1322 and D1840		
(1) Minimum smoke point (mm) or (2) minimum smoke point (mm) and maximum naphthalene content (vol.%)				
<i>Contaminants</i>				
Maximum existing gum (mg/100 mL)	7	D381	4	D381

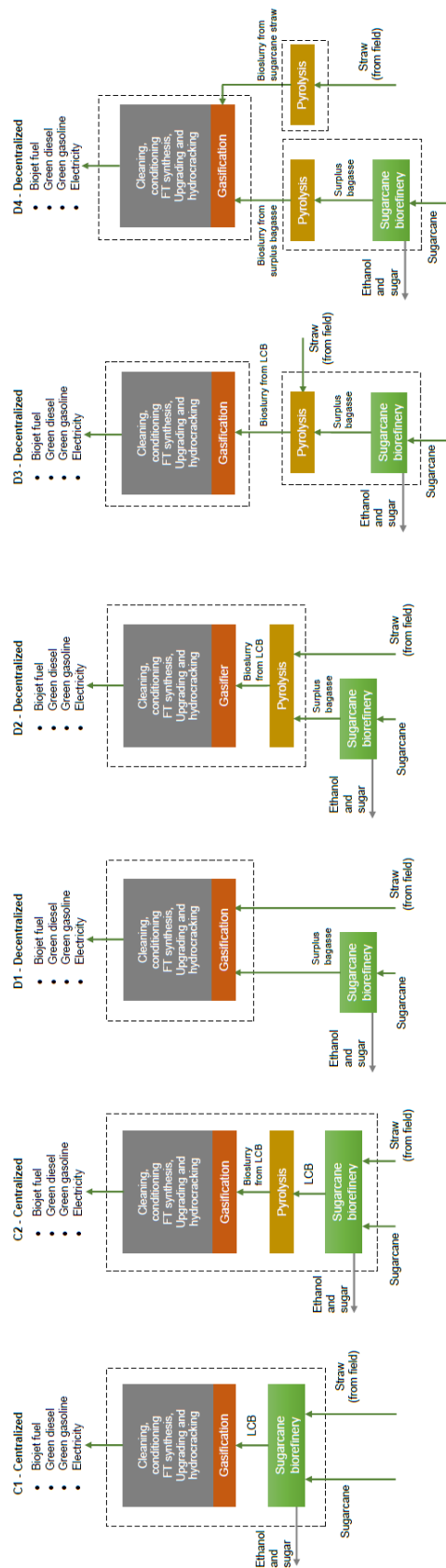


Figure 1. Possible scenarios with centralized and decentralized concepts of First-Generation sugarcane biorefinery integrated into the thermochemical process for biojet fuel production.

### 3 Chapter II

#### **Simulation and experiment of fast pyrolysis process of lignocellulosic biomass from First-Generation sugarcane biorefinery**

Renato Cruz Neves<sup>a,\*</sup>, Axel Funke<sup>b</sup>, Pablo Andrés Silva Ortiz<sup>c</sup>, Edgardo Olivares Gómez<sup>d</sup>, Nicolaus Dahmen<sup>b</sup>, Rubens Maciel Filho<sup>a,c</sup>

<sup>a</sup> Brazilian Bioethanol Science and Technology Laboratory (CTBE), Brazilian Center for Research in Energy and Materials (CNPEM), Zip Code 13083-970, Campinas, Brazil

<sup>b</sup> Institute for Catalysis Research and Technology (IKFT), Karlsruhe Institute of Technology (KIT), Hermann-von-Helmholtz-Platz 1, 76344 Eggenstein-Leopoldshafen, Germany

<sup>c</sup> School of Chemical Engineering, University of Campinas (UNICAMP), Campinas, São Paulo, Brazil.

<sup>d</sup> Mechanical Engineering Department, Federal University of Grande Dourados (UFGD), Dourados, Mato Grosso do Sul, Brazil

\* Corresponding author: Renato Cruz Neves.

Journal name: Fuel Processing Technology.

#### **ABSTRACT:**

The blend of sugarcane bagasse and straw, named as Lignocellulosic Biomass (LCB), is used to produce steam and electricity to the First-Generation (1G) sugarcane biorefinery. Surplus LCB from the optimized sugarcane biorefinery can be converted into bioslurry via fast pyrolysis. Bioslurry is a raw material used to produce energy, biofuels or biobased chemicals according to the bioliq<sup>®</sup> concept. In this work, fast pyrolysis of LCB from 1G sugarcane biorefinery was studied via experimental and two simulations models through kinetic and yield reactors. Considering the integration of LCB drying to the fast pyrolysis process, bioslurry mass fraction for the kinetic and yield model was 50% and 42%, respectively. Furthermore, energy efficiencies varied from 80% to 89%, while exergy efficiencies varied from 79% to 83%. The results of this work support future efforts of fast pyrolysis processes in integrated assessments.

**KEYWORDS:** fast pyrolysis; lignocellulosic biomass; sugarcane biorefinery; energy; exergy.

#### **Highlights:**

- *Experiment of fast pyrolysis process using sugarcane bagasse and straw*

- *Yield and kinetic simulation models to represent the fast pyrolysis process*
- *Evaluation of energy and exergy performances considering fast pyrolysis process*

## **1. Introduction**

Sugarcane (*Saccharum* spp.) is one of the most important crops produced in many regions of the world. Globally, Brazil can be considered the largest sugarcane producer in the world (CORTEZ et al., 2014), since the average productivity and total sugarcane production estimated at 2017/2018 harvest will be of 72.7 tons/ha and 635.6 million metric tons (CONAB, 2017), respectively. Therefore, sugarcane has been considered attractive to biofuel sector, once it has one of the highest production capacities of biogenic raw material, besides being used mainly to produce sugar and ethanol in the First-Generation (1G) sugarcane biorefineries (CORTEZ et al., 2014). The residual Lignocellulosic Biomass (LCB) from the sugarcane biorefinery, sugarcane bagasse and straw, besides being used for electricity generation, also has the potential to be the most suitable feedstock for Second-Generation (2G) liquid biofuels production (BONOMI, A., CAVALETT, O., DA CUNHA, M. P., & LIMA, 2016).

Recently, sugarcane biorefinery configuration for biofuel production has received attention due to the potential synergies from mass and energy integration (OLIVEIRA et al., 2017). 1G sugarcane biorefineries are categorized into three main configurations in Brazil considering ethanol and sugar the main products: sugar factories, autonomous distilleries and annexed distilleries (BONOMI, A., CAVALETT, O., DA CUNHA, M. P., & LIMA, 2016). In sugar factories is produced only sugar from sugarcane juice, which is a product obtained from the sugarcane milling process where separate sugarcane juice from sugarcane bagasse. In autonomous distilleries configuration, only ethanol is produced from sugarcane juice. Lastly, in the annexed distilleries configuration, both ethanol and sugar are produced from sugarcane juice. Sugarcane bagasse and straw can be considered as a fuel to supply heat and power for different configurations of biorefineries (MORAIS et al., 2016).

Depending on the optimization of the 1G sugarcane biorefinery configuration, surplus bagasse and straw can also be used for 2G biofuels (DIAS et al., 2012a). Accordingly, LCB can be used in the thermochemical process to produce 2G biofuels (KLEIN et al., 2018; MORAIS et al., 2016). Therefore, from an existing self-sufficient 1G sugarcane biorefinery in terms of heat and power demands, a self-sufficient fast pyrolysis plant can be installed consuming LCB from 1G sugarcane biorefinery to produce bioslurry, which is a blend of

biochar and bio-oil. The bioslurry produced from LCB fast pyrolysis process can be integrated into a centralized gasification facility where 2G biofuels can be produced according to the bioliq<sup>®</sup> concept (DAHMEN et al., 2017).

Therefore, currently, public and private institutions are seeking new technologies regarding the sugarcane chain to increase process efficiency and sustainability. One of the possible and fast actions to evaluate the potential of a new technology is the use of simulation models to represent unit processes and their combination in different process chains. With this purpose, the Brazilian Bioethanol Science and Technology Laboratory (CTBE) at the Brazilian Center for Research in Energy and Materials (CNPEM), has developed a simulation platform – called Virtual Sugarcane Biorefinery (VSB) – to assess process alternatives and configurations within the biorefinery designs (BONOMI, A., CAVALETT, O., DA CUNHA, M. P., & LIMA, 2016). One of the focuses of the VSB is to simulate the integration of a First-Generation (1G) ethanol and sugar plant to other processes such as thermochemical routes for biofuels and power production through different technologies, e.g. fast pyrolysis process. The main goal of this integration is to identify process configurations for sugarcane biorefineries in an integrated environment (BONOMI, A., CAVALETT, O., DA CUNHA, M. P., & LIMA, 2016; CHANDEL et al., 2014; DIAS et al., 2014; DUTTA et al., 2016; KLEIN et al., 2018).

One of the challenges involving process simulations is to define technical equipment and input parameters that will be used to represent the actual technology, besides to ensure mass balance (e.g. in kinetic models) and energy balance considering the overall integration processes. Considering thermochemical routes, LCB can be conducted to the fast pyrolysis process to be converted into bioslurry, which can be used as raw material for energy, biofuels and biobased chemicals (DAHMEN et al., 2017; FUNKE et al., 2016a, 2016b, 2018; NICOLEIT; DAHMEN; SAUER, 2016). So far, information about fast pyrolysis process from LCB to produce bioslurry considering experimental and simulation models are scarce due to lack of data in the literature such as: i) Non-conventional compounds in Aspen Plus<sup>®</sup> for LCB; ii) Lack of experimental and simulation data for fast pyrolysis process of LCB from 1G sugarcane biorefinery; iii) Unknown compounds for fast pyrolysis products from LCB (e.g. bio-oil can contain hundreds of components).

Furthermore, most of the literature considers a fast pyrolysis product mass balance using simplified hypothetical fast pyrolysis products (e.g. for bio-oil) and overall energy and exergy performances for integrated fast pyrolysis process are not evaluated. In fact, energy and exergy analysis are important tools for the optimization process. Generally, the exergy analysis

is based on the fundamental of thermodynamic looking for the major points of the process where the largest energy destruction occurs. Thus, exergy balance allows identifying the process irreversibilities aiming to improve the energy conversion process of the system.

Considering this context, the aim of this work is to carry out experimental and simulation models of fast pyrolysis process from LCB of 1G sugarcane biorefinery. In the experimental scope, the objective is to perform the fast pyrolysis process of LCB through the Python Process Development Unit (Python-PDU) in pilot scale. For the simulation scope, the main goal is to simulate the integration of LCB drying and fast pyrolysis process of LCB from 1G sugarcane biorefinery through Aspen Plus<sup>®</sup> using yield and kinetic simulation models to produce bioslurry. From the results of simulation models, energy and exergy performances are also presented.

## **2. Materials and Methods**

### **2.1 Fast pyrolysis process of LCB from 1G sugarcane biorefinery**

The scenario for fast pyrolysis process considering experiment and simulation models was based on the 1G sugarcane biorefinery. The chosen 1G sugarcane biorefinery was the optimized annexed plant (1G-Anx-Op) (BONOMI, A., CAVALETT, O., DA CUNHA, M. P., & LIMA, 2016), which consists of using 50 wt.% of the sugarcane juice to produce sugar and other 50 wt.%, together with molasses, to produce ethanol. The main characteristics of the 1G-Anx-Op biorefinery are:

- Season: 200 days
- Processing capacity:  $4.0 \times 10^6$  tons of cane (TC)
- Area of sugarcane crop:  $52.6 \times 10^3$  ha
- Anhydrous ethanol production: 35193 kg/h (42 kg/TC)
- Sugar production: 42820 kg/h (51 kg/TC)
- Surplus bagasse: 128143 kg/h (153 kg/TC) with 50 wt.% moisture
- Sugarcane straw: 39114 kg/h (47 kg/TC) with 30 wt.% moisture

The flowsheet of 1G-Anx-Op combining LCB fast pyrolysis process to produce bioslurry is schematically shown in Figure 1. The 1G-Anx-Op supplies the total heat demand for its operation via steam and electricity produced in the Combined Heat and Power plant, i.e.

1G-Anx-Op is a self-sufficient biorefinery. Surplus LCB is conducted to the fast pyrolysis plant. LCB is dried before entering the fast pyrolysis reactor due to the high moisture content: 50 wt.% moisture for sugarcane bagasse (from milling process) and 30 wt.% moisture for straw (collected from the field via bale). The water removed from the dryer goes to the water treatment plant. Non-Condensable Gas (NCG) and a fraction of biochar from fast pyrolysis process are burned in a combustor to provide heat to the dryer and to the fast pyrolysis reactions. The mixture of surplus biochar together with the organic-rich and aqueous condensates forms the bioslurry.

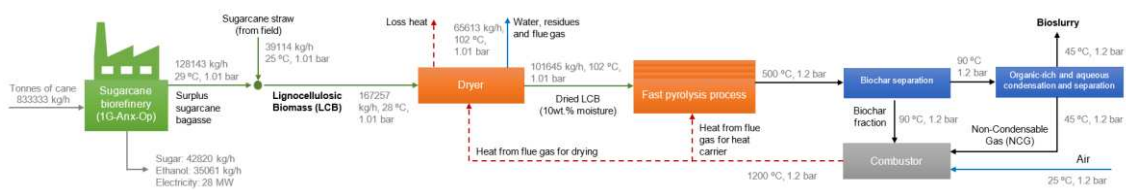


Figure 1. Flowsheet of the fast pyrolysis process using LCB from 1G sugarcane biorefinery for bioslurry production.

## 2.2. Fast pyrolysis experiments

Python-PDU is the fast pyrolysis process unit located at the Technikum of IKFT with an input capacity of 10 kg/h. An auger-type reactor, named as Twin-Screw mixing reactor, with two co-rotating screw was used as fast pyrolysis reactor. The flowsheet of the Python-PDU is shown in Figure 2. Further information about Python-PDU may be seen in work and video (FUNKE et al., 2016a, 2017a).

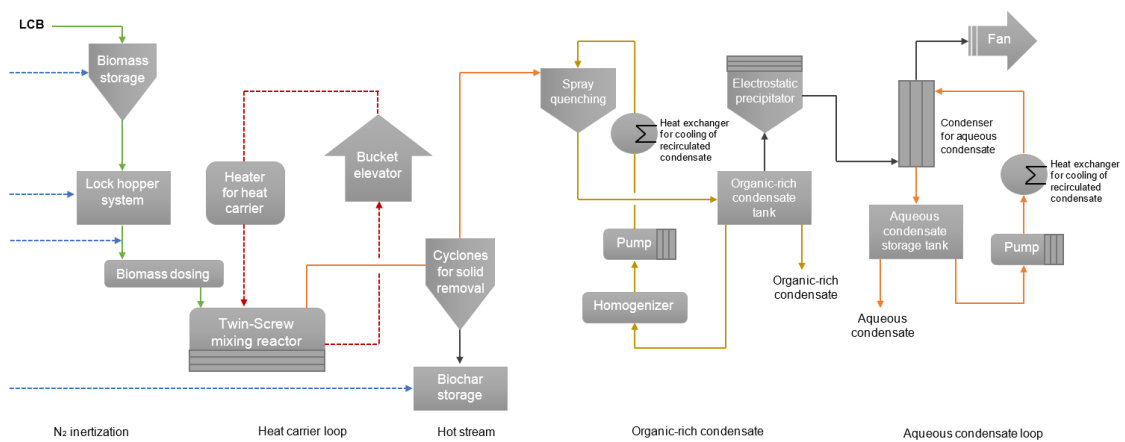


Figure 2. Python-PDU flowsheet.

The process parameters for the fast pyrolysis runs are shown in Table 1. NCG was analyzed in triplicates through Gas Chromatography (GC) Emerson Model 700 using helium as carrier gas. Prior to analysis, GC was calibrated with known composition ( $H_2$ ,  $CO$ ,  $CH_4$ ,  $CO_2$ ,  $C_2H_4$ ,  $C_2H_6$ ,  $C_3H_8$ ,  $C_4H_{10}$ , and compounds with carbons more than 5 named as  $C_{5+}$ ). Organic-rich and aqueous condensates were analyzed by Thünen Institute (Institute of wood Research, Hamburg, Germany), using Mass spectrometry (MS) as identification method and flame ionization detector (FID) as quantification method as described by Charon et al. (CHARON et al., 2015). Biochar composition was analyzed in triplicates according to the methodology presented in Supplementary Material.

Table 1. Parameters for the fast pyrolysis process.

Parameters	Value	Unit
LCB (Sugarcane straw/sugarcane bagasse) ratio	30	wt.% (10 wt.% of moisture content)
LCB feeding rate	7	kg/h
Temperature mixing adjusted by heat carrier	500	°C
Running time of pyrolysis process	3	h
Mass flow of spherical steel particles (heat carrier)	$10^3$	kg/h
Organic condensate temperature	< 90	°C
Aqueous condensate temperature	< 60	°C

### 2.3 Simulation models

The process simulation has been carried out through the commercial simulator Aspen Plus<sup>®</sup> V9.0. The simulation was carried out using the Redlich-Kwong-Soave equation of state with Boston-Mathias (RKS-BM) modification. This equation was selected because it considers the vapor-liquid multi-components stream (SELVATICO; LANZINI; SANTARELLI, 2016) giving satisfactory results in modeling hydrocarbons mixtures and light chemical species (ASPEN TECHNOLOGY, 2007).

To facilitate the modeling environment and give more representativeness using the process simulation software, some assumptions were also made (DAMARTZIS; MICHAÏLOS; ZABANIOTOU, 2012; RINGER; PUTSCHE; SCAHILL, 2006): Steady state operation and isothermal; Zero-dimensional model; Atmospheric pressure of 1.013 bar and ambient temperature of 25 °C; Solid, gas and liquid phases are uniformly distributed within each equipment.

Two fast pyrolysis simulation models for bioslurry production from LCB of the 1G-Anx-Op were performed. The first model was the yield model. In this model, experimental data from Python-PDU was inserted into the simulation process for representing the mass fraction of NCG, biochar, and organic-rich and aqueous condensates. The second model was the kinetic model based on Plug Flow reactor.

LCB composition inserted into the simulator program has been exactly obtained from 1G-Anx-Op from VSB (BONOMI, A., CAVALETT, O., DA CUNHA, M. P., & LIMA, 2016). The complete composition is presented in Supplementary Material. Surplus bagasse from 1G-Anx-Op contains 50 wt.% moisture while straw recovered from the field contains 30 wt.% moisture. A blend of these biomasses named as LCB needs to be dried before going to the fast pyrolysis process. Thus, LCB is conducted to the drying process to adequate moisture content. The drying of LCB to 10 wt.% moisture for yield and kinetic models was achieved by the heat from flue gas.

Besides heat to dry the LCB, it is also needed heat demand for the fast pyrolysis reactions via heat carrier. A combustor reactor (RSTOIC) supplies the overall heat required with temperature controlled by the combustion of NCG and a fraction of biochar. The amount of air (0.79 mole fraction of  $N_2$  and 0.21 mole fraction of  $O_2$ ) required by combustion is fixed by a DESIGN-SPEC in which controls mass flow of the stream considering 30 wt.% of excess in the combustion reactions. The overall heat integration demand is controlled by the combustor giving the outlet stream a temperature equal to 1200 °C.

In Aspen Plus<sup>®</sup> simulation area (flowsheet), surplus bagasse (from milling process of the 1G-Anx-Op) and straw (collected from the field in bales) are combined in a MIXER. This LCB blend goes to the drying process. This process is composed by a HEATX to exchange heat of flue gas from combustor and a FLASH2 model to separate the water removed from the LCB stream. The dried LCB (10 wt.% of moisture content) goes to the fast pyrolysis process whereas the water and residues are disposed off in a waste water treatment plant (not simulated in this work).

Subsequently drying process, LCB is conducted to the fast pyrolysis reactor simulated by kinetic or yield models. Later in the pyrolysis reactor, biochar is separated in a cyclone simulated as SEP model. The volatile compounds are cooled in a HEATX model and then NCG and bio-oil (composed by organic-rich and aqueous condensates) are separated in a SEP model. A fraction of biochar together with all amount of NCG are burned in the combustor.

The surplus biochar together with organic-rich and aqueous condensates are mixed in a MIXER model to form bioslurry.

The same configuration of integration processes between LCB drying and fast pyrolysis was designed for kinetic and yield models, i.e. all parameters presented in Figure 1. were considered identical for both simulation models in order to establish the comparison between them.

### 2.3.1 Yield model

The Yield model was performed using the mass balance according to experimental data. Basically, the mass flow of LCB was equal to the mass flow of fast pyrolysis products, i.e. the sum of mass flow of NCG, biochar and aqueous condensate and organic-rich condensates. The deficit value in the experimental study, which is a value set to ensure 100% in mass balance, was not considered in the yield model. Therefore, fast pyrolysis products in the yield model were adjusted to consider the sum of mass fraction of NCG, biochar and aqueous and organic-rich condensates equal to 100%.

### 2.3.2 Kinetic model

The kinetic model was based on the reactions of three main building blocks of LCB, i.e. cellulose, hemicellulose and lignin decompositions to represent the fast pyrolysis reactions and products in RPlug reactor. It was assumed that these reactions were based on the set of kinetic reactions for decomposition reaction, primary pyrolysis reactions, and secondary pyrolysis reactions proposed by Peters et al. (PETERS et al., 2017) in order to give satisfactory results to be comparable with experimental data of LCB proposed by this work. Cellulose (represented as CELLULOS), Hemicellulose (represented as ACETATE and XYLAN), and Lignin (represented as LIGNIN) were retrieved from VSB database (MORAIS et al., 2016).

Kinetic reactions were inserted in Aspen Plus<sup>®</sup> using the RPlug reactor. the parameters set for the Reactions folder are Liquid and Solid as reacting phase, and Reac (vol) as rate basis. RPlug reactor operated with pressure equal to 1.2 bar, 500 °C, volume equal to 44 m<sup>3</sup>, and vapor-Liquid as process stream. The kinetic reactions are based on powerlaw kinetic according equation 1.

$$k_f = k_o \exp\left(\frac{-E}{RT}\right) \quad (1)$$

where  $k_f$  is the reaction-rate constant,  $k_o$  is the pre-exponential factor,  $T$  is the temperature (K),  $E$  is the activation energy and  $R$  is the universal gas constant. Component ID and the 17 simplified kinetic reactions used for the simulation are shown in Table 2.

Table 2. Kinetic model.

Reaction number	Reaction (Based on Component ID)	$k_o$ (1/s)	$E$ (kJ/mole)	Assumption as proposed by Peters et al. (PETERS et al., 2017)	Reference adapted
1	<i>CELLULOS</i> → <i>CELLA</i>	$8 \times 10^{13}$	192.5	Primary pyrolysis reaction	(RANZI et al., 2008; SHEMAFE; GU; RANGANATHAN, 2015)
2	<i>CELLULOS</i> → $5H_2O + 6C$	$8 \times 10^7$	125.5	Primary pyrolysis reaction	(RANZI et al., 2008; SHEMAFE; GU; RANGANATHAN, 2015)
3	<i>CELLA</i> → <i>LEVOGLUC</i>	2000	41.8	Secondary pyrolysis reaction	(RANZI et al., 2008; SHEMAFE; GU; RANGANATHAN, 2015)
4	<i>CELLA</i> → <i>LEVOGLUC</i> + 0.95 <i>HAA</i> + 0.25 <i>GLYOXAL</i> + 0.2 <i>ACETALDE</i> + 0.27 <i>HMFU</i> + 0.2 <i>ACETONE</i> + 0.21 <i>CO</i> + 0.31 <i>CO</i> + 0.9 <i>H</i> <sub>2</sub> <i>O</i> + 0.15 <i>CH</i> <sub>4</sub> + 0.7 <i>C</i>	$1 \times 10^9$	133.9	Secondary pyrolysis reaction	(RANZI et al., 2008; SHEMAFE; GU; RANGANATHAN, 2015)
5	<i>XYLAN</i> → 0.4 <i>HCELL1</i> + 0.6 <i>HCELL2</i>	$1 \times 10^{10}$	129.7	Primary pyrolysis reaction	(RANZI et al., 2008; SHEMAFE; GU; RANGANATHAN,

6	<i>HCELL1</i> → <i>XYLANPYR</i>	1500	16	Secondary pyrolysis reaction	2015) (RANZI et al., 2008; SHEMAFE; GU; RANGANATHAN, 2015)
7	<i>HCELL1</i> → <i>2.5H2</i> + <i>0.125H2O + CO</i> + <i>CO2</i> + <i>0.5FORMALDE</i> + <i>0.125ETHANOL</i> + <i>C</i>	$3 \times 10^9$	116	Secondary pyrolysis reaction	(RANZI et al., 2008; SHEMAFE; GU; RANGANATHAN, 2015)
8	<i>HCELL2</i> → <i>CO2 + 0.5CH4</i> + <i>0.25C2H4 + H2</i> + <i>0.7FORMALDE</i> + <i>0.5METHANOL</i> + <i>0.125ETHANOL</i> + <i>0.125H2O + C</i>	$1 \times 10^{10}$	138.1	Secondary pyrolysis reaction	(RANZI et al., 2008; SHEMAFE; GU; RANGANATHAN, 2015)
9	<i>ACETATE</i> → <i>0.1814HCELL1</i> + <i>0.2715HCELL2</i>	$1 \times 10^{10}$	129.7	Primary pyrolysis reaction	(RANZI et al., 2008; SHEMAFE; GU; RANGANATHAN, 2015)
10	<i>LIGNIN</i> → <i>LGNSOL</i>	$9.6 \times 10^8$	107.6	Primary pyrolysis reaction	(ARDILA, 2015; MILLER; BELLAN, 1997)
11	<i>LGNSOL</i> → <i>0.5C8H8O</i> + <i>1.6C3H4O2</i> + <i>0.2PHENOL</i>	$1.5 \times 10^9$	143.8	Secondary pyrolysis reaction	(ARDILA, 2015; MILLER; BELLAN, 1997)
12	<i>LGNSOL</i> → <i>0.05H2</i> + <i>1.84H2O</i> + <i>0.38CO2</i> + <i>0.0665CH4</i> + <i>0.1CO</i> + <i>0.65ACETALDE</i> + <i>0.55METHANOL</i>	$3.5 \times 10^{14}$	194.8	Secondary pyrolysis reaction	(ARDILA, 2015; FERDOUS et al., 2002)

13	<i>C8H8O</i> → <i>CO</i> + 0.25 <i>C2H4</i> + 0.5 <i>BENZENE</i> + 0.5 <i>TOLUENE</i>	1x10 <sup>4.98</sup>	93.3	Secondary pyrolysis reaction	(ARDILA, 2015; BOROSON et al., 1989)
14	<i>C3H4O2</i> → <i>CO2</i> + <i>C2H4</i>	1x10 <sup>4.98</sup>	93.3	Secondary pyrolysis reaction	(ARDILA, 2015; MILLER; BELLAN, 1997)
15	<i>PHENOL</i> → 1.125 <i>CO2</i> + 0.25 <i>C2H4</i> + 0.875 <i>C</i> + 0.5 <i>C5H6</i> + 0.75 <i>CO</i> + 0.5 <i>C2H2</i> + 0.25 <i>CH4</i>	1x10 <sup>4.98</sup>	93.3	Secondary pyrolysis reaction	(ARDILA, 2015; MILLER; BELLAN, 1997)
16	<i>ACETALDE</i> → 0.5 <i>H2</i> + <i>CO</i> + 0.5 <i>CH4</i> + 0.25 <i>C2H4</i>	1x10 <sup>4.98</sup>	93.3	Secondary pyrolysis reaction	(ARDILA, 2015; MILLER; BELLAN, 1997)
17	<i>METHANOL</i> → 0.2 <i>CO</i> + 0.8 <i>H2</i> + 0.2 <i>DIETER</i> + 0.2 <i>H2O</i> + 0.2 <i>CH4</i> + 0.2 <i>CO2</i>	1x10 <sup>4.98</sup>	93.3	Secondary pyrolysis reaction	(ARDILA, 2015; MILLER; BELLAN, 1997)

While some components were retrieved from VSB database and others were considered conventional compounds from Aspen Plus<sup>®</sup> databank, there are still compounds without composition such as CELLA, HCELL1, HCELL2, and LGNSOL. In this case, CELLA was adopted as levoglucosan (C<sub>6</sub>H<sub>10</sub>O<sub>5</sub>), which is a glucosidic monomer referring to the initial formation of active cellulose (RANZI et al., 2008). HCELL1 and HCELL2 come from hemicellulose (represented as XYLAN) decomposition, where both were simulated as glutaric acid (xylose polymer) as proposed by Ranzi et al. (RANZI et al., 2008). Finally, LGNSOL was considered as active lignin compound (ARDILA, 2015; FERDOUS et al., 2002; MILLER; BELLAN, 1997). Its composition was retrieved equally to VSB database (BONOMI et al., 2016b).

## 2.4 Energy and exergy performance

Energy and exergy performances were conducted based on the volume fixed by the integration between LCB drying and fast pyrolysis process considering yield and kinetic models. Energy and exergy performances consist of using the First and Second laws of Thermodynamics together for furthering the goal of more effective energy resource use, for it allows the location, cause, and true magnitude of waste and loss to be determined. The exergy analysis was carried out to develop the procedure based on the methodology proposed by Ortiz et al. (ORTIZ; JÚNIOR, 2014). In this sense, a MS-Excel<sup>®</sup> tool was developed to perform the exergy analysis based on both simulation models.

The thermodynamic properties of the streams and substances present in the processes are evaluated at ambient temperature (25 °C) and pressure (1.013 bar). The exergy analysis throughout this work was conducted in Aspen Plus<sup>®</sup>, using the data from the different matter streams: mass flow rate, temperature, pressure and composition. The enthalpy and entropy of the streams with the same composition as well were obtained.

Note that the total specific exergy is calculated as in Szargut et al. (SZARGUT; MORRIS; STEWARD, 1988), as the sum of physical and chemical components. Furthermore, the standard chemical exergy calculation for each component was estimated using Szargut et al. (SZARGUT; MORRIS; STEWARD, 1988), as indicated in Ortiz et al. (ORTIZ; JR., 2016; ORTIZ; JÚNIOR, 2014) for LCB. However, data not available are calculated according to the technical fuels procedure based on Lower Heating Values (LHV) and atomic ratios (SZARGUT; MORRIS; STEWARD, 1988). Supplementary Material presents the standard chemical exergy of the compounds considered for the exergy analysis.

Finally, the quality of the energy conversion processes is quantified by the energy efficiency given by Equation 2 and the exergy efficiency by Equation 3. LHV correlation for sugarcane bagasse was retrieved from (HUGOT, 1986) and likewise for straw as presented in Equation 4.

$$\eta_E = \frac{\sum(LHV \cdot \dot{m})_{outputs}}{\sum(LHV \cdot \dot{m})_{inputs}} \quad (2)$$

$$\eta_B = \frac{\sum B_{outputs}}{\sum B_{inputs}} \quad (3)$$

$$LHV = 17790 - 50.23 * sucrose * 100 - 203 * MC * 100 \quad (4)$$

where *LHV* is the Low Heating Value (kJ/kg), *sucrose* is the sucrose mass fraction in biomass and *MC* is moisture mass fraction in biomass.

### 3. Results and discussion

#### 3.1 LCB characterization

Sugarcane bagasse and straw were collected in 2016/2017 harvest season at Sales Olivera, São Paulo State, Brazil, at Agrícola AgroQuatro-s, Fazenda Aliada. Sugarcane, variety RB966928 and 5th harvest, was collected in June 28th, 2016, and sugarcane straw was collected from the field in July 8th, 2016. Sugarcane bagasse was collected in July 13th, 2016, from the pile at Usina Alta Mogiana S/A – Açúcar e Álcool. The biomass transportation to IKFT-KIT was performed in bags.

After receiving the sugarcane bagasse and straw in IKFT-KIT, both biomasses were dried to 10 wt.% in open area. Then sugarcane straw was chopped to fit for milling process afterward using the chopper Viking GE260. Both sugarcane bagasse and straw were reduced to a particle size diameter with sieve equal to 2 mm using cross-beater mill Retsch SK100. These two materials were mixed manually with a mass ratio between sugarcane straw and sugarcane bagasse of 30% to suit the LCB (with 10 wt.% of moisture) composition from 1G-Anx-Op.

The sugarcane bagasse and straw characterization were carried out according to the standardize methodologies shown in Supplementary Material. Table 3 presents the bulk density, high heating value and ultimate analysis for the biomasses.

Table 3. Sugarcane bagasse, sugarcane straw and LCB blend characterizations.

Characterization	Sugarcane bagasse	Sugarcane straw of moisture content)	LCB blend	Unit
Bulk density <sup>1</sup>	104 <sup>2</sup>	123 <sup>3</sup>	110 <sup>4</sup>	kg/m <sup>3</sup>
Higher Heating Value	19.09	18.95	19.05	MJ/kg in dry basis
Ultimate analysis				
Carbon	48.13	47.31	47.88	wt.%
Hydrogen	5.88	6.01	5.91	dry basis
Oxygen <sup>5</sup>	42.86	41.61	42.48	
Nitrogen	0.36	0.55	0.42	
Ash	2.77	4.75	3.36	

<sup>1</sup> Biomass particle size < 2 mm.

<sup>2</sup> 5.5 wt.% of moisture content.

<sup>3</sup> 6.9 wt.% of moisture content.

<sup>4</sup> 5.9 wt.% of moisture content calculated.

<sup>5</sup> Calculated by difference.

### 3.2 Fast pyrolysis experiment

The fast pyrolysis experiment with LCB from 1G-Anx-op was carried in duplicates. Products of LCB fast pyrolysis process comprise NCG, biochar (solid fraction plus solid fraction found in bio-oil), bio-oil (organic-rich and aqueous condensates) and deficit, which is the calculated value to ensure mass balance equal to 100%. Mass balances of these products are presented in wet and dry basis as shown in Table 4. Dry basis was calculated as proposed by Funke et al. (FUNKE et al., 2016b).

Table 4. Mass balance of LCB fast pyrolysis products.

LCB	NCG (wt.%)	Biochar (wt.%)		Bio-oil (wt.%)		Deficit (wt.%)
		Solids	Solids in bio-oil	Organic-rich condensate	Aqueous condensate	
As received basis*	21.1	14.9	2.4	56.5	6.9	0.6
Dry basis	21.2	15.9	2.6	49.0	N/A	13.9

\*6.7 wt.% of moisture content.

Organic-rich condensate from LCB fast pyrolysis using dry basis calculation was equal to 49% whereas Funke et al. (FUNKE et al., 2016b) reported 50% for scrap wood, 46% for mischanthus, and 35% for wheat straw, i.e. LCB fast pyrolysis produced values comparable with scrap wood for organic-rich condensate. Thus, mass balance for fast pyrolysis process from Python-PDU using LCB and the comparison with other biomasses reported by Funke et al. (FUNKE et al., 2016b) using the same fast pyrolysis reactor showed good agreement.

NCG and biochar compositions are shown in Supplementary Material. Biochar was considered the solid fraction collected from cyclones and the solid fraction recovered with the bio-oil. Bio-oil is constituted of organic-rich and aqueous condensates and its compounds are simplified in Figure 3. The complete composition of organic-rich and aqueous condensates is given in Supplementary Material.

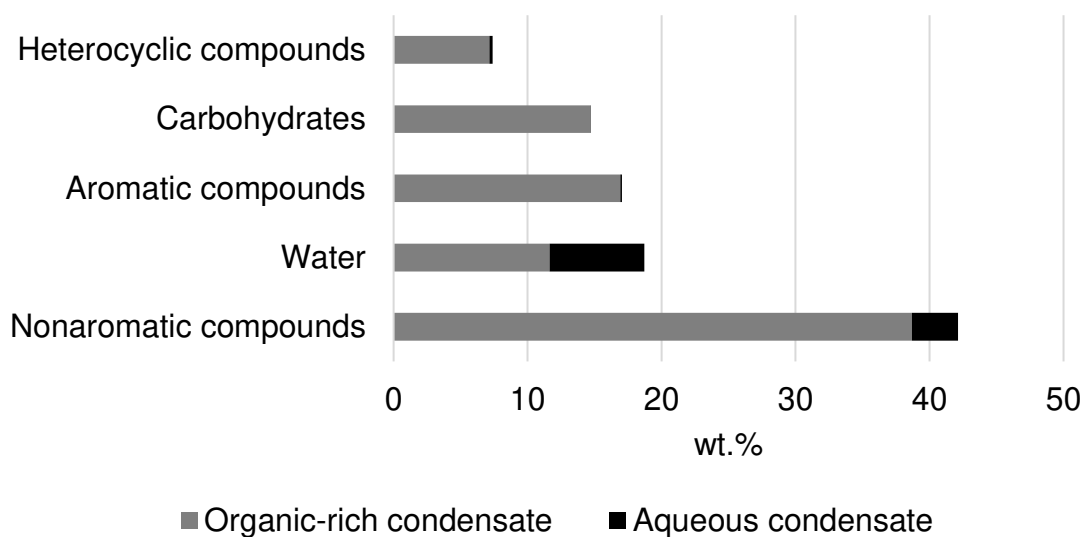


Figure 3. Simplified bio-oil compounds (wt.% as received basis) separated in organic-rich and aqueous condensate fractions.

### 3.2 Simulation models

#### 3.3.1 Yield model

Mass fraction of fast pyrolysis products of yield model was set according to the experimental data of fast pyrolysis process at Python-PDU and then inserted into simulation process. In this case, NCG was 21680 kg/h, biochar was 15243 kg/h, aqueous condensate was 11216 kg/h and organic-rich condensate was 53502 kg/h. Bio-oil fraction in fast pyrolysis products is 64%. Data from NCG, biochar and aqueous and organic-rich condensates can be found in Supplementary Material.

The heat demand for the fast pyrolysis reactions via heat carrier was limited to heat up the LCB temperature from 28 °C to 500 °C, i.e. the heat of reaction was assumed to be negligible. It is recognized that fast pyrolysis characterized by high liquid yield is endothermic and that this endothermicity is reduced the more biochar is being formed (MOK; ANTAL, 1983). High ash content in biomass (like wheat straw) leads to more biochar formation, which shifts the heat of reaction to slightly exothermic (HENRICH et al., 2016). In the case of this work, ash content in LCB (3.36 wt.%) is lower when compared to wheat straw (6.0 wt.%) (HENRICH et al., 2016). Thus, the heat of fast pyrolysis reactions was assumed negligible, i.e. round about zero, specially compared to the heat required for heating up the temperature of LCB. With this assumption, heat from the combustor for heat carrier was 30158 kW and heat to dry the LCB was equal to 50075 kW. To supply this demand, a biochar fraction, together

with NCG, to the combustion was equal to 60%, i.e. 40% of the biochar is mixed with bio-oil to form bioslurry. Bioslurry components from yield model are presented in Figure 4.

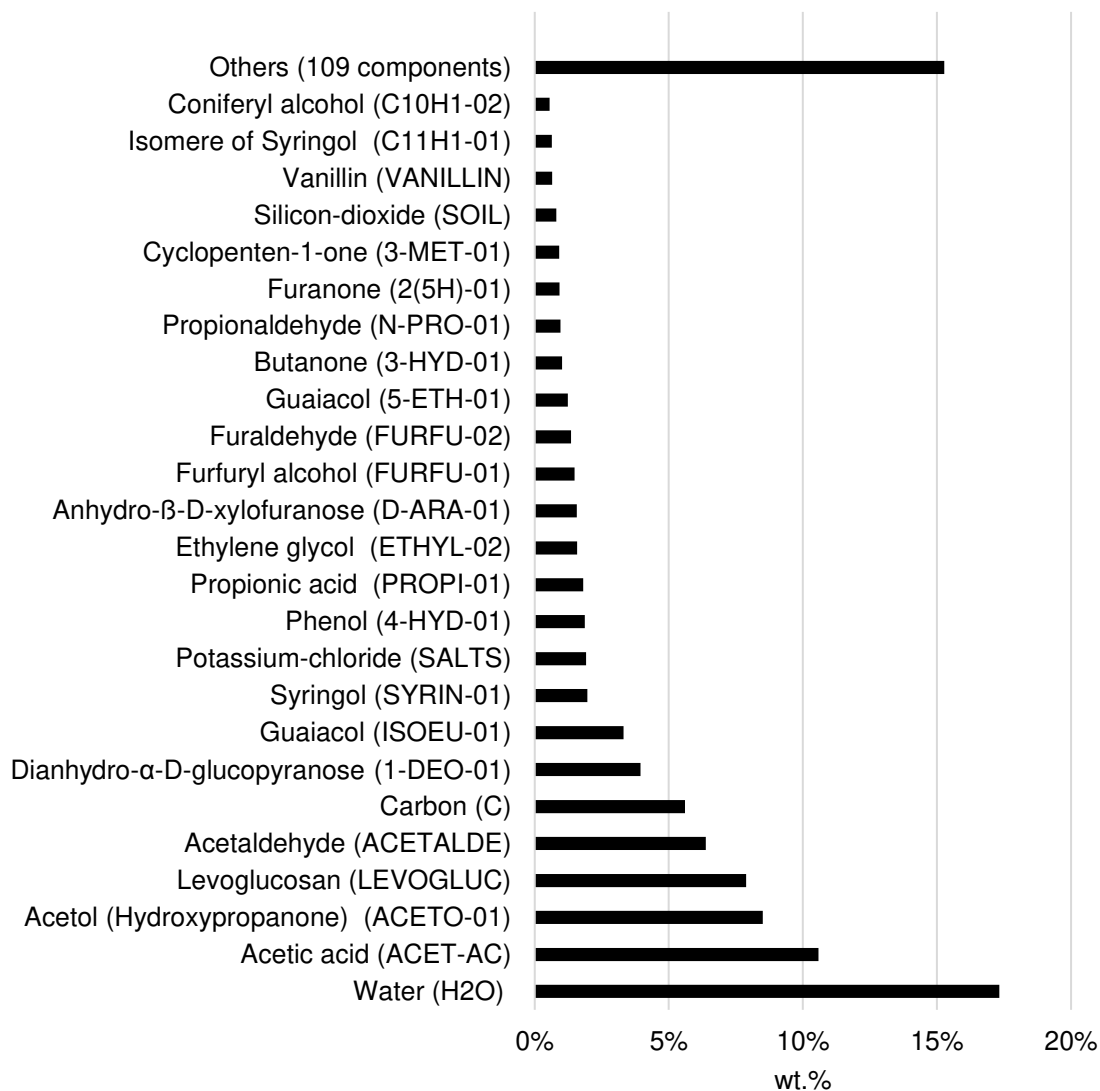


Figure 4. Simplified component (ID in Aspen Plus<sup>®</sup>) bioslurry for yield model at 500 °C.

### 3.3.2 Kinetic model

The complete composition of NCG, biochar, and aqueous and organic-rich condensates considering kinetic model with fast pyrolysis reactor temperature equal to 500 °C are given in Supplementary Material. In this case, NCG was 1191 kg/h, biochar was 41846 kg/h, aqueous condensate was 12311 kg/h and organic-rich condensate was 46313 kg/h. Aqueous condensate was considered only water in the simulation process. Thus, bio-oil mass flow is 58624 kg/h and its fraction in fast pyrolysis products is 57 wt.%. Heat from the

combustor for heat carrier was 25445 kW and heat to dry the LCB was equal to 50219 kW. To supply this demand, a biochar fraction, together with NCG, to the combustion was equal to 37%, i.e. 63% of the biochar is mixed with bio-oil for form bioslurry.

Using the fast pyrolysis reactor volume equal to 44 m<sup>3</sup> and the kinetic model with the reactions presented Supplementary Material, residence time was equal to 2.4 s. This residence time for fast pyrolysis process is within the range of 0.5-10 s (DEMIRBAS; ARIN, 2002; KAN; STREZOV; EVANS, 2016).

Figure 5 presents bioslurry components from 3 different temperatures sets in fast pyrolysis reactor. LGNSOL, a fraction of LIGNIN from LCB, in bioslurry was approximately 17% for fast pyrolysis reactions at 450 °C when compared with other fast pyrolysis temperatures (approximately 5%). This is due to the need of high energy demand for lignin decomposition (194.8 kJ/mole according to kinetic reaction); therefore, high values of lignin decomposition were observed with temperatures equal to 485 and 500 °C. The same behavior may be seen for 4-hydroxystyrene (C<sub>8</sub>H<sub>8</sub>O). Apart from these two components, the presented bioslurry composition showed similar agreement between the three different temperatures, where approximately 50% of bioslurry components are comprised by CELLA (represented by Levoglucosan), HCELL2 (represented by Glutaric-acid) and H<sub>2</sub>O (Water). Bioslurry mass flow and heat for the kinetic reactions were approximately equal for the 3 different temperatures evaluated.

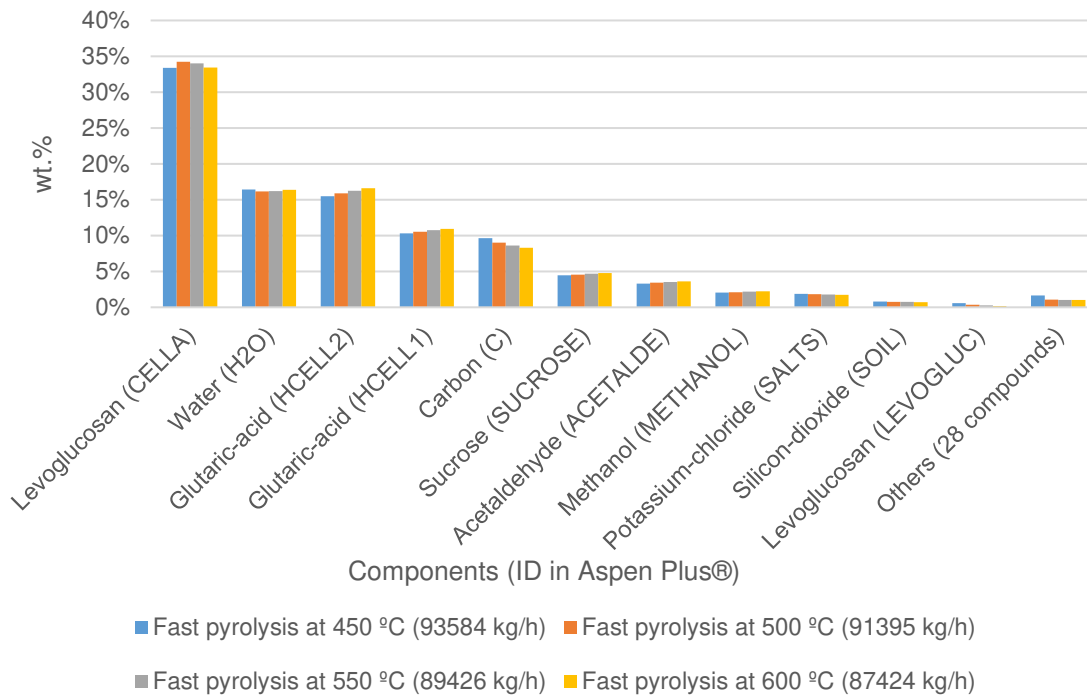


Figure 5. Bioslurry components for kinetic model considering different fast pyrolysis reactor temperatures.

### 3.4 Energy and exergy analysis

Energy and exergy values for the yield and kinetic models (at 500 °C) simulated in this work are reported in Table 5. The input for the fast pyrolysis process was the LCB. The outputs considered were heat and bioslurry.

Total mass flow of LCB equal to 167257 kg/h from 1G sugarcane biorefinery was used as input. In addition, the Low Heating Value for LCB was calculated using the previous correlation (equation 4) to compute energy efficiency. In relation to the outputs, heat and bioslurry were obtained through the internal correlations of the Aspen Plus<sup>®</sup> simulator.

Table 5. Energy and exergy efficiencies.

	Component	Yield	Kinetic	Unit
Energy Inputs	LCB Lower Heating Value	8467	8467	kJ/kg
	LCB mass flow	46.46	46.46	kg/s
Outputs	Bioslurry	13652	13603	kJ/kg
	Bioslurry mass flow	19.59	23.62	kg/s
	Heat	48551	27330	kW

	Energy efficiency (%)		80.36	88.64	
Exergy	Inputs	Sugarcane straw	134616	134616	kW
		Sugarcane bagasse	318972	318972	kW
		Air	188	630	kW
		Specific exergy of sugarcane straw	12390	12390	kJ/kg
		Specific exergy of sugarcane bagasse	8961	8961	kJ/kg
	Outputs	Bioslurry	309052	350916	kW
		Heat	48551	27330	kW
		Specific exergy of the bioslurry	15769	14854	kJ/kg
	Exergy efficiency (%)		78.81	83.27	

---

Considering the results reported in Table 5 it is possible to define the irreversibilities for the simulation models. The irreversibilities represent the exergy destruction rate of the system. Hence, the yield model indicated the higher irreversibilities rate of 96173 kW because of the lower exergy efficiency when compared with kinetic model. In fact, the exergy destruction for the kinetic model was 75973 kW due to mainly to the better performance of the fast pyrolysis process in terms of the bioslurry mass flow rate.

### 3.5 Comparison between the simulation and experiment

Bridgwater (BRIDGWATER, 2012a) considers fast pyrolysis at 500 °C when products of fast pyrolysis are around 60% of organic phase, 15% of aqueous phase (only water), 12% of solid and 13% of gas phases. The same author considers intermediate pyrolysis at 500 °C when this fraction is around 25% for organic phase, 25% for aqueous phase (only water), 25% for solid and 25% for gas phase. Thus, the results obtained from the experimental and the yield model are classified between intermediate pyrolysis and fast pyrolysis. The NCG mass fraction of kinetic model leads to an uncertainty of pyrolysis classification. These results and a comparison with other biomasses are shown in Figure 6.

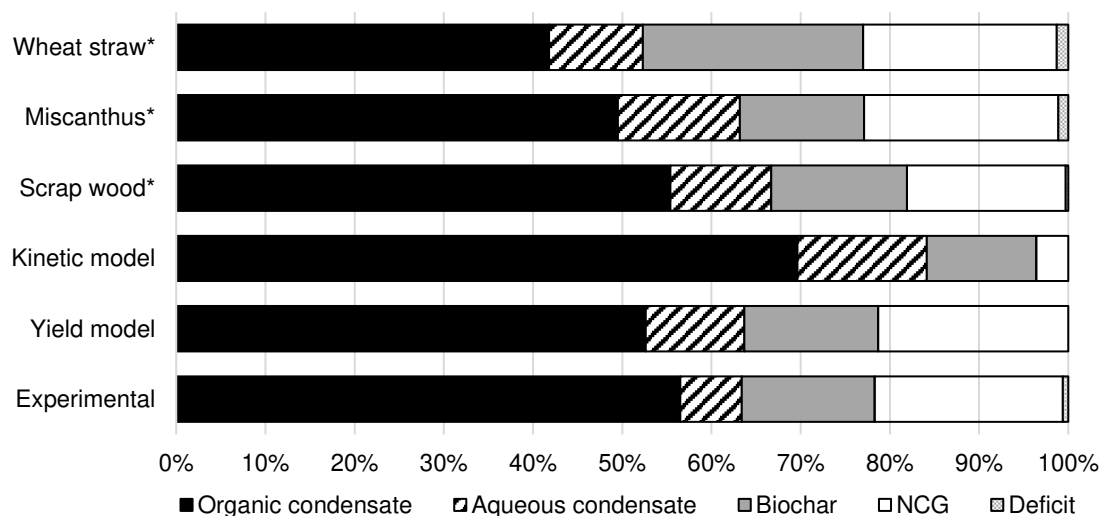


Figure 6. Comparison of fast pyrolysis fraction products (wt.%). \* Collected from Funke et al. (FUNKE et al., 2016b).

Although yield model in Aspen Plus<sup>®</sup> is based on experimental data, there is a slight difference reported for the organic and aqueous condensates when compared these values with experimental data. This difference is due to water content. It was only considered water in the aqueous condensate fraction for kinetic and yield models whereas water is also presented in both aqueous and organic-rich condensate fractions in the experimental data.

Kinetic model presented a bio-oil fraction of 58% whereas for the yield model this value was 64%, showing that bio-oil fraction in yield model and experimental were identical. For NCG fraction, kinetic and yield models were 1% and 21%, respectively. This fraction difference regarding both models may be explained by the need of surplus kinetic reactions for biochar decomposition into NCG. Moreover, once LCB composition was equal for yield and kinetic models, this fraction difference may also be explained by mass balance considered for yield model, i.e. taking the example that all salts are found in the biochar fraction in the simulator, the mass flow of salts should be the same value in biochar fraction, however this is different for yield model. Mass balance for yield model was considered based on each fast pyrolysis product fractions (NCG, biochar and aqueous and organic condensates) from experimental data as described before, differently from kinetic model in which uses building block decomposition where salts are fully considered a biochar component.

Although the results of Kinetic model used in this work can be somehow compared with Yield model and fast pyrolysis experimental data, further kinetic reactions through

algorithm implementation can be added to represent secondary pyrolysis reactions as reported by Peters et al. (PETERS et al., 2017), which could also solve the issue related to low NGC production (RANZI et al., 2008). While Peters et al. (PETERS et al., 2017) used 144 kinetic reactions to describe the fast pyrolysis reactions and Shemfe et al. (SHEMFE; GU; RANGANATHAN, 2015) used 15 reactions, this work used 16 to represent the fast pyrolysis reactions. Possibly, this is the major limitation of the simpler kinetic model used in this work, since it requires the secondary pyrolysis reactions, especially for NCG production, in order to compare with Yield model and experimental data.

Combustor temperature was set equal to 1200 °C with an error of 4 °C. If this temperature was not assumed equal for both simulation models, biochar fraction for the combustor would change and subsequently the flue gas temperature would be lower for yield model than kinetic model. As consequence, biochar fraction in bioslurry would be different and the excess heat could be used for other purposes such as further integration processes.

Higher and Lower Heating Values, and molecular weight of bioslurry considering yield and kinetic models are presented in Table 6. These values were similar when compared the complexity of fast pyrolysis products between yield model and kinetic model.

Table 6. Molecular weight and heating values for bioslurry.

Parameter	Unit	Yield model		Kinetic model	
		500 °C	450 °C	485 °C	500 °C
Molecular weight	g/mol	50.4	64.9	61.7	59.8
Higher Heating Value	MJ/kg	14.8	11.8	13.8	14.6
Lower heating Value	MJ/kg	13.7	10.9	12.8	13.6

#### 4. Conclusion

Experimental results showed great complexity of fast pyrolysis products, especially for aqueous and organic-rich condensates. Regarding the integrated process simulation between LCB drying and fast pyrolysis, the bioslurry mass fraction was 50% for kinetic model and 42% for yield model. Energy efficiencies were 80% for yield model and 89% for kinetic model. Furthermore, exergy efficiencies were 79% and 83% for yield and kinetic models, respectively. The results presented in this work are useful for further assessments of fast pyrolysis processes in integrated scenarios considering 1G sugarcane biorefinery and centralized gasification facilities to produce 2G biofuels according to the bioliq<sup>®</sup> concept.

### Acknowledgements

We would like to thank the Brazilian Bioethanol Science and Technology Laboratory (CTBE) from Brazilian Center for Research in Energy and Materials (CNPEN), Coordination for the Improvement of Higher Education Personnel (CAPES) for the scholarship, BE MUNDUS Project from Erasmus Mundus Programme by the PhD mobility scholarship (BM15DM0953) and the São Paulo Research Foundation (FAPES) for grant 2017/03091-8. Furthermore, the authors also thank Daniel Richter and Renata Moreira for their experimental support, and Pia Griesheimer, Jessica Maier, Jessica Heinrich for their laboratory analyses.

### Supplementary Material

This Supplementary Material presents the main data issued from the experimental and simulations of fast pyrolysis process.

Table 1. Methodologies for sugarcane bagasse and straw characterization.

Characterization		Deutsches Institut für Normung (DIN) and European Norm (EN) with International Organization for Standardization (ISO)
Bulk density		DIN EN ISO 17828 - Solid biofuels - Determination of bulk density (ISO 17828:2015)
Elemental analysis	Ash content	DIN EN ISO 18122 - Solid biofuels - Determination of ash content (ISO 18122:2015)
	CHN content	DIN EN ISO 16948:2015 - Solid biofuels - Determination of total content of carbon, hydrogen and nitrogen
	Oxygen content	ISO 16993 - Solid biofuels - Conversion of analytical results from one basis to another
High Heating Value (HHV)		BS EN 14918:2009 - Solid biofuels - Determination of calorific value
Sampling preparation		DIN EN 14778-09 and DIN EN 14780-09

Table 2. Methodologies for biochar composition.

Parameter	Method
Ash Content	DIN EN 14775 (prEN ISO 18122): 60 min @ 250 °C, 120 min @ 550 °C (atmospheric conditions) (±0.5 %)

Carbon, hydrogen and nitrogen contents	DIN 51732: Elemental analysis without correction of water content
Higher Heating Value	DIN 51900-2/3: Bomb calorimeter ( $\pm 200$ J/g)
Moisture content	DIN EN 14774-3: Drying at 105 °C; ( $\pm 0.1$ %)

Table 3. Non-Condensable Gas (NCG) composition.

NGC compound	Value (%mole)	Standard deviation (%mole)	Mole fraction (%)
H <sub>2</sub>	4.5	0.6	4.6
CO	38.3	1.7	39.1
CH <sub>4</sub>	6.8	0.4	6.9
CO <sub>2</sub>	44.9	2.6	45.9
C <sub>2</sub> H <sub>4</sub>	0.7	0.1	0.7
C <sub>2</sub> H <sub>6</sub>	0.7	0.1	0.7
C <sub>3</sub> H <sub>8</sub>	0.9	0.1	0.9
C <sub>4</sub> H <sub>10</sub>	1.1	0.4	1.1
C <sub>5</sub> +	2.1	0.4	N/A

Table 4. Biochar composition.

Biochar parameter	Value	Standard deviation	Unit
Moisture	3.3	0.1	%wt. wet basis
Ash	32.6	0.1	%wt. dry basis
Carbon	63.2	0.2	%wt. dry basis
Hydrogen	3.5	~ 0	%wt. dry basis
Nitrogen	0.7	~ 0	%wt. dry basis
Heating Value	24.2	1.4	MJ/kg

Table 5. Organic-rich condensate composition.

Name (Component ID in Aspen Plus®)		Mass fraction (wt.% basis)
<b>NONAROMATIC COMPOUNDS</b>		
<b>Acids</b>		15.249
1	Acetic acid (ACET-AC)	11.611
2	Propionic acid (PROPI-01)	2.136
3	Butyric acid (N-BUT-01)	0.457
4	2-Propenoic acid (ACRYL-01)	0.077
5	3-Butenoic acid (3-BUT-01)	0.075
6	2-Butenoic acid (CROTO-01), (Z)-(cis) (NIST MQ 87)	0.433

7	2-Pentenoic acid ((Z)-2-01) (cis or trans) (NIST MQ 84)	0.125
8	Possible: Pentanoic acid, 4-oxo- (ETHYL-01) (NIST MQ 77)	0.214
9	Possible: Pentanoic acid, 4-oxo- (ETHYL-01) (NIST MQ 77)	0.121

---

<b>Nonaromatic Esters</b>	1.023
---------------------------	-------

10	Acetic acid 2-hydroxyethyl ester (2-HYD-01)	0.06
11	Acetic acid, hydroxy-, methyl ester (GLYCO-01)	0.035
12	Possible: Oxopropanoic acid methylester, 2- (METHY-01)	0.61
13	Possible: 2-Butenoic acid, methyl ester (C7H12-01)	0.025
14	Possible: Propanoic acid, ethenyl ester (VINYL-01)	0.060
15	Butanedioic acid, dimethyl ester or Isomere (DIMET-01)	0.051
16	Possible: 2-Propenoic acid, 3-(4-hydroxyphenyl)-, methyl ester (C10H1-01)	0.156
17	Butanedioic acid, dimethyl ester or Isomere (DIMET-01)	0.009
18	Possible: 2-Propenoic acid, 3-(4-hydroxyphenyl)-, methyl ester (C10H1-01)	0.017

---

<b>Nonaromatic Alcohols</b>	1.278
-----------------------------	-------

19	Ethylene glycol (ETHYL-02)	1.203
20	2-Propen-1-ol (ALLYL-01)	0.040
21	Possible: 2-Propanol, 2-methyl- (ISOPR-01)	0.035

---

<b>Nonaromatic Aldehydes</b>	9.705
------------------------------	-------

22	Acetaldehyde, hydroxy- (ACETALDE)	7.872
23	Propionaldehyde, 3-hydroxy (N-PRO-01)	1.182
24	2-Butenal (CIS-C-02)	0.096
25	Possible: 2-Pentenal, (E)- (2-PEN-01)	0.017
26	Butanedial or Propanal (N-PRO-02)	0.538

---

<b>Nonaromatic Ketones</b>	16.166
----------------------------	--------

27	Acetol (Hydroxypropanone) (ACETO-01)	9.771
28	Acetylacetone (Hexandione, 2,5-) (2:5-H-01)	0.031
29	Butanone, 2- (METHY-02)	0.065
30	Butanone, 1-hydroxy-2- (3-HYD-01)	1.167
31	Butandione, 2,3- (Diacyl) (DIACE-01)	0.108
32	Acetoin (Hydroxy-2-butanone, 3-) (3-HYD-02)	0.135
33	Propan-2-one, 1-acetyloxy- (ACETO-02)	0.545
34	Cyclopentanone (CYCLO-01)	0.138
35	Cyclopenten-1-one, 2- (CYCLO-02)	0.527
36	Cyclopenten-1-one, 2,3-dimethyl-2- (2:3-D-01)	0.199
37	Cyclopenten-1-one, 2-methyl-2- (2-MET-01)	0.171
38	Cyclopenten-1-one, 3-methyl-2- (METHY-03)	0.231
39	Cyclopenten-1-one, 2-hydroxy-2- (2-MET-02)	0.414
40	Cyclopenten-3-one, 2-hydroxy-1-methyl-1- (3-MET-01)	1.043
41	Cyclopenten-1-one, 3-ethyl-2-hydroxy-2- (3-ETH-01)	0.618

42	Cyclohexen-1-one, 2- (2-CYC-01)	0.088
43	Possible: 3-Buten-2-one = 2-Butenone (METHY-04)	0.031
44	3-Pentanone (DIETH-01)	0.097
45	3-Buten-2-one, 3-methyl- (METHY-04)	0.082
46	Possible: 2,3-Pentanedione (or Methyl-Isobutyl Ketone) (2:3-P-01)	0.054
47	3-Penten-2-one (MESIT-01)	0.021
48	Isomere of 2-Cyclopenten-1-one, 3-methyl- (2-MET-03)	0.026
49	2-Butanone, 1-hydroxy-3-methyl- (METHY-05)	0.042
50	Isomer of Cyclopentenone, 3,4-dimethyl- (3::4:-01)	0.029
51	4-Cyclopentene-1,3-dione (3::4:-01)	0.098
52	Possible: Butan-2-one, 1-(acetyloxy)- (METHY-06)	0.111
53	Possible: Cyclopentanone, ethyl-vinyl- (1-PEN-01)	0.059
54	2-Cyclopenten-1-one, 2,3,4-trimethyl- (2:3:4-01)	0.051
55	Isomer of Cyclopenten-1-one, 3-ethyl-2-hydroxy- (3-ETH-02)	0.051
56	Possible: Cyclohexanone, 3-methyl- (CYCLO-03)	0.082
57	Possible: 2-Cyclohexene-1,4-dione (2-CYC-02)	0.021
58	Possible: 1,3-Cyclopentanedione, 2,4-dimethyl- (1:3-C-01)	0.032
59	2-Cyclopenten-1-one, 3-ethyl- (CYCLO-04)	0.029

**Hydrocarbons**

0.005

---

60	Possible: 2-Hexene, 4-methyl- (CIS-2-01)	0.005
----	--	-------

**Furans**

8.011

---

61	Furfuryl alcohol, 2- (FURFU-01)	0.273
62	Furanone, 2(3H)- (GAMMA-01)	0.262
63	Furanone, 2(5H)- (2(5H)-01)	0.720
64	Furaldehyde, 2- (FURFU-02)	1.516
65	Furaldehyde, 3- (3-FUR-01)	0.547
66	Furaldehyde, 5-methyl-2- (5-HYD-01)	0.124
67	Furaldehyde, 5-(hydroxymethyl)-, 2- (5-HYD-02)	0.421
68	Ethanone, 1-(2-furanyl)- (C15H1-01)	0.457
69	Furan-2-one, 3-methyl-, (5H)- (6:7-D-01)	0.193
70	Furan-x-on, x,x-dihydro-x-methyl- (6:7-D-01)	0.314
71	Angelicalactone, $\alpha$ - (Furan-2-one, 2,3-dihydro-5-methyl-) (FURFU-03)	0.219
72	Butyrolactone, $\gamma$ - (GAMMA-01)	0.319
73	Butyrolactone, 2-hydroxy-, $\gamma$ - (3-HYD-03)	0.394
74	Furan, tetrahydro-2-methoxy- (TETRA-01)	0.20
75	Possible: 2(3H)-Furanone, dihydro-4-hydroxy- (GAMMA-01)	0.045
76	Possible: 2(5H)-Furanone, 5-methyl- (2(5H)-01)	0.237
77	Furandione-2,5-, 3-methyl- (SUCCI-01)	0.120
78	Possible: 2(5H)-Furanone, 5-ethyl- ((2(5H)-01))	0.101
79	Possible: 2-Furancarboxylic acid, methyl ester (ALPH-01)	0.085
80	2,5-Furandicarboxaldehyde (ALPH-01)	0.077
81	Furan-2-one, 4-methyl-(5H)- (ALPH-01)	0.182

82	Lactone derivative (Possible: (S)-(+)-2',3'-Dideoxyribonolactone (ALPH-01)	0.353
83	Isomer of 2-Furanone, 2,5-dihydro-3,5-dimethyl- (ALPH-01)	0.268
84	Lactone derivative (Furanone derivative)(unspecific spectrum) (ALPH-01)	0.132
85	Lactone derivative = Furanone derivative (unspecific spectrum) (ALPH-01)	0.092
86	Lactone derivative (unspecific spectrum) (ALPH-01)	0.188
87	Lactone derivative = Furanone derivative (unspecific spectrum) (ALPH-01)	0.171
<b>Pyrans</b>		0.676
88	Pyran-2-one, 2H- (ALPH-02)	0.064
89	Maltol (Pyran-4-one, 3-Hydroxy-2-methyl-4H-) (MALTO-01)	0.242
90	Pyran-4-one, 3-hydroxy-5,6-dihydro-, (4H)- (4-PYR-01)	0.304
91	unknown Pyranone or Furanone derivative (4-PYR-01)	0.066
<b>AROMATIC COMPOUNDS</b>		
<b>Benzenes</b>		0.045
92	Inden-1-one, 2,3-dihydro-1H- (ALPH-03)	0.041
93	Benzene (BENZENE)	0.004
<b>Aromatic Aldehydes</b>		0.223
94	Benzaldehyde (BENZA-01)	0.041
95	Possible: Benzaldehyde, methyl- (BENZA-01)	0.053
96	Possible: Benzaldehyde, 3-hydroxy- (BENZA-01)	0.128
<b>Aromatic Ketones</b>		0.015
97	Acetophenone (METHY-07)	0.015
<b>Lignin derived Phenols</b>		7.730
98	Phenol (PHENOL)	0.532
99	Cresol, o- (O-CRE-01)	0.177
100	Cresol, p- (P-CRE-01)	0.293
101	Cresol, m- (M-CRE-01)	0.146
102	Phenol, 2,5-dimethyl- (2:5-X-02)	0.067
103	Phenol, 2,4-dimethyl- (2:4-X-01)	0.061
104	Phenol, 2,3-dimethyl- (2:3-X-01)	0.027
105	Phenol, 3,5-dimethyl- (3:5-X-01)	0.021
106	Phenol, 3-ethyl- (M-ETH-01)	0.072
107	Phenol, 4-ethyl- (P-ETH-01)	0.587
108	Phenol, 4-vinyl- (4-HYD-01)	2.298
109	Phenol, 4-propenyl-, cis (ISOEU-01)	2.556
110	Phenol, 4-propenyl-, trans (ISOEU-01)	0.074
111	Benzaldehyde, 4-hydroxy- (BENZA-02)	0.261
112	Acetophenone, 4-hydroxy- (4-HYD-02)	0.318

113	Phenol, ethyl-methyl- (2-ETH-01)	0.069
114	Phenol, trimethyl- (MESIT-02)	0.044
115	Possible: Phenol, allyl- or propenyl- (2-ALL-01)	0.044
116	unknown phenolic dimere compound (2-ALL-01)	0.043
117	Phenol, 3-methoxy-5-methyl- (2-ALL-01)	0.015
118	unknown phenolic dimere compound (2-ALL-01)	0.025

---

**Guaiacols (Methoxy phenols)**

6.009

---

119	Guaiacol (GUAIA-01)	0.490
120	Guaiacol, 3-methyl- (2-MET-04)	0.042
121	Guaiacol, 4-methyl- (4-MET-01)	0.310
122	Guaiacol, 4-ethyl- (5-ETH-01)	0.268
123	Guaiacol, 4-vinyl- (5-ETH-01)	1.243
124	Guaiacol, 4-allyl- (Eugenol) (4-ALL-01)	0.170
125	Guaiacol, 4-propyl- (4-PRO-01)	0.037
126	Guaiacol, 4-propenyl- cis (Isoeugenol) (ISOEU-01)	0.306
127	Guaiacol, 4-propenyl-(trans) (Isoeugenol) (ISOEU-01)	1.136
128	Vanillin (VANILLIN)	0.799
129	Phenylacetaldehyde, 4-hydroxy-3-methoxy- (Homovanillin) (BENZE-01)	0.109
130	Dihydroconiferyl alcohol (C10H1-02)	0.236
131	Coniferyl alcohol (trans) (C10H1-02)	0.230
132	Coniferyl alcohol, Isomer of (C10H1-02)	0.213
133	Phenylethanone, 4-hydroxy-3-methoxy- (Acetoguaiacone) (METHY-08)	0.157
134	Propioguaiacone (METHY-08)	0.079
135	Guaiacyl acetone (METHY-08)	0.092
136	Coniferylaldehyde (METHY-08)	0.062
137	Possible: Guaiacol, 3-ethyl- (METHY-08)	0.030

---

**Syringols (Dimethoxy phenols)**

4.574

---

138	Syringol (SYRIN-01)	0.629
139	Syringol, 4-methyl- (SYRIN-01)	0.425
140	Syringol, 4-ethyl- (SYRIN-01)	0.133
141	Syringol, 4-vinyl- (SYRIN-01)	0.464
142	Syringol, 4-allyl- (SYRIN-01)	0.254
143	Syringol, 4-propyl- (SYRIN-01)	0.085
144	Syringol, 4-(1-propenyl)-, cis (SYRIN-01)	0.221
145	Syringol, 4-(1-propenyl)-, trans (SYRIN-01)	0.824
146	Syringaldehyde (SYRIN-02)	0.368
147	Homosyringaldehyde (DIALL-01)	0.243
148	Acetosyringone (DIALL-01)	0.142
149	Propiosyringone (C11H1-01)	0.115
150	Syringyl acetone (C11H1-01)	0.199
151	Sinapaldehyde (trans) (C11H1-01)	0.137
152	Syringol, 4-(1,2-propandione)- (C11H1-01)	0.133

153	Sinapaldehyde (trans) (C11H1-01)	0.126
154	Syringol, 4-(1,2-propandione)- (C11H1-01)	0.037
155	Isomere of Syringol (C11H1-01)	0.041

### CARBOHYDRATES

	<b>Sugars</b>	16.502
156	Anhydro- $\beta$ -D-arabinofuranose, 1,5- (D-ARA-01)	0.777
157	Anhydro- $\beta$ -D-xylofuranose, 1,5- (D-ARA-01)	1.153
158	Anhydro- $\beta$ -D-glucopyranose, 1,6- (Levoglucosan) (LEVOGLUC)	9.312
159	Anhydro- $\beta$ -D-glucofuranose, 1,6- (LEVOGLUC)	0.394
160	Dianhydro- $\alpha$ -D-glucopyranose, 1,4:3,6- (1-DEO-01)	1.298
161	Anhydrosugar unknown (unspecific spectrum) (1-DEO-01)	0.760
162	unknown sugar derived compound (unspecific spectrum) (no NIST spectrum found) (1-DEO-01)	0.199
163	Possible: 2,3-Anhydro-d-galactosan (NIST MQ 78) (1-DEO-01)	0.310
164	Possible: 2,3-Anhydro-d-mannosan (NIST MQ 84) (1-DEO-01)	0.368
165	unknown sugar derived compound (no NIST spectrum found) (1-DEO-01)	0.179
166	unknown sugar derived compound (1-DEO-01)	0.448
167	Anhydrosugar unknown (unspecific spectrum) (1-DEO-01)	0.586
168	Anhydrosugar unknown (unspecific spectrum) (1-DEO-01)	0.361
169	unknown sugar derived compound (no NIST spectrum found) (1-DEO-01)	0.247
170	Anhydrosugar unknown (no NIST spectrum found) (1-DEO-01)	0.110

### OTHER ORGANIC COMPOUNDS

	<b>N-compounds</b>	0.012
171	Pyridine (PYRIDINE)	0.012
	<b>Miscellaneous</b>	0.130
172	1,3-Dioxolane, 2-methyl- (DIOXOLAN)	0.022
173	1,4-Dioxin, 2,3-dihydro- (DIOXIN)	0.025
174	Benzopyran-2-one, 3,4-dihydro-6-hydroxy-; 2H-1- (DIHYDROC)	0.037
175	similar to Ferulic acid methyl ester = 2-Propenoic acid, 3-[4-(acetyloxy)-3-methoxy+B579phenyl]-, methyl ester (C3H4O2)	0.033
176	Naphthalene, 1-phenyl- (impurity in IS = Fluoranthene) (NAPHTALE)	0.013
177	<b>Water (H2O)</b>	13.321
	<b>TOTAL</b>	100

Table 6. Aqueous condensate composition.

Name (Component ID in Aspen Plus®)	Mass fraction (wt. % basis)
<b>NONAROMATIC COMPOUNDS</b>	

	<b>Acids</b>	13.022
1	Acetic acid (ACET-AC)	11.490
2	Propionic acid (PROPI-01)	0.735
3	2-Propenoic acid (ACRYL-01)	0.227
4	2-Butenoic acid, (Z)- (CROTO-01)	0.061
5	2-Butenoic acid, (E)- (CROTO-01)	0.176
6	2-Butenoic acid, 2-methyl- ((CROTO-01))	0.075
7	Pentanoic acid, 4-oxo- (ETHYL-01)	0.071
8	Butyric acid (BUTYRIC)	0.186
	<b>Nonaromatic Alcohols</b>	7.086
9	Methanol (METHANOL)	1.188
10	Ethylene glycol (ETHYL-02)	5.897
	<b>Nonaromatic Aldehydes</b>	0.552
11	Crotonaldehyde, trans (TRANS-01)	0.552
	<b>Nonaromatic Ketones</b>	10.773
12	Acetol (Hydroxypropanone) (ACETO-01)	5.764
13	Butanone, 2- (METHY-02)	0.694
14	Butanone, 1-hydroxy-2- (3-HYD-01)	0.704
15	Butandione, 2,3- (Diacetyl) (DIACE-01)	0.857
16	Propanone, acetyloxy-2-	0.270
17	Possible: 2-Butenone (METHY-04)	0.354
18	3-Buten-2-one, 3-methyl- (METHY-04)	0.102
19	Possible: 2,3-Pentanedione (2:3-P-01)	0.082
20	3-Penten-2-one (2:3-P-01)	0.213
21	Possible: 3-Penten-2-one, 4-methyl- (MESIT-01)	0.076
22	2-Butanone, 3-hydroxy- (METHY-05)	0.046
23	2-Butanone, 4-hydroxy- (METHY-05))	0.013
24	Cyclopentanone (CYCLO-01)	0.081
25	Cyclopenten-1-one, 2- (CYCLO-02)	0.238
26	Cyclopenten-1-one, 2-methyl-2- (2-MET-03)	0.122
27	Cyclopenten-1-one, 3-methyl-2- (3-MET-01)	0.076
28	Cyclopenten-1-one, 2-hydroxy-2- (2-MET-02)	0.513
29	Cyclopenten-3-one, 2-hydroxy-1-methyl-1- (3-MET-01)	0.239
30	Cyclopenten-1-one, 3-ethyl-2-hydroxy-2- (3-MET-01)	0.034
31	similar to Cyclopenten-1-one (3-MET-01)	0.153
32	4-Cyclopentene-1,3-dione (3-MET-01)	0.089
33	2-Cyclohexene-1,4-dione (3-MET-01)	0.036
34	2-Cyclopenten-1-one, 2-hydroxy-3,4-dimethyl- (3-MET-01)	0.017
	<b>HETEROCYCLIC COMPOUNDS</b>	
	<b>Furans</b>	2.293

35	Furan, 2-methyl- (2-MET-06)	0.024
36	Furfuryl alcohol, 2- (FURFU-01)	0.053
37	Furanone, 2(5H)- (2(5H)-01)	0.458
38	Furaldehyde, 2- (FURFU-02)	1.198
39	Furaldehyde, 5-methyl-2- (5-HYD-01)	0.088
40	Furaldehyde, 5-(hydroxymethyl)-, 2- (5-HYD-02)	0.027
41	Ethanone, 1-(2-furanyl)- (C15H1-01)	0.052
42	Furan-2-one, 3-methyl-, (5H)- (6:7-D-01)	0.079
43	2(5H)-Furanone, 5-methyl- (2(5H)-01)	0.089
44	Furan-2-one, 4-methyl-(5H)- (2(5H)-01)	0.044
45	Furan-2-one, 2,5-dihydro-3,5-dimethyl- (2(5H)-01)	0.048
46	Furan-x-on, x,x-dihydro-x-methyl- (2(5H)-01)	0.034
47	Butyrolactone, $\gamma$ - (GAMMA-01)	0.100

**CARBOHYDRATES**

**Sugars** 0.183

---

48	Anhydro- $\beta$ -D-glucopyranose, 1,6- (Levogluconan) (LEVOGLUC)	0.108
49	Anhydrosugar unknown (unspecific spectrum) (LEVOGLUC)	0.040
50	unknown sugar derived compound (no NIST spectrum found) (LEVOGLUC)	0.035

**AROMATIC COMPOUNDS**

**Lignin derived Phenols** 0.331

---

51	Phenol (PHENOL)	0.119
52	Cresol, o- (O-CRE-01)	0.046
53	Cresol, m- (M-CRE-01)	0.019
54	Phenol, 2,6-dimethyl- (2:6-X-01)	0.005
55	Phenol, 3-ethyl- (M-ETH-01)	0.004
56	Phenol, 4-ethyl- (P-ETH-01)	0.084
57	Phenol, 4-vinyl- (4-HYD-01)	0.051
58	Phenol, tetramethyl- (4-HYD-01)	0.004

**Guaiacols (Methoxy phenols)** 0.552

---

59	Guaiacol (GUAIA-01)	0.168
60	Guaiacol, 3-methyl- (2-MET-04)	0.033
61	Guaiacol, 4-methyl- (4-MET-01)	0.096
62	Guaiacol, 4-ethyl- (5-ETH-01)	0.035
63	Guaiacol, 4-vinyl- (5-ETH-01)	0.042
64	Guaiacol, 4-allyl- (Eugenol) (4-ALL-01)	0.027
65	Guaiacol, 4-propyl- (4-PRO-01)	0.015
66	Guaiacol, 4-propenyl- cis (Isoeugenol) (ISOEU-01)	0.029
67	Guaiacol, 4-propenyl-(trans) (Isoeugenol) (ISOEU-01)	0.052
68	Vanillin (VANILLIN)	0.025
69	Phenylethanone, 4-hydroxy-3-methoxy- (Acetoguaiacone) (METHY-08)	0.019

70	Guaiacyl acetone (METHY-08)	0.011
<b>Syringols (Dimethoxy phenols)</b>		0.165
71	Syringol (SYRIN-01)	0.080
72	Syringol, 4-methyl- (SYRIN-01)	0.021
73	Syringol, 4-ethyl- (SYRIN-01)	0.012
74	Syringol, 4-allyl-(SYRIN-01)	0.017
75	Syringol, 4-(1-propenyl)-, cis (SYRIN-01)	0.008
76	Syringol, 4-(1-propenyl)-, trans (SYRIN-01)	0.012
77	Syringaldehyde (SYRIN-02)	0.001
78	Acetosyringone (SYRIN-02)	0.005
79	Propiosyringone (SYRIN-02)	0.005
80	Syringyl acetone (SYRIN-02)	0.004
<b>OTHER ORGANIC COMPOUNDS</b>		
<b>Nonaromatic Esters</b>		0.039
81	Propanoic acid, ethenyl ester (PROPI-01)	0.039
<b>Miscellaneous</b>		0.415
82	Possible: 1,2-Ethanediol, 1-(2-furanyl)- (DIOXOLAN)	0.003
83	1,3-Dioxolane, 2-methyl- (DIOXOLAN)	0.177
84	1,3-Dioxol-2-one (DIOXOLAN)	0.025
85	Possible: 1,2-Ethanediol, monoacetate (DIOXOLAN)	0.211
<b>unknown compounds</b>		0.039
86	unknown compound (unspecific spectrum) (no NIST spectrum found)	0.107
87	unknown aliphatic acid compound MW=?	0.033
88	unknown compound (unspecific spectrum) (no NIST spectrum found)	0.015
89	unknown compound (no NIST spectrum found) MW 98	0.033
90	unknown compound (no NIST spectrum found) MW 98	0.094
91	unknown aromatic compound MW 180	0.027
92	<b>Water (H2O)</b>	64.552
<b>TOTAL</b>		100

Table 7. LCB mass fraction composition in Aspen Plus<sup>®</sup>.

Component ID	Component name	Alias	Surplus bagasse	Sugarcane straw	LCB
ACETATE	Acetic-acid	C2H4O2	1.21E-02	1.86E-02	1.36E-02
CELLULOS	Cellulose	USER DEFINED	2.16E-01	2.61E-01	2.27E-01
GLUCOSE	Dextrose	C6H12O6	8.39E-04	1.84E-03	1.07E-03

H2O	Water	H2O	5.00E-01	2.98E-01	4.53E-01
H3PO4	Orthophosphoric-acid	H3PO4	5.43E-05	1.83E-04	8.45E-05
LIGNIN	Lignin	USER DEFINED	1.17E-01	1.66E-01	1.29E-01
MINERALS	Potassium-oxide	K2O	1.24E-03	1.14E-04	9.76E-04
ORG-AC	Trans-aconitic-acid	C6H6O6	8.91E-04	4.06E-03	1.63E-03
SALTS	Potassium-chloride	KCL	9.79E-03	1.78E-02	1.17E-02
SOIL	Silicon-dioxide	SIO2	3.76E-03	8.64E-03	4.90E-03
SUCROSE	Sucrose	C12H22O11	1.96E-02	4.26E-02	2.50E-02
XYLAN	Xylan	USER DEFINED	1.18E-01	1.81E-01	1.33E-01

Surplus bagasse and straw mass flow are 128143 kg/h and 39114 kg/h, respectively.

Macromolecules, such as Cellulose, lignin and xylan, were added in Aspen Plus® through USER DEFINED function according to the component properties obtained from other physical property database (ASPEN TECHNOLOGY, 2012; WOOLEY; PUTSCHE, 1996) and an adaption has been performed to match the characteristics of sugarcane components according to Junqueira et al. (JUNQUEIRA et al., 2016) proposed by VSB framework.

Table 8. NCG, biochar and bio-oil compositions in Aspen Plus® for yield model considering fast pyrolysis temperature equal to 500 °C.

Fast pyrolysis product	Mass flow (kg/h)	Component ID in Aspen Plus®	Mass fraction
NCG	21680	CO2	0.597
		CO	0.324
		CH4	0.033
		C4H10	0.019
		C3H8	0.012
		C2H6	0.006
		C2H4	0.006
		H2	0.003
Biochar	15243	C	0.660
		SALTS	0.225
		SOIL	0.095
		MINERALS	0.019
		H3PO4	0.002
Bio-oil	70558	H2O	1.73E-01
		ACET-AC	1.06E-01
		ACETO-01	8.50E-02

---

LEVOGLUC	7.88E-02
ACETALDE	6.38E-02
C	5.60E-02
1-DEO-01	3.94E-02
ISOEU-01	3.31E-02
SYRIN-01	1.96E-02
SALTS	1.91E-02
4-HYD-01	1.87E-02
PROPI-01	1.81E-02
ETHYL-02	1.58E-02
D-ARA-01	1.56E-02
FURFU-01	1.48E-02
FURFU-02	1.35E-02
5-ETH-01	1.23E-02
3-HYD-01	1.02E-02
N-PRO-01	9.58E-03
2(5H)-01	9.26E-03
3-MET-01	9.11E-03
SOIL	8.04E-03
VANILLIN	6.50E-03
C11H1-01	6.38E-03
C10H1-02	5.50E-03
GAMMA-01	5.18E-03
3-ETH-01	5.00E-03
METHY-01	4.94E-03
P-ETH-01	4.84E-03
CYCLO-02	4.51E-03
PHENOL	4.43E-03
3-FUR-01	4.43E-03
ACETO-02	4.42E-03
N-PRO-02	4.36E-03
6:7-D-01	4.20E-03
GUAIA-01	4.14E-03
2-MET-02	3.88E-03
CROTO-01	3.83E-03
C15H1-01	3.75E-03
N-BUT-01	3.70E-03
5-HYD-02	3.44E-03
METHY-08	3.43E-03
3-HYD-03	3.19E-03
DIAL-01	3.12E-03
SYRIN-02	3.00E-03
4-PYR-01	3.00E-03

---

---

ETHYL-01	2.79E-03
4-MET-01	2.61E-03
4-HYD-02	2.58E-03
P-CRE-01	2.37E-03
BENZA-02	2.12E-03
DIACE-01	2.02E-03
MALTO-01	1.96E-03
METHY-03	1.87E-03
CO2	1.85E-03
BENZA-01	1.81E-03
FURFU-03	1.78E-03
TETRA-01	1.62E-03
2:3-D-01	1.61E-03
MINERALS	1.60E-03
O-CRE-01	1.48E-03
4-ALL-01	1.41E-03
C10H1-01	1.40E-03
2-MET-01	1.38E-03
METHY-04	1.38E-03
METHY-02	1.24E-03
METHANOL	1.21E-03
M-CRE-01	1.20E-03
CYCLO-01	1.20E-03
5-HYD-01	1.10E-03
3-HYD-02	1.09E-03
2-ALL-01	1.03E-03
3::4:-01	1.03E-03
(Z)-2-01	1.01E-03
CO	1.01E-03
SUCCI-01	9.69E-04
METHY-06	9.03E-04
BENZE-01	8.86E-04
ACRYL-01	8.54E-04
DIETH-01	7.85E-04
CIS-C-02	7.80E-04
2:3-P-01	7.36E-04
2-CYC-01	7.12E-04
CYCLO-03	6.63E-04
3-BUT-01	6.08E-04
DIOXOLAN	5.98E-04
M-ETH-01	5.85E-04
TRANS-01	5.62E-04
2-ETH-01	5.60E-04

---

---

2:5-X-02	5.45E-04
ALPH-02	5.19E-04
2:4-X-01	4.97E-04
DIMET-01	4.92E-04
VINYL-01	4.90E-04
2-HYD-01	4.85E-04
1-PEN-01	4.80E-04
3-ETH-02	4.17E-04
2:3:4-01	4.16E-04
METHY-05	3.97E-04
2-MET-04	3.71E-04
MESIT-02	3.58E-04
2-MET-03	3.34E-04
ALPH-03	3.29E-04
ALLYL-01	3.23E-04
4-PRO-01	3.16E-04
DIHYDROC	3.01E-04
GLYCO-01	2.82E-04
ISOPR-01	2.80E-04
C3H4O2	2.64E-04
1:3-C-01	2.59E-04
MESIT-01	2.49E-04
2:5-H-01	2.47E-04
CYCLO-04	2.31E-04
2:3-X-01	2.21E-04
DIOXIN	2.05E-04
C7H12-01	2.03E-04
BUTYRIC	1.90E-04
3:5-X-01	1.69E-04
2-CYC-02	1.67E-04
H3PO4	1.39E-04
2-PEN-01	1.39E-04
METHY-07	1.25E-04
NAPHTALE	1.05E-04
CH4	1.02E-04
PYRIDINE	9.89E-05
C4H10	5.99E-05
CIS-2-01	4.26E-05
C3H8	3.72E-05
BENZENE	3.42E-05
2-MET-06	2.47E-05
C2H6	1.97E-05
C2H4	1.84E-05

---

	H2	8.50E-06
	2:6-X-01	4.69E-06

Table 9. Component ID in Aspen Plus® for the kinetic model.

Component ID	Type	Component name	Alias
ACETALDE	Conventional	Acetaldehyde	C2H4O-1
ACETATE	Solid	Acetic-acid	C2H4O2-1
ACETONE	Conventional	Acetone	C3H6O-1
BENZENE	Conventional	Benzene	C6H6
C	Solid	Carbon-graphite	C
C2H2	Conventional	Acetylene	C2H2
C2H4	Conventional	Ethylene	C2H4
C3H4O2	Conventional	Acrylic-acid	C3H4O2-1
C5H6	Conventional	Cyclopentadiene	C5H6
C8H8O	Conventional	4-hydroxystyrene	C8H8O-D1
CELLA	Conventional	Levoglusosan	C6H10O5-N1
CELLULOS	Solid	Cellulose	USER DEFINED
CH4	Conventional	Methane	CH4
CO	Conventional	Carbon-monoxide	CO
CO2	Conventional	Carbon-dioxide	CO2
DIETER	Conventional	Dimethyl-ether	C2H6O-1
ETHANOL	Conventional	Ethanol	C2H6O-2
FORMALDE	Conventional	Formaldehyde	CH2O
GLUCOSE	Conventional	Dextrose	C6H12O6
GLYOXAL	Conventional	Glyoxal	C2H2O2
H2	Conventional	Hydrogen	H2
H2O	Conventional	Water	H2O
H3PO4	Conventional	Orthophosphoric-acid	H3PO4
HAA	Conventional	Glycol-aldehyde	C2H4O2-D1
HCELL1	Conventional	Glutaric-acid	C5H8O4
HCELL2	Conventional	Glutaric-acid	C5H8O4
HMFU	Conventional	Furfural	C5H4O2
LEVOGLUC	Conventional	Levoglusosan	C6H10O5-N1
LGNSOL	Solid	Lignin	USER DEFINED
LIGNIN	Solid	Lignin	USER DEFINED
METHANOL	Conventional	Methanol	CH4O
MINERALS	Conventional	Potassium-oxide	K2O
N2	Conventional	Nitrogen	N2
O2	Conventional	Oxygen	O2
ORG-AC	Conventional	Trans-aconitic-acid	C6H6O6
PHENOL	Conventional	Phenol	C6H6O
SALTS	Conventional	Potassium-chloride	KCL

SOIL	Solid	Silicon-dioxide	SIO2
SUCROSE	Conventional	Sucrose	C12H22O11
TOLUENE	Conventional	Toluene	C7H8
XYLAN	Solid	Xylan	USER DEFINED
XYLANPYR	Conventional	Glutaric-acid	C5H8O4

Macromolecules, such as Cellulose, lignin and xylan, were added in Aspen Plus® through USER DEFINED function according to the component properties obtained from other physical property database (ASPEN TECHNOLOGY, 2012; WOOLEY; PUTSCHE, 1996) and an adaption has been performed for match the characteristics of sugarcane components according to Junqueira et al. (JUNQUEIRA et al., 2016) proposed by VSB framework.

Table 10. NCG, biochar and bio-oil compositions in Aspen Plus® for kinetic model considering fast pyrolysis temperature equal to 500 °C.

Fast pyrolysis products	Mass flow (kg/h)	Component ID in Aspen Plus®	Mass fraction
NCG	1191	CO2	0.510
		CH4	0.315
		CO	0.096
		C2H4	0.074
		H2	0.005
Biochar	41846	CELLA	0.849
		C	0.082
		SALTS	0.046
		SOIL	0.019
		MINERALS	0.004
Bio-oil	58625	HCELL2	0.248
		H2O	0.210
		HCELL1	0.164
		C3H4O2	0.100
		LGNSOL	0.082
		SUCROSE	0.071
		C8H8O	0.052
		ACETALDE	0.017
		PHENOL	0.016
		CELLA	0.012
		METHANOL	0.011
		LEVOGLUC	0.006
		ORG-AC	0.005
		GLUCOSE	0.003
HAA	0.001		

Others	0.002
--------	-------

Table 11. Standard chemical exergy of the compounds used in the exergy analysis.

Formula	Component	ID Aspen	Molecular mass (kg/kmol)	Standard chemical exergy (kJ/kmol)	
C	CARBON-GRAPHITE	C	12.01	410260	*
C10H12O2	ISOEUGENOL	ISOEU- 01	164.20	8260490	**
C10H8	NAPHTHALENE	TAR	128.17	5255000	*
C10H8	NAPHTHALENE	NAPHT ALE	128.17	5255000	*
C12H22O11	SUCROSE	SUCRO SE	342.30	6007800	*
C2H4	ETHYLENE	C2H4	28.05	1361100	*
C2H4O	ACETALDEHYDE	ACETA LDE	44.05	1163300	*
C2H4O2	ACETIC-ACID	ACET- AC	44.05	1163300	*
C2H4O2	ACETIC-ACID	ACETA TE	60.05	908000	*
C2H6	ETHANE	C2H6	30.07	1495840	*
C2H6O	ETHANOL	ETHAN OL	46.07	1250900	*
C2H6O2	ETHYLENE-GLYCOL	ETHYL- 02	62.06	1207300	*
C3H6O	ALLYL-ALCOHOL	ALLYL- 01	58.08	1791500	*
C3H6O	N-PROPIONALDEHYDE	N-PRO- 01	60.09	1998600	*
C3H6O	N-PROPIONALDEHYDE	N-PRO- 02	60.09	1998600	*
C3H6O2	PROPIONIC-ACID	PROPI- 01	58.08	1791500	*
C3H6O2	ACETOL	ACETO- 01	58.08	1791500	*
C3H8	PROPANE	C3H8	44.09	2163190	*
C3H8O	1-PROPANOL	C3H7O H	60.09	1998600	*
C3H8O	ISOPROPYL-ALCOHOL	ISOPR- 01	60.09	1998600	*
C3H8O3	GLYCEROL	GLYCE ROL	92.09	1705600	*
C4H10	N-BUTANE	C4H10	58.12	2818930	*
C4H8O	METHYL-ETHYL- KETONE	METHY -02	72.10	2432600	*
C4H8O	METHYL-ETHYL- KETONE	METHY -05	88.10	2269000	*
C4H8O	METHYL-ETHYL- KETONE	METHY -06	88.10	2269000	*
C4H8O2	N-BUTYRIC-ACID	N-BUT- 01	88.10	2215800	*
C4H8O2	3-HYDROXY-2- BUTANONE	3-HYD- 01	88.40	2278750	*
C4H8O2	N-BUTYRIC-ACID	BUTYRI C	88.10	2215800	*

C5H10O	METHYL-ISOPROPYL-KETONE	METHY-03	86.13	3109700	*
C5H10O	DIETHYL-KETONE	DIETH-01	86.13	3109700	*
C5H10O5	D-XYLOSE	XYLOLI G	150.13	1835300	*
C5H10O5	D-XYLOSE	XYLOS E	150.13	1835300	*
C5H10O5	D-ARABINOSE	D-ARA-01	86.13	3121220	*
C5H12	N-PENTANE	C5H12	72.15	3463300	*
C5H12O	3-METHYL-1-BUTANOL	ISOAMI L	88.15	3275700	*
C5H12O	2-METHYL-2-BUTANOL	2-MET-02	88.15	3258	*
C5H4O2	FURFURAL	FURFU RAL	96.08	2338700	*
C5H4O2	FURFURAL	HMFU	96.08	2338700	*
C5H4O2	FURFURAL	FURFU-02	96.08	2338700	**
C5H6O2	FURFURYL-ALCOHOL	FURFU-01	98.10	2687700	*
C5H6O2	FURFURYL-ALCOHOL	FURFU-03	98.10	2687700	*
C5H8O4	XYLAN	XYLAN	132.12	2533665	**
C6H10O5	CELLULOSE	CELLU LOS	162.14	3060411	**
C6H10O5	LEVOGLUCOSAN	LEVOG LUC	162.14	3060411	*
C6H12	2.3-DIMETHYL-2-BUTENE	2:3-D-01	84.16	3970900	*
C6H12	CIS-2-HEXENE	CIS-2-01	84.16	3970900	*
C6H12O5	1-DEOXY-D-GLUCOPYRANOSE	1-DEO-01	164.16	3800470	**
C6H12O6	DEXTROSE	GLUCO LIG	180.16	2982800	*
C6H12O6	DEXTROSE	GLUCO SE	180.16	2982800	*
C6H6	BENZENE	BENZE NE	78.11	3303600	*
C6H6O	PHENOL	PHENO L	94.11	3128500	*
C6H6O6	TRANS-ACONITIC-ACID	ORG-AC	174.11	312850	*
C6H8O	3-METHYL-2-CYCLOPENTEN-1-ONE	3-MET-01	96.13	5102763	**
C7.3H13.9O1.3	LIGNIN	LIGNIN	122.49	3449500	**
C8H10O3	SYRINGOL	SYRIN-01	154.17	5897285	**
C8H18	2.3.4-TRIMETHYLPENTANE	2:3:4-01	114.23	5431100	*
C8H8O	4-HYDROXYSTYRENE	4-HYD-01	120.15	5954310	**
C9H12O2	5-ETHYLGUAIACOL	5-ETH-01	152.19	8640696	**
CA(OH)2	CALCIUM-HYDROXIDE	CAOH2	74.09	53700	*

CA3(PO4)2	CALCIUM-PHOSPHATE	CAL-PHOS	310.18	19400	*
CAO	CALCIUM-OXIDE	CAO	56.08	110200	*
CH1.57N0.29O0.31S0.007	ENZYME	ENZYM E		570246	**
CH1.8O0.9N0.1		YEAST		524490	**
CH4	METHANE	CH4	16.04	831650	*
CH4N2O	UREA	UREA	60.05	689000	**
CH4O	METHANOL	METHA NOL	32.04	718000	*
CL2	CHLORINE	CL2	70.9	123600	*
CO	CARBON-MONOXIDE	CO	28	275100	*
CO2	CARBON-DIOXIDE	CO2	44	19870	*
H2	HYDROGEN	H2	2	236100	*
H2O	WATER	H2O	18	900	*
H2S	HYDROGEN-SULFIDE	H2S	34.08	812000	*
H2SO4	SULFURIC-ACID	H2SO4	98.07	163400	*
H3N	AMMONIA	NH3	17	337900	*
H3PO4	ORTHOPHOSPHORIC-ACID	H3PO4	98	104000	*
HCL	HYDROGEN-CHLORIDE	HCL	36.46	84500	*
K2O	POTASSIUM-OXIDE	MINER ALS	94.20	413100	*
KCL	POTASSIUM-CHLORIDE	SALTS	75.56	19600	*
LIGNIN	LGNSOL	LGNSO L	122.49	3449500	**
N2	NITROGEN	N2	28	720	*
NAOH	SODIUM-HYDROXIDE	NAOH	39.99	74900	*
O2	OXYGEN	O2	32	3970	*
O2S	SULFUR-DIOXIDE	SO2	64.06	313400	*
S	SULFUR	SULFU R	32.06	609600	*
SIO2	SILICON-DIOXIDE	SOIL	60.08	3545	**

\* From Szargut et al. (SZARGUT; MORRIS; STEWARD, 1988).

\*\* Calculated using the correlations linking the ratio of the standard chemical exergy and the net calorific value of the substances (Szargut, J., Morris, D., Steward, F., 1988).

## 4 Chapter III

### **Complete 1G2G biorefinery evaluation regarding simulation and economic assessment.**

Renato Cruz Neves<sup>a,\*</sup>, Edgardo Olivares Gómez<sup>b</sup>, Rubens Maciel Filho<sup>a,c</sup>

<sup>a</sup> Brazilian Bioethanol Science and Technology Laboratory (CTBE), Brazilian Center for Research in Energy and Materials (CNPEM), Zip Code 13083-970, Campinas, Brazil

<sup>b</sup> Mechanical Engineering Department, Federal University of Grande Dourados (UFGD), Dourados, Mato Grosso do Sul, Brazil

<sup>c</sup> School of Chemical Engineering, University of Campinas (UNICAMP), Campinas, São Paulo, Brazil.

\* Corresponding author: Renato Cruz Neves.

Journal name: Biofuels, Bioproducts and Biorefining

This Chapter uses previous information depicted in Chapters I and II and gives the complete 1G2G biorefinery evaluation regarding simulation and economic assessment. For this reason, this Chapter presents downstream processes from fast pyrolysis process presented in Chapter II, i.e. follow the stream from fast pyrolysis process where the next step is the gasification hierarchy.

#### *4.1 Materials and methods*

##### *4.1.1 Gasification Process hierarchy*

Gasification Process hierarchy plays an important role as an intermediate product in the conversion of bioslurry into producer gas. Bioslurry comes from the upstream hierarchy and gas cleaning and conditioning hierarchy is set downstream. Only after gas cleaning and conditioning hierarchy the producer gas will be named as syngas.

A pressurized entrained-flow gasification was chosen. Many parameters were collected from the technological point of view considering experiment and simulation process in Aspen Plus<sup>®</sup> according to Trippe et al. (TRIPPE et al., 2011). Moreover, this gasification reactor type was selected because of the benefits in terms of higher partial pressure conducting to a suitable stream for Fischer-Tropsch process hierarchy (IM-ORB; SIMASATITKUL; ARPORNWICHANOP, 2016b). Finally, this gasification guarantees elevated temperature (1200-2000 °C) which produces high carbon conversion rates and short residence time, besides no tar production (TRIPPE et al., 2011).

The bioslurry coming from pyrolysis hierarchy needs to present low water content (up to 20 wt.%) and maximum of solid contents equal to 50 wt.% (HE; PARK; NORBECK, 2009). Entrained flow gasifier according to bioliq<sup>®</sup> can operate with liquid/solid content up to 2/1 wt.% (TRIPPE et al., 2010).

Since there is no experimental data from gasification of bioslurry produce from LCB, a simplified flowsheet is shown in Figure 2. The parameters inputs are shown in Table 11. To control the gasification hierarchy a couple of Design Spec and Calculators in Aspen Plus<sup>®</sup> were carried out.

The first Design Spec controls the gasification temperature around 1200 °C by fixing the amount of oxygen flow from Air Separation Unit. The entrained flow gasifier is also controlled by the steam input, which controls the mole fraction between H<sub>2</sub> and CO according to a second Design Spec. Water from deaerator passes through a pump and a heater to reach 40 bar and 280 °C, respectively, before entering the entrained flow gasifier. The amount of steam is fixed by a molar ratio equal to 1 of H<sub>2</sub>/CO at the exit of the gasifier. These values are based on Trippe et al. (TRIPPE et al., 2011).

The producer gas is conducted to the Quench system, which is the bottom part of the entrained flow reactor vessel. This system is controlled by a Design Spec. The slag, after the Sep block which presents the removals according to Table 11, goes to a split where 2 wt.% of this amount goes to the disposal off.

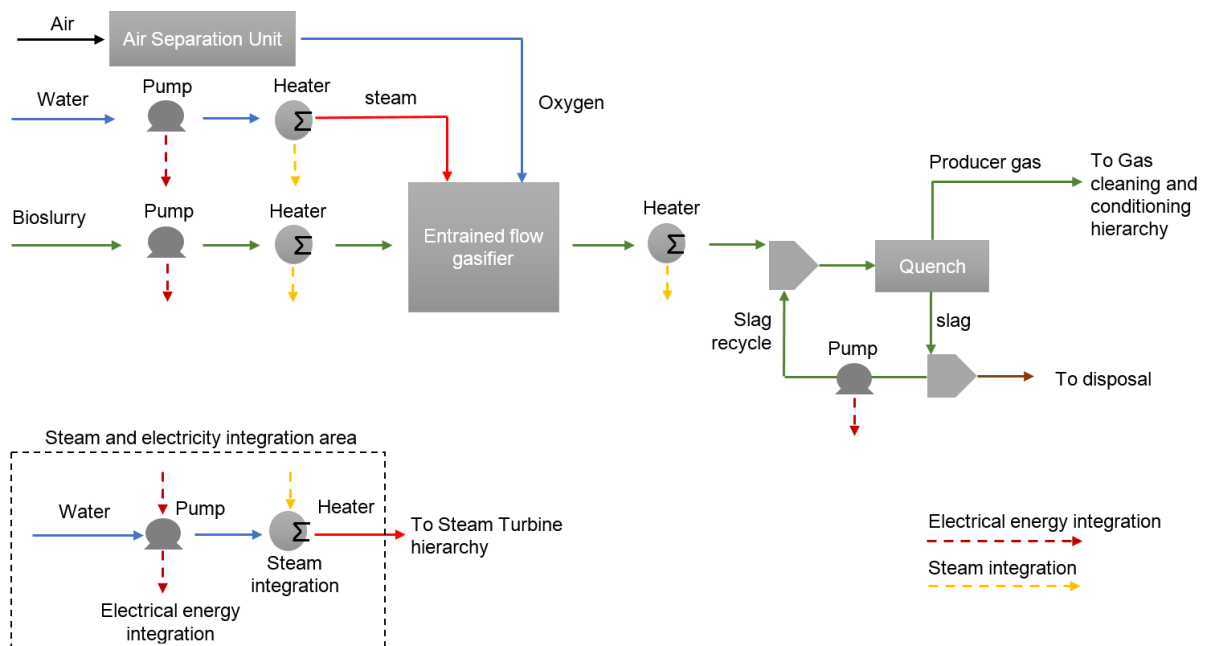


Figure 2. Simplified flowsheet of gasification hierarchy.

Table 11. Block parameters for gasification hierarchy.

Block (Aspen Plus®)	Parameter	Value	Unit
Entrained flow gasifier (RGibbs)	Pressure	40	bar
	Heat duty	0	kW
	Identify possible products	CH <sub>4</sub> , CO <sub>2</sub> , H <sub>2</sub> O, N <sub>2</sub> , O <sub>2</sub> , SO <sub>2</sub> , SOIL, C, H <sub>2</sub> , CO, CL <sub>2</sub> , HCL, H <sub>2</sub> S, H <sub>3</sub> PO <sub>4</sub> , SALTS, MINERALS, COS, NH <sub>3</sub> , HCN	
Quench (Sep)	Removal of H <sub>3</sub> PO <sub>4</sub>	0.99	
	Removal of MINERALS	0.99	
	Removal of SALTS	0.99	
	Removal of SOIL	0.99	
	Removal of C	0.99	

The Air Separation Unit (ASU) consists of several unit operations processes. Basically, ASU compress, purifies, and separates air into its principal components. Due to its complex simulation in Aspen Plus® environment, only the required flow of oxygen (stream with 95 wt.% oxygen and 5 wt.% of nitrogen) for the Entrained Flow Gasifier was simulated (TRIPPE et al., 2011). In this simulation, nitrogen from ASU unit was not assumed to be used on-site or sold, i.e. a conservative estimate was selected according to Trippe et al. (TRIPPE et al., 2011).

#### 4.1.2 Gas cleaning and conditioning hierarchy

The simplified flowsheet of gas cleaning and conditioning hierarchy is shown in Figure 3. This hierarchy is responsible to deliver a gas free of impurities to Fischer-Tropsch synthesis. This hierarchy is comprised mainly by different areas like ceramic filters, direct quench, monoethanolamine which removes acid gases, and zinc oxide guard bed area. Moreover, it is also needed a Low-Cost Aerial Target (LOCAT) area to guarantee the proper disposal. The main parameter inputs are shown in Table 12.

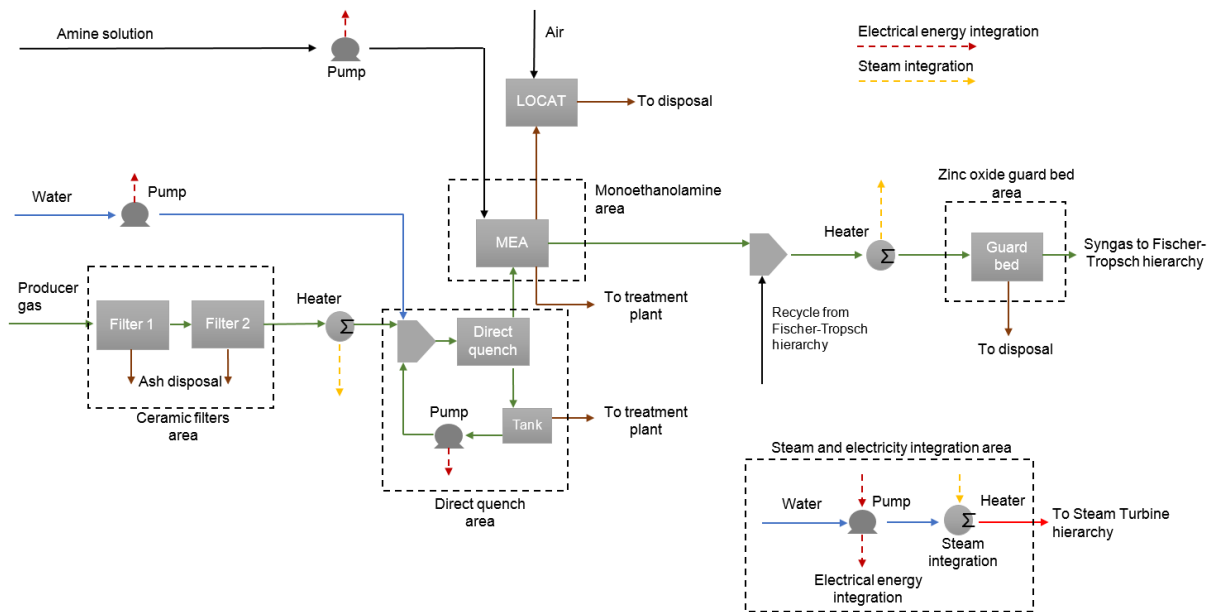


Figure 3. Simplified flowsheet of Gas cleaning and conditioning hierarchy.

Table 12. Block parameters for gas cleaning and conditioning hierarchy.

Block (Aspen Plus®)	Parameter	Value	Unit	Additional information
Filter 1 (Sep) and Filter 2 (Sep)	Removal of H <sub>3</sub> PO <sub>4</sub>	0.99		(MORRIS; ALLEN, 1997; SIKARWAR et al., 2017)
	Removal of MINERALS	0.99		(MORRIS; ALLEN, 1997; SIKARWAR et al., 2017)
	Removal of SALTS	0.99		(MORRIS; ALLEN, 1997; SIKARWAR et al., 2017)
	Removal of SOIL	0.99		(MORRIS; ALLEN, 1997; SIKARWAR et al., 2017)
	Discharge pressure	-0.02	bar	KIT specification
Direct quench (Flash2)	Pressure	-0.1	bar	
	Duty	0	kW	
MEA (Sep)	Removal of CH <sub>4</sub>	0.0013		(SWANSON et al., 2010)
	Removal of CO <sub>2</sub>	0.9		(SWANSON et al., 2010)
	Removal of H <sub>2</sub> O	0.7		(SWANSON et al., 2010)
	Removal of H <sub>3</sub> PO <sub>4</sub>	0.4		(SWANSON et al., 2010)
	Removal of N <sub>2</sub>	0.05		(SWANSON et al., 2010)
	Removal of NH <sub>3</sub>	0.99		(SWANSON et al., 2010)

	Removal of H <sub>2</sub> S	0.99	(SWANSON et al., 2010)
	Removal of HCN	0.05	(SWANSON et al., 2010)
Guard bed (Sep)	Removal of H <sub>3</sub> PO <sub>4</sub>	1	Consideration
	Removal of MINERALS	1	Consideration
	Removal of H <sub>2</sub> S	0.945	(SWANSON et al., 2010)
	Removal of HCL	0.945	Consideration
LOCAT (Rstoic)	Temperature	60	°C
	Reaction 1	H <sub>2</sub> S + 0.5O <sub>2</sub> → H <sub>2</sub> O + S (H <sub>2</sub> S conversions is 0.98)	(SWANSON et al., 2010)
	Reaction 1	SO <sub>2</sub> → S + O <sub>2</sub> (SO <sub>2</sub> conversion is 0.98)	(SWANSON et al., 2010)

Producer gas from Gasification hierarchy passes through two ceramic filters according to Trippe et al. (TRIPPE et al., 2011). Ash is collected and removed from the stream to disposal off. Ceramic filter removal efficiencies were based no literature (MORRIS; ALLEN, 1997; SIKARWAR et al., 2017). Pressure drop around 0.2 bar was set to represent pressure drop due the ceramic filter. This value was collected via experts from the KIT bioliq<sup>®</sup> plant.

Direct quench is set after ceramic filters to mainly remove impurities as ammonia and chloric acid. Producer gas, recycle stream and water are put in contact using a quench system simulated by Flash2 block and the phase separation occurs after a tank simulated by a separation block. Flash2 block estimates the composition of the chemical equilibrium of the phases, thus the removal efficiency is a consequence of this block. After the Flash2 block, there is a separation block controlled by a Design Spec. The values of this Design Spec is set according to Swanson et al. (SWANSON et al., 2010) which determines that 22 wt.% of the producer gas entering the direct quench goes to the recycle stream. This recycle is pumped again to the direct quench system. The water needed to the direct quench system is controlled by another Design Spec, and the main purpose of this stream is to guarantee the functionality of the quench system. Water required for the direct quench system was set equal to 0.11 wt.% of the producer gas, also in accordance with Swanson et al. (SWANSON et al., 2010).

The next area is the Monoethanolamine (MEA) area to guarantee further removal of acid gases. This MEA reactor uses an aqueous solution based on AMINE mainly to remove H<sub>2</sub>S, besides CO<sub>2</sub> to avoid the accumulation of this compound. Basically, this area is explained as follows (SWANSON et al., 2010). This process consists of two columns: one of absorption and the other of regeneration. In the absorption column, the gas is conducted countercurrent to the AMINE solution, where AMINE solution absorbs mainly the H<sub>2</sub>S and CO<sub>2</sub> compounds present in producer gas. The producer gas is removed at the top of the column and passes through a separator where the droplets are carried out by the gas and, then, there is a separation between liquid and gas phases. The solution, now containing H<sub>2</sub>S and CO<sub>2</sub>, is conducted by the regeneration column. This column has a steam generation at the bottom and a condenser at the top. The condensed phase is conveyed to a phase separator from which a gas stream flow with the acid gases (mainly CO<sub>2</sub> and H<sub>2</sub>S) and AMINE solution. This solution in the condenser and the reboiler is reused in the absorption column. Through the mass and molar balance of the compounds present in the synthesis as proposed by Swanson et al. (SWANSON et al., 2010), the solution AMINE (20 wt.% of AMINE compound) is capable of remove 0.35 mol of acid gases by AMINE mol. Considering this complex modeling process of AMINE system, the simulation process only considered a separation block where the producer gas is mixed with a recycle from Pressure Swing Adsorption from Fischer-Tropsch hierarchy, and the acid gas stream goes to treatment plant at LOCAT area.

The gas from MEA block presents high content of acid gases, therefore it is needed a specific treatment. In this case, a Low-Cost Aerial Target (LOCAT) process can treat this gas. LOCAT recuperates solid sulfur via an aqueous process around environment temperature using iron-based catalyst (MERICHEM, 2017). This process is selective for H<sub>2</sub>S while other compounds such as CO<sub>2</sub> crosses the systems with no interaction. The acid gas stream goes to an oxidant vessel where occurs the oxidization of hydrosulfide ions to elemental sulfur by reducing from ferric iron (Fe<sup>+3</sup>) to ferrous iron (Fe<sup>+2</sup>) and, as a final step, there is a reoxidation step of ferrous ions to ferric ions through air contact (MERICHEM, 2017). The simulation of LOCAT was performed according to Swanson et al. (SWANSON et al., 2010) where a Design Spec was fixed to control the air entrance in the reactor vessel LOCAT. This control is set to give a mole flow of O<sub>2</sub> equal to 2 times more than the mass flow of H<sub>2</sub>S varying the air entering the LOCAT reactor. After this vessel, the stream goes to discard.

The producer gas from MEA block is mixed with a recycle from Pressure Swing Adsorption (PSA) which is part of the Fischer-Tropsch hierarchy. After the mixing step, this

stream crosses a Guard Bed composed mainly by zinc oxide (ZnO) and activated carbon (BOERRIGTER; UIL; CALIS, 2002). These compounds are capable of remove the last impurities in producer gas to guarantee a desired syngas quality to the Fischer-Tropsch synthesis and avoid the impurities accumulation (BOERRIGTER; UIL; CALIS, 2002). The impurities are moved to the disposal while the clean producer gas, named as syngas, is conducted to the Fischer-Tropsch hierarchy.

#### 4.1.3 Fischer-Tropsch hierarchy

The simplified flowsheet of Fischer-Tropsch hierarchy is shown in Figure 4. This hierarchy is responsible to produce biojet fuel, besides green naphtha production and light gases which will be conducted to the gas turbine hierarchy. Moreover, there is also a recycle stream to the gas cleaning and conditioning hierarchy. Fischer-Tropsch hierarchy is comprised mainly by a Water-Gas-Shift (WGS) reactor, Fischer-Tropsch reactor, and column to separate biojet fuel, green naphtha, wax and light gases. The main parameter inputs for this hierarchy are shown in Table 13.

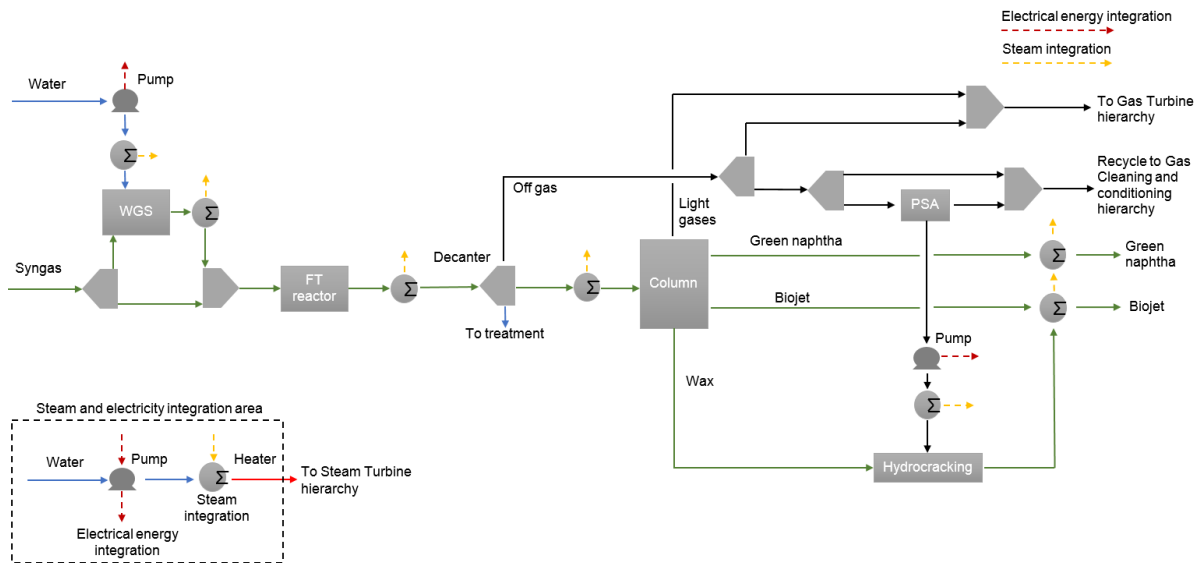


Figure 4. Simplified flowsheet of Fischer-Tropsch hierarchy.

Table 13. Block parameters for Fischer-Tropsch hierarchy.

Block (Aspen Plus®)	Parameter	Value	Unit	Additional information
WGS (REquil)	Pressure	25	bar	(PONDINI; EBERT, 2013)
	Duty	0	kW	
	Pressure drop	50	mbar	(PONDINI; EBERT, 2013)

	Reaction	$\text{CO} + \text{H}_2\text{O} \rightarrow \text{H}_2 + \text{CO}_2$		(PONDINI; EBERT, 2013)
FT reactor (RStoic)	Temperature	180	°C	(KLERK, 2011)
	Pressure drop	1	bar	(PONDINI; EBERT, 2013)
Decanter (Flash3)	Temperature	35	°C	
	Key component in 2nd liquid phase	H <sub>2</sub> O		
Column (RadFrac)	Calculation type	Equilibrium		(KLEIN et al., 2018) and CTBE internal data
	Number of Stages	35		(KLEIN et al., 2018) and CTBE internal data
	Condenser	Partial-Vapor-Liquid		(KLEIN et al., 2018) and CTBE internal data
	Reboiler	Kettle		(KLEIN et al., 2018) and CTBE internal data
	Valid Phases	Vapor-Liquid		(KLEIN et al., 2018) and CTBE internal data
	Convergence	Petroleum/Wide-boiling		(KLEIN et al., 2018) and CTBE internal data
	Feed stream (above-stage)	28		(KLEIN et al., 2018) and CTBE internal data
	Wax stream (liquid)	35		(KLEIN et al., 2018) and CTBE internal data
	Biojet stream (liquid)	30		(KLEIN et al., 2018) and CTBE internal data
	Green naphtha stream (liquid)	1		(KLEIN et al., 2018) and CTBE internal data
	Light gases (vapor)	1		(KLEIN et al., 2018) and CTBE internal data
	Pressure state	1.013	bar	(KLEIN et al., 2018) and CTBE internal data
Hydrocracking (RYield)	1/condenser pressure			
	C <sub>8</sub> H <sub>18</sub>	0.220	wt. %	Adpated from (KLERK, 2011)
	C <sub>9</sub> H <sub>20</sub>	0.179	wt. %	Adpated from (KLERK, 2011)
	C <sub>10</sub> H <sub>22</sub>	0.146	wt. %	Adpated from (KLERK, 2011)
	C <sub>11</sub> H <sub>24</sub>	0.119	wt. %	Adpated from (KLERK, 2011)
	C <sub>13</sub> H <sub>28</sub>	0.097	wt. %	Adpated from (KLERK, 2011)
	C <sub>14</sub> H <sub>30</sub>	0.079	wt. %	Adpated from (KLERK, 2011)
	C <sub>15</sub> H <sub>32</sub>	0.064	wt. %	Adpated from (KLERK, 2011)
	C <sub>16</sub> H <sub>34</sub>	0.043	wt. %	Adpated from (KLERK, 2011)
PSA (Sep) - stream to hydrocracking reactor	CH <sub>4</sub>	0.007	wt. %	Adpated from (KLERK, 2011)
	CO <sub>2</sub>	0.007	wt. %	Adpated from (KLERK, 2011)
	N <sub>2</sub>	0.007	wt. %	Adpated from (KLERK, 2011)
	O <sub>2</sub>	0.007	wt. %	Adpated from (KLERK, 2011)
	H <sub>2</sub>	0.930	wt. %	Adpated from (KLERK, 2011)

CO	0.007	wt. %	Adpated from (KLERK, 2011)
NH3	0.007	wt. %	Adpated from (KLERK, 2011)
C2H6	0.007	wt. %	Adpated from (KLERK, 2011)
C3H8	0.007	wt. %	Adpated from (KLERK, 2011)
C4H10	0.007	wt. %	Adpated from (KLERK, 2011)

WGS is responsible to adequate the molar ratio of H<sub>2</sub>/CO for the Fischer-Tropsch reactor. This reactor is fixed by two Design Specs. Basically, one Design Specs depends on another. The first Design Spec controls the amount of steam to the WGS reactor regulating a mole flow of steam equal to four times the CO molar flow in syngas. This value needs to be higher than 3 to guarantee no carbon deposition (PONDINI; EBERT, 2013). The second Design Spec controls the split fraction to the WGS by fixing the H<sub>2</sub>/CO molar ratio equal to 1.7 at the entrance of the FT reactor.

The Fischer-Tropsch reactor is responsible to convert CO and H<sub>2</sub> into liquid hydrocarbons. Due to syngas characteristics after WGS reactor (H<sub>2</sub>/CO molar ratio 1.7, temperature around 180 °C) and biojet range from FT reactions, a slurry Co-based Low-Temperature Fischer-Tropsch reactor was selected with reactor volume up to 190 m<sup>3</sup> (HU, 2012; IM-ORB; SIMASATITKUL; ARPORNWICHANOP, 2016b). Moreover, the simulation of the FT reactor was chosen according to the proposed models by some authors (IM-ORB; SIMASATITKUL; ARPORNWICHANOP, 2016b; PONDINI; EBERT, 2013).

The Anderson-Schulz-Flory (ASF) distribution was selected to predict the chain growth probability  $\alpha$  of the FT products. Equations are presented from Equation 1 to 4 (IM-ORB; SIMASATITKUL; ARPORNWICHANOP, 2016b):

$$\alpha = 0.75 - 0.373\sqrt{-\log S_{C_{5+}}} + 0.25S_{C_{5+}} \quad \text{Equation 5}$$

$$S_{C_{5+}} = 1.7 - 0.0024T - 0.088\frac{[H_2]}{[CO]} + 0.18([H_2] + [CO]) + 0.0079P_{total} \quad \text{Equation 6}$$



$$M_n = \alpha^{n-1}(1 - \alpha) \quad \text{Equation 8}$$

Where  $S_{C_{5+}}$  is the selectivity of hydrocarbon with a chain length longer than 5,  $n$  is number of carbon range,  $[H_2]$  and  $[CO]$  are the molar concentration of H<sub>2</sub> and CO in the syngas before FT

reactor,  $T$  and  $P_{total}$  are the operating temperature (K) and pressure (bar), respectively. These equations are governed by the CO conversion equal to 40% (SWANSON et al., 2010).

The ASF distribution can also be performed using mass fraction instead of molar fraction as presented by the following equation (PONDINI; EBERT, 2013):

$$M_n = \alpha^{n-1}(1 - \alpha)^2 n \quad \text{Equation 9}$$

The equations presented only consider paraffins compounds ( $C_nH_{2n+2}$ ). To guarantee more reliable FT products from FT reactor, olefins compounds ( $C_nH_{2n}$ ) were also added to this distribution according to the equation as follows (PONDINI; EBERT, 2013):

$$O/P = e^{-cn} \quad \text{Equation 10}$$

Where the number of olefins  $O$  is a relation between the amount of paraffins  $P$ , carbon range  $n$  valid for C8-C16, and  $c$  is a number between 0.19 and 0.49. In this case, it was adopted  $c$  equal to 0.40.

After the FT reactor, the stream is conducted to a flash followed by a decanter simulated only by a decanter block (PONDINI; EBERT, 2013). This block separates liquid fraction which goes to the treatment plant, liquid hydrocarbons which goes to the separation column, and off gas which is separated between PSA, recycle and Gas turbine hierarchy. The PSA reactor is a zeolite-based reactor responsible for adsorption for all components, except hydrogen, allowing it to separate from the stream. The main purpose of the recycle stream is to increase the conversion of the unconverted syngas left after the FT reactor. The separated gas from PSA joins to the recycle stream while hydrogen from PSA is used in the hydrocracking reactor. The recycle ratio of off-gas to the gas cleaning and conditioning hierarchy was set equal to 0.6, which is near to 0.51 reported by Swanson (SWANSON et al., 2010) and in the range of 0.1-0.9 according to Im-Orb et al. (IM-ORB; SIMASATITKUL; ARPORNWICHANOP, 2016a). Liquid hydrocarbons from decanter pass through column to be separated into various fraction: light gases, green naphtha, wax, and biojet fuel. Light gases are mixed with the separated fraction of off gas and both are conducted to the Gas Turbine hierarchy. Green naphtha is a final product due to complexity or advanced configuration to convert into biojet fuel (PONDINI; EBERT, 2013). Wax is hydrocracked using hydrogen from PSA to produce more biojet fuel. This conversion can reach up to 85-99% of conversion using Pt/ZSM-22 catalyst in the hydrocracking reactor (BOUCHY et al., 2009; CALEMMMA et al., 2010) considering 0.5 wt.% of Pt (STEYNBERG; DRY, 2004). Hydrocracking reactor reduces the long carbon chains and introduces branching chain in paraffinics in the biojet fuel range

(KLEIN et al., 2018; MCCALL et al., 2009). Biojet fuel from column together with biojet fuel from hydrocracking reactor are mixed to produce the final amount of biojet fuel.

There is a Design Spec to control the hydrogen amount required by the hydrocracking reactor. In the case of FT reactor selected to this simulation, hydrocracking technology was carried out to convert wax into biojet fuel range considering the ratio of hydrogen per wax equal to 1 wt.% (KLERK, 2011). Therefore, the Design Spec fixes the separation block of syngas to the PSA reactor.

As biojet fuel is not restrictive concerning molecular composition (KLERK, 2011), the configuration represented in this work via FT reactor and hydrocracking reactor for biojet fuel production gives a suitable biojet fuel to be mixed with conventional jet fuel (KLEIN et al., 2018; KLERK, 2011).

#### 4.1.4 Gas turbine hierarchy

Gas turbine hierarchy is responsible for producing electricity and steam for the overall combined heat and power integration. Figure 5 shows a simplified flowsheet for this hierarchy. The main parameter inputs for this hierarchy are shown in Table 14.

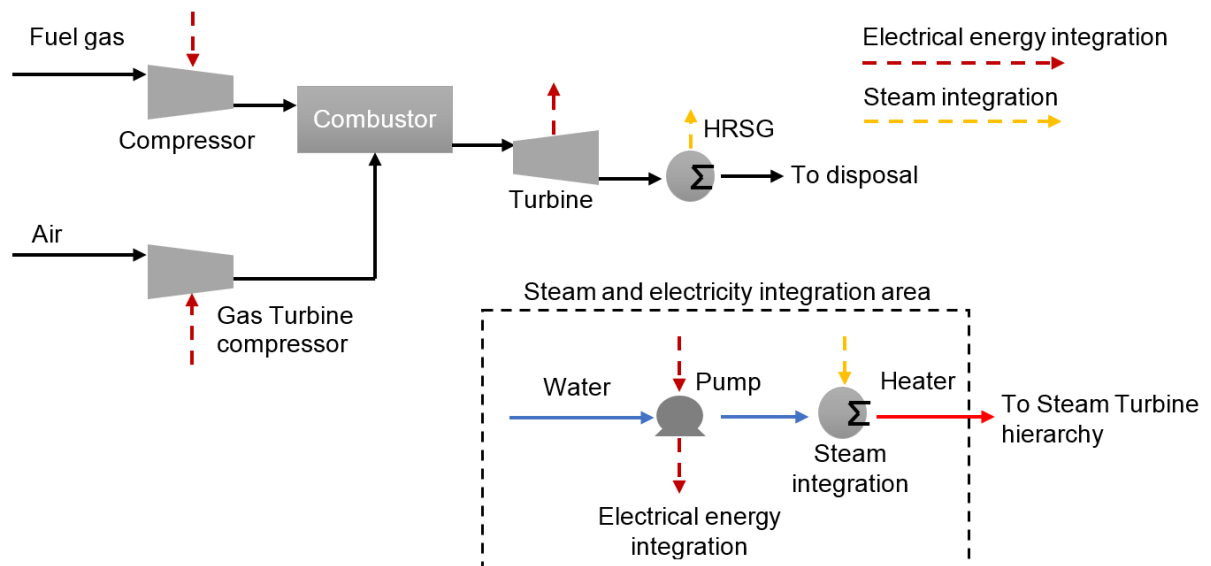


Figure 5. Simplified flowsheet of Gas Turbine hierarchy.

Table 14. Block parameters for Gas Turbine hierarchy.

Block (Aspen Plus®)	Parameter	Value	Unit	Additional information
Fuel gas compressor (Compr)	Model	Compressor		
	Type	Isentropic		
	Discharge pressure	21	bar	
	Isentropic efficiency	0.9433		CTBE database
	Mechanical efficiency	0.99		CTBE database
Combustor (RStoic)	Pressure	0	bar	Generate combustion reactions
	Duty	0	kW	
Air compressor (Compr)	Model	Compressor		
	Type	Isentropic		
	Discharge pressure	21	bar	CTBE database
	Isentropic efficiency	0.9433		CTBE database
	Mechanical efficiency	0.99		CTBE database
Turbine (Compr)	Model	Turbine		
	Discharge pressure	1.2	bar	CTBE database
	Isentropic efficiency	0.9433		CTBE database
	Mechanical efficiency	0.99		CTBE database

Fuel gas from Fischer-Tropsch hierarchy is compressed and then is mixed with compressed air to be burned in a combustor. Gas burned is expanded in a gas turbine providing power and energy. Power is converted into electrical energy while flue gas goes to the Heat Recovery Steam Generator (HRSG) to produce steam. Flue gas from HRSG is disposed off while steam is conducted to the Steam turbine hierarchy.

The outlet temperature of the combustor before expanding is fixed by a Design Spec. The temperature equal to 1350 °C is controlled by the air amount into the combustor chamber.

#### 4.1.5 *Steam turbine hierarchy*

Steam turbine hierarchy is responsible for producing electricity and water (or steam) for the overall combined heat and power integration, including the 1G sugarcane integration. Figure 6 shows a simplified flowsheet for this hierarchy. The main parameter inputs for this hierarchy are shown in Table 15



Compressors and gas and steam turbines in the gas turbine hierarchy and steam turbine hierarchy, respectively, were simulated assuming common isentropic and mechanical efficiencies as shown in Table 14 and Table 15.

Steams with different pressures and temperatures are produced across the hierarchies. Different hierarchies produce different sort of steam dependently on the heat consumed/generated by each hierarchy. Three values of steam with the respective temperatures were considered: 90 bar, 22 bar, and 2.5 bar. The steam with 90 bar is expanded in a back-pressure steam turbine to produce power and the outlet stream is then mixed with steam at 22 bar. A fraction is collected to supply the steam demand for the integration into 1G sugarcane biorefinery while the other fraction is expanded in a back-pressure steam turbine to 2.5 bar. Two extractions are performed. The first extraction is for the integration into 1G sugarcane biorefinery, the second extraction is for controlling steam parameters for the deaerator (1.4 bar and 105 °C). The remaining fraction is conducted to a condensing extracting steam turbine up to 0.83 bar. The outlet stream is conducted to a cooling tower and, after a pump, is mixed with all stream coming out of this hierarchy. The outlet stream is then conducted to the deaerator and to the overall steam integration. A Design Spec controls the temperature to integration (deaerator) by fixing the steam control coming from extraction separator. The temperature set is equal to 105 °C. Power demand converted into electricity is integrated to supply electricity for the overall integration process regarding thermochemical plant and 1G sugarcane biorefinery.

#### 4.1.6 *Steam and electricity integration*

Water treated from the treatment water plant is mixed with water from steam turbine hierarchy. Two water streams are separated. The first stream water is the process integration of water, which is converted into steam within the hierarchies. In this case, water is conducted to five hierarchies: Biomass Handling and Feeding, Pyrolysis, Gasification, Gas Cleaning and Conditioning, and Gas Turbine. The second stream water is consumed by the hierarchies. In this case, water is consumed into the direct quench area in the Gas Cleaning and Conditioning hierarchy, water to the entrained flow gasifier in the Gasification hierarchy, and water to the Water Gas Shift reactor in the Fischer-Tropsch hierarchy. Additional water was performed by a water makeup controlled by a Design Spec set equal to 5% of more water for each loop varying the amount of water that comes from the water treatment plant.

Water from deaerator passes through a pump, simulated as Pump using liquid-only option, which was simulated with 0.7 of pump efficiency and 0.99 of driver efficiency. After the pump, the stream passes through a heater simulated by Heater using valid phase as Vapor-Only. These values were the same according to the First-Generation simulation by Bonomi et al (BONOMI, A., CAVALETT, O., DA CUNHA, M. P., & LIMA, 2016). Pressure of steam produced is in accordance with the available thermal energy for each hierarchy, where process steam is produced in heat recovery generators.

Electricity is used across the hierarchies through pumps, bucket elevator, among others. Moreover, electricity is also needed for the integration into 1G sugarcane biorefinery. Then, a split block controls the 1G electricity demands, thermochemical plant demand, and surplus electricity.

#### 4.1.7 *Scenarios*

Two scenarios were simulated as presented in Figure 7. Centralized scenario considers the overall integration from sugarcane and straw collected from the field via bales to biojet fuel and green naphtha production, covering also heat and power integration. The decentralized scenario considers bioslurry production from surplus sugarcane bagasse and straw collected from the field and the transportation of this material to the central facility to produce biojet fuel and green naphtha.

Different scenarios lead to different simulation models, especially due to the difference of sugarcane bagasse and straw for centralized and decentralized scenarios. However, this simulation difference is mainly caused by the steam and electricity integration. Therefore, equipment and parameter inputs for both scenarios were set equal for both scenarios of simulation.

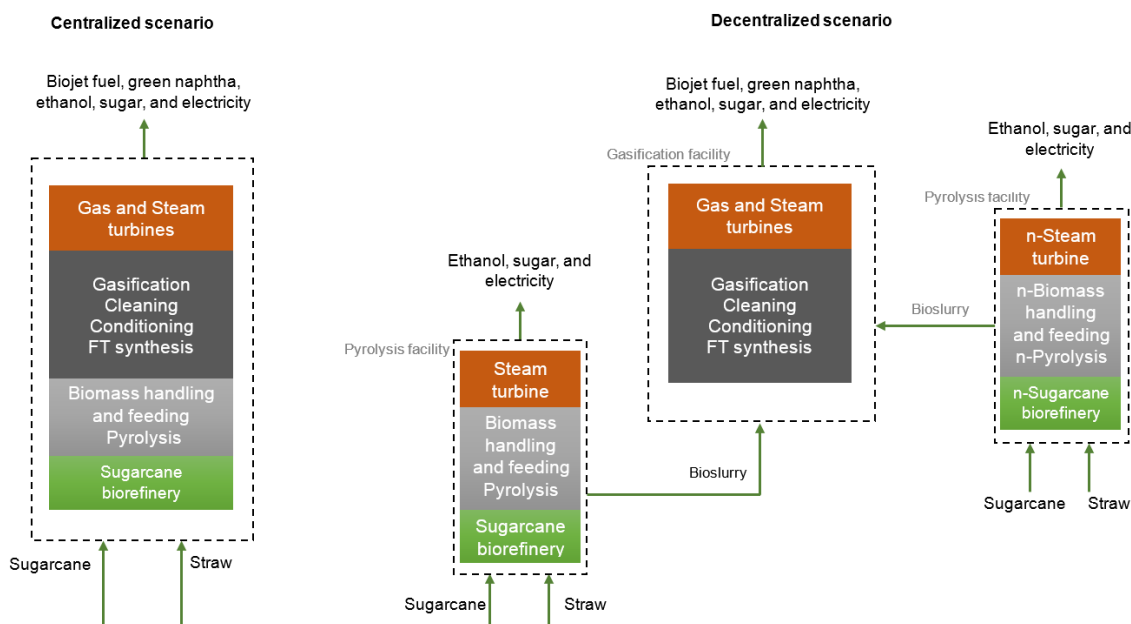


Figure 7. Centralized and decentralized biorefinery scenarios.

#### 4.1.8 Economic assessment

To perform economic feasibility between two scenarios presented, an economic study was carried out in accordance with CTBE database and correlated works, i.e. all input and output parameters, analysis and modeling were retrieved from Virtual Sugarcane Biorefinery, where agricultural system is fully integrated to the industrial scenarios (BONOMI, A., CAVALETT, O., DA CUNHA, M. P., & LIMA, 2016; DIAS et al., 2014; KLEIN et al., 2018) via CanaSoft model (CAVALETT et al., 2016). The main parameters for economic feasibility are presented in Table 16.

Table 16. Main parameters considered for economic feasibility.

Item	Value	Reference
Expected plant lifetime	25 years	(WATANABE et al., 2016)
Discount rate	12%/year	(WATANABE et al., 2016)
Exchange rate	3.352 R\$/US\$ or 3.528 R\$ per € (Dez/2016)	(WATANABE et al., 2016)
Depreciation	10 years (linear)	(WATANABE et al., 2016)
Construction time	2	(DIAS et al., 2012b)
Anhydrous ethanol price	1.70 R\$/L	CTBE database (KLEIN et al., 2018)
Sugar price	1.00 R\$/kg	CTBE database
Electricity price	193 R\$/MWh	Ministério de minas e energia

Jet fuel price	2.02 R\$/L	CTBE database CTBE database (KLEIN et al., 2018)
Green naphtha price	2.04 R\$/L	CTBE database CTBE database (KLEIN et al., 2018)

The main parameters used were based on CTBE database considering economic parameters where the assessment is based on cash flow analysis for each scenarios, taking into account all expenses, investment, and revenues for each scenario considered (WATANABE et al., 2016). Economic parameters are set as payback period, net present value (NPV), internal rate of return (IRR), the production cost, and cost allocation (WATANABE et al., 2016).

Payback period or time is the required period for the profit to equal the cost of the investment. NPV is the difference between the cash inflows and the present value of cash outflows. IRR is the average interest rate paid per year by the evaluated project, in which the minimum acceptable rate of return is 12% per year, this value is reasonable for sugarcane mill in Brazil (WATANABE et al., 2016) considering the plant 100% equity financed. Cost allocation is the cost allocated among the products according to the share on the total revenues. Basically, the equations are:

$$NPV = \sum_{n=0}^{n=N} \frac{C_n}{(1+r)^n}$$

$$\sum_{n=0}^{n=N} \frac{C_n}{(1+IRR)^n} = 0$$

The information data was collected from hierarchies involving the overall process, for example, the determination of data for calculation basis, equipment considered in simulation processes and/or similar processes, information based on raw materials, and close scenarios for comparative purposes. Equipment costing data, and installation factors, are collected from direct quotation, published data, or CTBE database.

Cost of specific equipment is correlated by the following equation:

$$Ce = Cr \left( \frac{Se}{Sr} \right)^n$$

Where  $Ce$  is the cost of equipment,  $Cr$  is the cost of reference,  $Se$  is the size of equipment,  $Sr$  is the size of reference, and  $n$  is the exponential growth factor (FONSECA, 2015; WRIGHT et al., 2010). Working capital is considered 15% of the fixed capital investment (DO; LIM; YEO, 2014). After estimating the equipment costs, a contingency factor of 35% was

applied to project the total equipment costs, which includes, pumps, heaters, among others (D.W. GREEN, 2008).

## 5 Discussion

In order to ensure the complete discussion of this thesis, the next sessions cover the discussion from the Gasification hierarchy to techno-economic indicators, since the previous discussions have already been approached in Chapters I and II.

### 5.1 Gasification hierarchy

A summary of gasification hierarchy results is presented in Table 17. The mass flow from ASU unit to the entrained flow gasifier is 75517 kg/h and 80989 kg/h for centralized and decentralized scenarios, respectively. Steam required is 53740 and 58194 kg/h for centralized and decentralized scenarios, respectively. With these values simulated, oxygen to bioslurry ratio for both scenarios was 0.35. Dahmen et al. (DAHMEN et al., 2012) reported an oxygen/(oxygen + biomass) ratio in the range of 0.4-0.5. Steam to bioslurry ratio simulated was 0.55, Im-Orb et al. (IM-ORB; SIMASATITKUL; ARPORNWICHANOP, 2016a) reported a value from 0.57 to 2.86 and Chiodini et al. (CHIODINI et al., 2017) reported values in the range of 0.20-0.78. Lower Heating Value (LHV) of the producer gas was around 6.9 kJ/kg for both scenarios, leading to a thermal power demand equal to 500 MW for centralized scenario and 523 MW for decentralized scenario. These results are sufficient to reach a temperature near to 1240 °C with H<sub>2</sub>/CO molar ratio equal to 1.01 for both scenarios, as proposed for entrained flow gasification reactors (LA VILLETТА; COSTA; MASSAROTTI, 2017; TRIPPE et al., 2011).

Steam produced in this hierarchy reached 530 °C and 90 bar, which is conducted to the steam turbine hierarchy. Power required was around 1600 kW for both scenarios, however it is not neglected ASU unit. ASU unit consumes 0.45 kWh (electrical) per Nm<sup>3</sup> of oxygen (HENRICH; DAHMEN; DINJUS, 2009), therefore, it was calculated around 26 MW of electrical energy for each scenario considering the mass flow of oxygen for the specific consumption within entrained flow reactor.

Table 17. Summary results of gasification hierarchy.

Process or parameters	Variable	Unit	Centralized	Decentralized
			Value	Value

Bioslurry mass flow from pyrolysis hierarchy	Mass flow	kg/h	131508	141115	
Mass flow from ASU unit to Entrained flow gasifier	Temperature	°C	120	120	
	Pressure	bar	40	40	
	N2	kg/h	3335	3567	
	O2	kg/h	72382	77421	
	Temperature	°C	280	280	
Steam to Entrained flow gasifier	Pressure	bar	40	40	
	H2O	kg/h	56740	58194	
	Temperature	°C	1235.04	1239	
Producer gas	Pressure	bar	40	40	
	CH4	kg/h	1.74E+01	1.87E+01	
	CO2	kg/h	7.45E+04	7.85E+04	
	H2O	kg/h	8.19E+04	8.56E+04	
	H3PO4	kg/h	1.84E+01	1.96E+01	
	MINERALS	kg/h	2.12E+02	2.25E+02	
	N2	kg/h	3.53E+03	3.77E+03	
	O2	kg/h	8.19E-08	9.18E-08	
	SALTS	kg/h	2.54E+03	2.70E+03	
	SOIL	kg/h	1.07E+03	1.13E+03	
	C	kg/h	1.19E-15	1.47E-15	
	H2	kg/h	6.94E+03	7.41E+03	
	CO	kg/h	9.32E+04	1.01E+05	
	CL2	kg/h	1.37E-16	1.52E-16	
	NH3	kg/h	7.22E+00	7.67E+00	
	HCL	kg/h	1.17E-02	1.26E-02	
	HCN	kg/h	2.44E-01	2.71E-01	
	Total mass flow	kg/h	2.64E+05	2.80E+05	
	To disposal	Temperature	°C	252	252
		Pressure	bar	40	40
		H3PO4	kg/h	1.80E+01	1.91E+01
		MINERALS	kg/h	2.07E+02	2.20E+02
		SALTS	kg/h	2.48E+03	2.64E+03
SOIL		kg/h	1.04E+03	1.11E+03	
Total mass flow		kg/h	3.75E+03	3.98E+03	
Producer gas to gas cleaning and conditioning hierarchy	Temperature	°C	252	252	
	Pressure	bar	40	40	
	CH4	kg/h	1.74E+01	1.87E+01	
	CO2	kg/h	7.45E+04	7.85E+04	
	H2O	kg/h	8.19E+04	8.56E+04	
	H3PO4	kg/h	4.37E-01	4.64E-01	
	MINERALS	kg/h	5.04E+00	5.35E+00	
	N2	kg/h	3.53E+03	3.77E+03	
	O2	kg/h	8.19E-08	9.18E-08	
	SALTS	kg/h	6.04E+01	6.41E+01	
	SOIL	kg/h	2.53E+01	2.69E+01	

	H2	kg/h	6.94E+03	7.41E+03
	CO	kg/h	9.32E+04	1.01E+05
	NH3	kg/h	7.22E+00	7.67E+00
	HCL	kg/h	1.17E-02	1.26E-02
	HCN	kg/h	2.44E-01	2.71E-01
	Total mass flow	kg/h	2.60E+05	2.76E+05
Steam produced	Temperature	°C	530	530
	Pressure	bar	90	90
	Mass flow	kg/h	118518	127836
Electricity needed	Power required	kW	1537	1676
ASU demand	Power required	kW	25759	27552
Total power required	Power required	kW	27296	29228

Producer gas contains impurities which must be removed before the Fischer-Tropsch synthesis. Therefore, producer gas stream exiting the gasification hierarchy is connected to the gas cleaning and conditioning hierarchy.

## 5.2 Gas cleaning and conditioning hierarchy

The main goal of this hierarchy is to ensure the clean producer gas to the Fischer-Tropsch hierarchy. Therefore, Table 18 presents a summary of the main results of this hierarchy.

The mass flow of producer gas after MEA reactor was 111325 kg/h and 120132 kg/h for centralized and decentralized scenarios, respectively. This stream is mixed with the recycle of the Fischer-Tropsch hierarchy. The mass flow of the recycle stream from Fischer-Tropsch is 150847 kg/h and 163524 kg/h for centralized and decentralized scenarios. This mixture is conducted to the guard bed reactor. Considering these values of mass flow, the mass ratio of recycle stream per producer gas was 1.35 for both scenarios. These mixed streams lead to the composition presented in Table 18, in which contain a small fraction of the light Fischer-Tropsch products.

Table 18. Summary results of gas cleaning and conditioning hierarchy.

Process or parameters	Variable	Unit	Centralized	Decentralized
			Value	Value
Amine solution	Temperature	°C	25	25
	Pressure	bar	1.01	1.01
	AMINE	kg/h	2	2

	Phase		Liquid	Liquid
Water to direct quench	Temperature	°C	30	30
	Pressure	bar	1.01	1.01
	H2O	kg/h	2.94E+03	3.13E+03
Air to LOCAT	Temperature	°C	30	30
	Pressure	bar	1.01	1.01
	N2	kg/h	7.67E-02	7.67E-02
	O2	kg/h	2.33E-02	2.33E-02
Ash disposal from filter 1	Temperature	°C	247	247
	Pressure	bar	25.00	25.00
	H3PO4	kg/h	4.37E-01	4.64E-01
	MINERALS	kg/h	5.03E+00	5.35E+00
	SALTS	kg/h	5.98E+01	6.35E+01
	SOIL	kg/h	2.51E+01	2.67E+01
	Total mass flow	kg/h	9.03E+01	9.59E+01
Ash disposal from filter 2	Temperature	°C	247	247
	Pressure	bar	24.98	24.98
	H3PO4	kg/h	4.37E-04	4.64E-04
	MINERALS	kg/h	5.03E-03	5.35E-03
	SALTS	kg/h	5.98E-01	6.35E-01
	SOIL	kg/h	2.51E-01	2.67E-01
	Total mass flow	kg/h	8.54E-01	9.07E-01
To treatment plant from direct quench	Temperature	°C	59	59
	Pressure	bar	24.88	24.88
	CH4	kg/h	4.78E-04	5.00E-04
	CO2	kg/h	1.94E+01	2.00E+01
	H2O	kg/h	8.35E+04	8.73E+04
	H3PO4	kg/h	2.15E-10	2.24E-10
	MINERALS	kg/h	1.84E-07	1.91E-07
	N2	kg/h	1.13E-02	1.18E-02
	O2	kg/h	4.36E-12	4.78E-12
	SALTS	kg/h	6.04E-03	6.41E-03
	SOIL	kg/h	2.53E-03	2.69E-03
	H2	kg/h	7.77E-02	8.11E-02
	CO	kg/h	3.12E-01	3.30E-01
	NH3	kg/h	5.48E+00	5.79E+00
	HCL	kg/h	3.98E-05	4.16E-05
	HCN	kg/h	3.00E-04	3.26E-04
Total mass flow	kg/h	8.36E+04	8.74E+04	

To treatment plant from MEA	Temperature	°C	59	59	
	Pressure	bar	24.88	24.88	
	AMINE	kg/h	2.00	2.00	
To disposal from LOCAT	Temperature	°C	60	60	
	Pressure	bar	1.01	1.01	
	CH4	kg/h	2.27E-02	2.43E-02	
	CO2	kg/h	6.71E+04	7.07E+04	
	H2O	kg/h	8.82E+02	9.44E+02	
	H3PO4	kg/h	1.75E-07	1.86E-07	
	N2	kg/h	1.76E+02	1.89E+02	
	O2	kg/h	2.33E-02	4.66E-02	
	NH3	kg/h	1.66E+00	1.79E+00	
	HCN	kg/h	1.22E-02	1.35E-02	
	Total mass flow	kg/h	6.82E+04	7.19E+04	
	To disposal from Guard Bed	Temperature	°C	200	200
		Pressure	bar	24.88	24.88
H3PO4		kg/h	2.62E-07	2.78E-07	
MINERALS		kg/h	4.85E-06	5.16E-06	
HCL		kg/h	1.14E-02	1.22E-02	
Total mass flow		kg/h	1.14E-02	1.22E-02	
Syngas to Fischer-Tropsch hierarchy (Considering recycle)		Temperature	°C	200	200
	Pressure	bar	24.88	24.88	
	CH4	kg/h	6.79E+03	7.30E+03	
	CO2	kg/h	8.61E+04	9.38E+04	
	H2O	kg/h	6.58E+02	7.07E+02	
	N2	kg/h	8.38E+03	8.96E+03	
	O2	kg/h	2.05E-07	2.29E-07	
	H2	kg/h	1.09E+04	1.17E+04	
	CO	kg/h	1.35E+05	1.46E+05	
	NH3	kg/h	9.46E-02	1.02E-01	
	HCL	kg/h	6.65E-04	7.12E-04	
	C2H6	kg/h	4.74E+03	5.10E+03	
	C3H8	kg/h	3.50E+03	3.76E+03	
	C4H10	kg/h	2.57E+03	2.76E+03	
	C5H12	kg/h	1.78E+03	1.92E+03	
	METHANOL	kg/h	4.85E+01	5.23E+01	
	HCN	kg/h	5.41E-01	6.02E-01	
	C6H14	kg/h	1.07E+03	1.15E+03	
	C7H16	kg/h	5.21E+02	5.63E+02	

C8H18	kg/h	1.99E+02	2.15E+02
C9H20	kg/h	6.71E+01	7.26E+01
C10H22	kg/h	2.14E+01	2.32E+01
C11H24	kg/h	6.76E+00	7.32E+00
C12H26	kg/h	2.11E+00	2.28E+00
C13H28	kg/h	6.92E-01	7.51E-01
C14H30	kg/h	2.43E-01	2.63E-01
C15H32	kg/h	7.92E-02	8.60E-02
C16H34	kg/h	2.81E-02	3.05E-02
C17H36	kg/h	8.48E-03	9.20E-03
C18H38	kg/h	3.02E-03	3.27E-03
C19H40	kg/h	1.06E-03	1.15E-03
C20H42	kg/h	3.26E-04	3.54E-04
C21H44	kg/h	1.22E-04	1.33E-04
C22H46	kg/h	5.04E-05	5.48E-05
C23H48	kg/h	1.55E-05	1.68E-05
C24H50	kg/h	5.50E-06	5.99E-06
C25H52	kg/h	2.15E-06	2.34E-06
C26H54	kg/h	7.61E-07	8.26E-07
C27H56	kg/h	2.29E-07	2.49E-07
C28H58	kg/h	1.14E-07	1.24E-07
C29H60	kg/h	5.23E-08	5.70E-08
C30H62	kg/h	2.06E-08	2.24E-08
C31H64	kg/h	4.78E-08	5.21E-08
C32H66	kg/h	4.08E-09	4.45E-09
C33H68	kg/h	9.72E-09	1.06E-08
C34H70	kg/h	3.13E-08	3.41E-08
C35H72	kg/h	2.10E-09	0.00E+00
C8H16	kg/h	1.91E+01	2.07E+01
C9H18	kg/h	9.73E+00	1.05E+01
C10H20	kg/h	8.74E+00	9.45E+00
C11H22	kg/h	1.35E-01	1.46E-01
C12H24	kg/h	9.29E-01	1.01E+00
C13H26	kg/h	1.34E-02	1.45E-02
C14H28	kg/h	1.87E-03	2.02E-03
C15H30	kg/h	3.71E-03	4.03E-03
C16H32	kg/h	8.62E-04	9.35E-04
Total mass flow	kg/h	2.62E+05	2.84E+05
Steam produced	Temperature	°C	130
			130

	Pressure	bar	2.50	2.50
	Mass flow	kg/h	6.46E+04	6.66E+04
Electricity needed	Power required	kW	7	6

Table 19 presents the impurities after gasification hierarchy and before Fischer-Tropsch hierarchy. This hierarchy is responsible for removing 100% of particulate matter, 99.99% of nitrogen compounds, and 90.66% of chlorine compounds. These values are reached due to equipment used for impurities removal along with the mass flow of the recycle stream from Fischer-Tropsch hierarchy. Just after the guard bed reactor, the syngas is conducted to the Fischer-Tropsch hierarchy.

Table 19. Impurities in the producer gas.

Impurity	Producer gas after gasification hierarchy	Producer gas after gas cleaning and conditioning hierarchy	Reference
Particulates matter simulated as MINERALS, SALTS, SOILS, and H <sub>3</sub> PO <sub>4</sub>	9.81E-05	0	0 mg/Nm <sup>3</sup> (i)
Nitrogen in NH <sub>3</sub> +HCN	9614 ppm	8.04E-5 ppm	< 0.1(i) or < 1(ii) ppm (v.%)
Chlorine in HCl	0.0238 ppm	0.0022 ppm	< 0.01 <sup>(viii)</sup> ppm (wt.%) (iii)

(i) (KALTSCHMITT; NEULING, 2018); (ii) (BOERRIGTER et al., 2004); (iii) (TIJMENSEN et al., 2002)

### 5.3 Fischer-Tropsch hierarchy

Syngas entering the FT hierarchy is not suitable for Fischer-Tropsch synthesis due to the H<sub>2</sub>/CO molar ratio being equal to 1.1. This ratio must be equal to 1.7 for Fischer-Tropsch synthesis using Lower-Temperature slurry Co-based reactor (HU, 2012; IM-ORB; SIMASATITKUL; ARPORNWICHANOP, 2016b). Therefore, a WGS reactor was set to adequate this molar ratio and, to avoid carbon deposition, the steam/CO mole flow ratio must be higher than 3 (PONDINI; EBERT, 2013). A fraction of syngas was collected and passes through WGS reactor and then is mixed again with syngas to present the H<sub>2</sub>/CO molar ratio equal to 1.7 for both scenarios. This syngas is now ready for Fischer-Tropsch reactor. A summary results of WGS cycle, steam produced, and electricity demand is shown in Table 20.

Table 20. WGS cycle, steam produced, and electricity needed for Fischer-Tropsch hierarchy.

Process or parameters	Variable	Unit	Centralized	Decentralized
			Value	Value
WGS cycle	Temperature	°C	200	200
	Pressure	bar	24.88	24.88
	Mass flow of syngas to WGC reactor	kg/h	61521	67880
	Steam to WGS reactor	°C	350	350
		bar	25	25
	Steam mole flow to WGS reactor	kmol/h	4576	4958
	CO mole flow to WGS reactor	kmol/h	1129	1244
	Steam/CO molar ratio in WGS reactor		4.05	3.99
Steam produced	Temperature	°C	130	130
	Pressure	bar	2.5	2.5
	Mass flow	kg/h	1.27E+05	1.37E+05
Electricity needed	Power required	kW	97	106

Considering the ASF distribution for paraffins and olefins production in the FT reactor, the mole fraction for each carbon range was set according to the data presented in Table 21.

Table 21. ASF distribution for paraffins and olefins from Fischer-Tropsch reactor.

Carbon number ( $n$ )	$W_n$	Paraffins ( $C_nH_{2n+2}$ )	Olefins ( $C_nH_{2n}$ )
1	0.18548	0.07419	
2	0.15108	0.06043	
3	0.12306	0.04922	
4	0.10023	0.04009	
5	0.08164	0.03266	
6	0.06650	0.02660	
7	0.05416	0.02167	
8	0.04412	0.01765	0.00239
9	0.03593	0.01437	0.00151
10	0.02927	0.01171	0.00096
11	0.02384	0.00954	0.00061
12	0.01942	0.00777	0.00039
13	0.01582	0.00633	0.00025
14	0.01288	0.00515	0.00016
15	0.01049	0.00420	0.00010
16	0.00855	0.00342	0.00006
17	0.00696	0.00278	

18	0.00567	0.00227
19	0.00462	0.00185
20	0.00376	0.00150
21	0.00306	0.00123
22	0.00250	0.00100
23	0.00203	0.00081
24	0.00166	0.00066
25	0.00135	0.00054
26	0.00110	0.00044
27	0.00089	0.00036
28	0.00073	0.00029
29	0.00059	0.00024
30	0.00048	0.00019
31	0.00039	0.00016
32	0.00032	0.00013
33	0.00026	0.00010
34	0.00021	0.00009
35	0.00017	0.00007

Green naphtha and biojet fuel produced considering both scenarios are presented Figure 8 while the complete streams of Fischer-Tropsch is shown in Appendix.

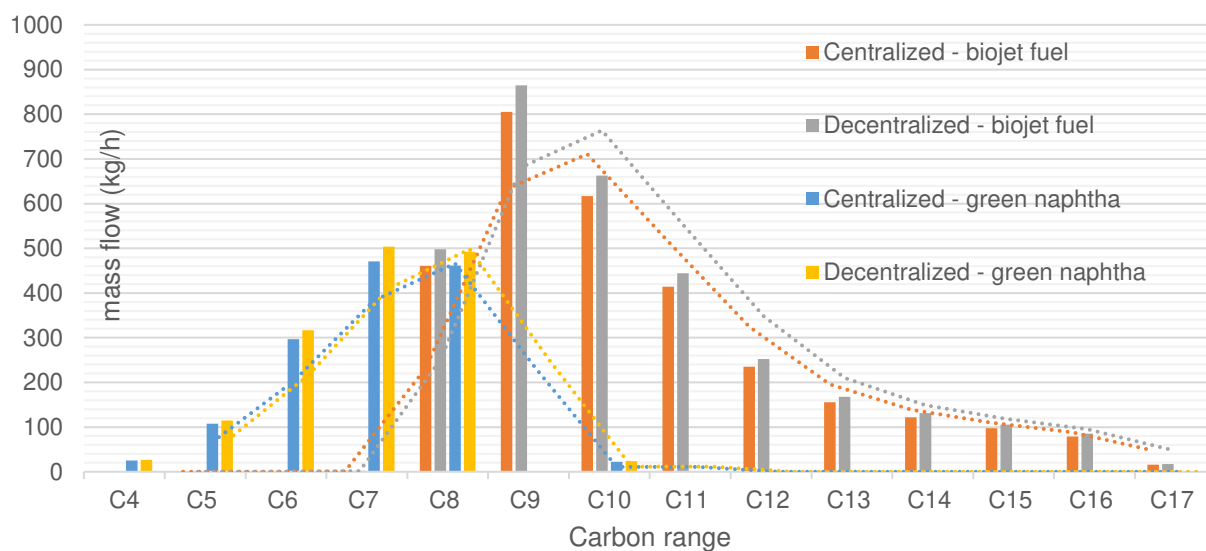


Figure 8. Carbon range for biojet fuel and green naphtha production for centralized and decentralized scenarios.

Total mass flow of green naphtha in centralized and decentralized scenarios was 1400 kg/h and 1495 kg/h, respectively. Considering the mass flow of LCB entering the fast pyrolysis reactor, the efficiency for both scenarios was around 0.74%. LHV of green naphtha is around 43 MJ/kg, within the range of petroleum naphtha which is around 41.8-46.5 MJ/kg (IPCC, 2006).

The mass flow of biojet fuel was 3088 kg/h for centralized scenario and 3321 kg/h for decentralized scenarios. Klerk et al. (KLERK, 2011) reported that biojet fuel mass flow is around three times higher than gasoline type using LTFT for jet fuel production. The results of this simulation found a value equal to 2.2, i.e. biojet fuel mass flow is around two times than the mass flow of green naphtha.

Considering the mass flow of LCB entering the fast pyrolysis reactor, the efficiency for both scenarios was around 1.64% considering biojet fuel production, i.e. for each 1 kg of LCB, around 0.016 g of biojet fuel is produced. If it is considered 4 Mt of sugarcane and 0.18 Mt of straw per year, this value is 0.004 while Klein et al (KLEIN et al., 2018) reported 0.009 using the same biorefinery configuration (4 Mt per season of sugarcane processed plus 0.18 Mt of straw). Also, for comparison issues, Alves et al. (ALVES et al., 2017) reported the value around 0.052, however it is not detailed such information of biomass mass flow, besides the different LCB consideration.

The mass density simulated of biojet fuel was 670 kg/m<sup>3</sup> considering 25 °C and ambient pressure, while the final requirement for the blend with conventional jet fuel must reach a value from 755 to 800 kg/m<sup>3</sup> at 15°C (ASTM, 2011, 2017), this value is around 20% of difference, i.e. this range can be reached by blending biojet fuel with conventional jet fuel according to regulation bodies.

Considering water, nitrogen and halogen contents and minimum carbon and hydrogen contents in biojet fuel, Table 22 shows a comparison with regulatory bodies. The only case out of range according to D6304 is water content in biojet fuel. This issue may be solved by adding conventional jet fuel into biojet fuel to guarantee the maximum of 75 mg/kg of biojet fuel in the blend. Nitrogen and chlorine contents are below the maximum value. Minimum carbon and hydrogen contents are higher than the target specified by D5291. LHV of biojet fuel simulated is 43.26 MJ/kg, which is in accordance with D4529, D3338, or D4809 and within the range of 43.92-46.23 MJ/kg reported by IEA (IEA, 2005)

Table 22. Biojet fuel components in comparison with regulatory bodies.

Parameter	Simulated for both scenarios	ASTM	Unit	Reference
Water	79	75	mg/kg of biojet fuel	D6304
Nitrogen	5E-05	2	mg/kg of biojet fuel	D4629
Halogen (Chlorine)	1E-12	1	mg/kg of biojet fuel	D7359
Minimum carbon and hydrogen content	99.9	99.5	%	D5291
Minimum Lower Heating Value	43.3	42.8	MJ/kg	D4529, D3338, or D4809

#### 5.4 Gas turbine hierarchy

Table 23 presents a summary of the main results of this hierarchy. The main goal of this hierarchy is to guarantee the electricity production in the Gas Turbine and steam production in the HRSG system, which the last will be used in the Steam Turbine hierarchy.

Table 23. Summary results of Gas Turbine hierarchy.

Process or parameters	Variable	Unit	Centralized Value	Decentralized Value
Fuel gas from Fischer-Tropsch synthesis	Temperature	°C	25	25
	Pressure	bar	1.01	1.01
Fuel gas to combustor	Temperature	°C	325	325
	Pressure	bar	21	21
	CH4	kg/h	4.52E+03	4.86E+03
	CO2	kg/h	5.27E+04	5.76E+04
	H2O	kg/h	1.91E+02	2.07E+02
	N2	kg/h	3.35E+03	3.59E+03
	O2	kg/h	8.18E-08	9.17E-08
	H2	kg/h	2.64E+03	2.84E+03
	CO	kg/h	2.77E+04	2.98E+04
	NH3	kg/h	5.04E-03	5.47E-03
	HCL	kg/h	2.66E-04	2.85E-04
	C2H6	kg/h	3.18E+03	3.42E+03
	C3H8	kg/h	2.38E+03	2.55E+03
	C4H10	kg/h	1.80E+03	1.93E+03
	C5H12	kg/h	1.31E+03	1.41E+03
	METHANOL	kg/h	3.58E+01	3.86E+01
HCN	kg/h	2.22E-01	2.47E-01	
C6H14	kg/h	8.13E+02	8.76E+02	
C7H16	kg/h	4.04E+02	4.37E+02	
C8H18	kg/h	1.51E+02	1.64E+02	

	C9H20	kg/h	4.47E+01	4.84E+01
	C10H22	kg/h	1.43E+01	1.55E+01
	C11H24	kg/h	4.50E+00	4.88E+00
	C12H26	kg/h	1.40E+00	1.52E+00
	C13H28	kg/h	4.61E-01	5.00E-01
	C14H30	kg/h	1.62E-01	1.76E-01
	C15H32	kg/h	5.28E-02	5.73E-02
	C16H34	kg/h	1.87E-02	2.03E-02
	C17H36	kg/h	5.65E-03	6.14E-03
	C18H38	kg/h	2.01E-03	2.18E-03
	C19H40	kg/h	7.05E-04	7.66E-04
	C20H42	kg/h	2.17E-04	2.36E-04
	C21H44	kg/h	8.14E-05	8.85E-05
	C22H46	kg/h	3.36E-05	3.65E-05
	C23H48	kg/h	1.03E-05	1.12E-05
	C24H50	kg/h	3.67E-06	3.99E-06
	C25H52	kg/h	1.43E-06	1.56E-06
	C26H54	kg/h	5.07E-07	5.52E-07
	C27H56	kg/h	1.53E-07	1.67E-07
	C28H58	kg/h	7.60E-08	8.28E-08
	C29H60	kg/h	3.50E-08	3.81E-08
	C30H62	kg/h	1.38E-08	1.50E-08
	C31H64	kg/h	3.20E-08	3.48E-08
	C32H66	kg/h	2.73E-09	2.97E-09
	C33H68	kg/h	6.50E-09	7.09E-09
	C34H70	kg/h	2.09E-08	2.28E-08
	C35H72	kg/h	1.40E-09	1.53E-09
	C8H16	kg/h	1.33E+01	1.44E+01
	C9H18	kg/h	6.48E+00	7.02E+00
	C10H20	kg/h	6.68E+00	7.22E+00
	C11H22	kg/h	9.01E-02	9.76E-02
	C12H24	kg/h	6.19E-01	6.71E-01
	C13H26	kg/h	8.91E-03	9.66E-03
	C14H28	kg/h	1.24E-03	1.35E-03
	C15H30	kg/h	2.47E-03	2.69E-03
	C16H32	kg/h	5.75E-04	6.24E-04
	Total mass flow	kg/h	1.01E+05	1.10E+05
Air to compressor	Temperature	°C	25	25
	Pressure	bar	1.01	1.01
	O2	kg/h	2.40E+05	2.58E+05
	N2	kg/h	7.90E+05	8.49E+05
Air to combustor	Temperature	°C	444	444
	Pressure	bar	21	21
Flue gas to HRSG	Temperature	°C	617	617
	Pressure	bar	1.20	1.20

Flue gas to flue gas stack (to disposal)	Temperature	°C	102	102
	Pressure	bar	1.20	1.20
	CO <sub>2</sub>	kg/h	1.39E+05	1.50E+05
	H <sub>2</sub> O	kg/h	5.05E+04	5.43E+04
	N <sub>2</sub>	kg/h	7.94E+05	8.52E+05
	O <sub>2</sub>	kg/h	1.48E+05	1.59E+05
	NH <sub>3</sub>	kg/h	5.04E-03	5.47E-03
	HCL	kg/h	2.66E-04	2.85E-04
	HCN	kg/h	2.22E-01	2.47E-01
	Total mass flow	kg/h	1.13E+06	1.22E+06
Steam produced from HRSG	Temperature	°C	341	341
	Pressure	bar	22	22
	Mass flow	kg/h	244039	262430
Electricity needed	Power required	kW	13531	14606
	Power produced (gas turbine)	kW	161951	174152

LHV of the fuel gas to gas turbine combustor is 12.7 MJ/kg and operating pressure at 21 bar. This LHV matches the requirements for Low-BTU gas turbines, which varies from 10 to 35 MJ/kg, therefore, this fuel gas can be used in industrial gas turbines for electricity production (SIEMENS, 2008).

The electrical energy produced in this hierarchy is 161 MW and 174 MW for centralized and decentralized scenarios, respectively, where electricity is also used to operate the water pump and the air and fuel gas compressors.

The flue gas from HSRG is conducted to disposal via flue gas stack whereas steam produced is conducted to the Steam Turbine Hierarchy.

### 5.5 *Steam turbine hierarchy*

The steam produced throughout hierarchies depends on steam availability. Therefore, steam turbine hierarchy is presented in the Decentralized pyrolysis facility, Decentralized gasification facility, and Centralized scenario. Table 24 presents the results of steam turbine hierarchy regarding specific steam turbine for different scenarios.

Table 24. Summary results of Steam Turbine hierarchy.

Process or parameters	Variable	Unit	Centralized Value	Decentralized - each pyrolysis facility Value	Decentralized - gasification facility Value
Backpressure turbine (90 bar)	Steam inlet temperature	°C	530	530	530

	Steam outlet temperature	°C	341	341	341
	Steam inlet pressure	bar	90	90	90
	Steam outlet pressure	bar	22	22	22
	Mass flow	kg/h	156080	20179	127836
	Electricity produced	kW	15017	1941	12300
Backpressure turbine (22 bar)	Steam inlet temperature	°C	341	341	341
	Steam outlet temperature	°C	131	131	131
	Steam inlet pressure	bar	22	22	22
	Steam outlet pressure	bar	2.5	2.5	2.5
	Mass flow	kg/h	427097	38118	390266
	Electricity produced	kW	45512	4443	41588
Condensing-extracting turbine (2.5 bar)	Steam inlet temperature	°C	131	131	131
	Steam outlet temperature (to cooling tower)	°C	54	54	54
	Steam inlet pressure	bar	2.5	2.5	2.5
	Steam outlet pressure (to cooling tower)	bar	0.15	0.15	0.15
	Mass flow (to cooling tower)	kg/h	307214	38118	542484
	Electricity produced	kW	43960	5456	77626
Cooling tower	Power	kW	168735	20492	297960
Steam control	Mass flow	kg/h	36900	3578	50940
To integration (deaerator)	Temperature	°C	105	105	105
	Pressure	bar	1.4	1.4	1.4
	Mass flow	kg/h	642582	41697	593426
Electricity	Power required	kW	16	2	28
	Power produced (by steam turbines)	kW	104488	6384	131514

The back-pressure turbine operating at 90 bar inlet uses steam from biomass handling and feeding hierarchy and from gasification hierarchy. The back-pressure turbine operating at 22 bar inlet uses steam from 90 bar outlet turbine and Pyrolysis and Steam Turbine hierarchies. Finally, the condensing-extracting turbine operating at 2.5 bar inlet uses steam from 22 bar outlet turbine along with Gas Cleaning and Conditioning and Fischer-Tropsch hierarchies.

The mass flow for steam turbines differs for each scenario due to different configuration and steam availability throughout hierarchies. This difference can be verified by

checking each hierarchy, which corresponds to different steam availability. Therefore, a higher amount of electricity can be produced, especially concerning the decentralized gasification facility, which can produce around 30% more electrical energy when compared to centralized scenario.

Table 25 presents the integration and consumed water throughout hierarchies are controlled by a SPLIT block. In general, all demands in order to integrate 1G biorefinery and thermochemical plant are provided by the Centralized scenario while decentralized scenarios are self-sufficient in terms of steam and electricity.

Table 25. Summary results of steam and electricity integration.

Process or parameters	Variable	Unit	Centralized	Decentralized - each pyrolysis facility	Decentralized - gasification facility
			Value	Value	Value
Electricity to 1G biorefinery	Power required	kW	26378	N/A	N/A
Steam to 1G biorefinery (22 bar)	Mass flow	kg/h	23854	N/A	N/A
Steam to 1G biorefinery (2.5 bar)	Mass flow	kg/h	274616	N/A	N/A
Water	Water consumed	kg/h	142131	N/A	150662
	Water integrated	kg/h	515605	41697	456872
	Water makeup	kg/h	7107	2085	7533

Electricity integration demands are shown in Table 26. ASU unit is responsible for 53% of electricity consumed in centralized scenario (already discounted the demands for 1G biorefinery), while around 38% of electricity consumed in the gasification facility. In both cases are also discounted the ASU unit electricity demand.

Electricity produced in decentralized scenario is around 66 MW higher than centralized scenario. This difference can be explained mainly by 1G integration. 1G Anx-Op requires around 27 MW to operate in centralized scenario, while decentralized scenario does not contain such integration. In total, decentralized scenario can produce around 312 MW, consuming around 75 MW, there is a surplus equal to 237 MW, whereas the centralized scenario can sell to the grid around 193 MW.

Table 26. Surplus electricity.

Process or parameters	Variable	Unit	Centralized	Decentralized Pyrolysis facility (each one)	Decentralized Gasification facility
Electricity	Electricity produced	MW	240	6	306

Electricity consumed	MW	47	3	72
Surplus electricity (to be sold)	MW	193	3	234

## 5.6 *Economic assessment*

A summary of CAPEX and OPEX of centralized and decentralized scenarios is presented in Table 27. The full CAPEX and OPEX analyses are shown in Appendix.

Table 27. Summary of CAPEX and OPEX for centralized and decentralized scenarios.

Hierarchy	Centralized		Decentralized	
	CAPEX	OPEX	CAPEX	OPEX
Biomass handling and feeding	R\$ 131,397,375.47	R\$ 2,275,279.23	R\$ 165,286,377.30	R\$ 2,851,433.82
Pyrolysis	R\$ 1,126,762,661.72	R\$ 47,662,060.59	R\$ 1,457,282,784.04	R\$ 83,502,303.53
Gasification	R\$ 130,245,243.85	R\$ 8,594,080.30	R\$ 145,816,338.56	R\$ 9,161,243.32
Gas cleaning and conditioning	R\$ 115,153,354.82	R\$ 1,152,539.15	R\$ 120,903,061.12	R\$ 1,224,175.82
Fischer-Tropsch	R\$ 148,043,067.58	R\$ 10,690,203.62	R\$ 155,554,819.29	R\$ 11,524,798.13
Gas turbine	R\$ 90,965,528.14	R\$ 4,093,448.77	R\$ 96,800,431.96	R\$ 4,356,019.44
Steam Turbine	R\$ 220,151,213.80	R\$ 9,906,804.62		
Gasification facility			R\$ 253,514,451.54	R\$ 11,408,150.32
Pyrolysis facility			R\$ 60,126,383.55	R\$ 2,705,687.26
Water, steam, and electricity integration	R\$ 7,122,436.89	R\$ 9,873,253.97		
Gasification facility			R\$ 6,650,342.81	R\$ 5,769,969.74
Pyrolysis facility			R\$ 2,715,856.62	R\$ 4,770,534.37
Total	R\$ 1,969,840,882.27	R\$ 94,247,670.25	R\$ 2,464,650,846.79	R\$ 137,274,315.74

Hierarchy	Centralized		Decentralized	
	CAPEX	OPEX	CAPEX	OPEX
Biomass handling and feeding	6.67%	2.41%	6.71%	2.08%
Pyrolysis	57.20%	50.57%	59.13%	60.83%
Gasification	6.61%	9.12%	5.92%	6.67%
Gas cleaning and conditioning	5.85%	1.22%	4.91%	0.89%
Fischer-Tropsch	7.52%	11.34%	6.31%	8.40%
Gas turbine	4.62%	4.34%	3.93%	3.17%
Steam Turbine	11.18%	10.51%	12.73%	10.28%
Water, steam, and electricity integration	0.36%	10.48%	0.38%	7.68%
Total	100%	100%	100%	100%

The fast pyrolysis hierarchy is the most expensive one (1126 MR\$). Fibria and Cenibra will spend around half billion in order to build a fast pyrolysis plant in Brazil to operate in 2020 (SEIXAS, 2018). This unit will be able to deliver 110 kton of bio-oil per year, i.e., fast pyrolysis plant for bioslurry production in this work will be 900 kton of bioslurry per year,

resulting in around 8 times larger than Fibria and Cenibra's fast pyrolysis plant. Although the size will be 8 times larger, the CAPEX will be around 2 times due to the exponential factor considered by CAPEX. Thus, due to difficult to build a fast pyrolysis plant, high values for CAPEX is still in accordance with literature data.

Table 28 shows the main inputs for economic assessments. 1G represents the chosen sugarcane biorefinery which produces ethanol and sugar, while 2G represents the hierarchies simulated in this work. CAPEX from decentralized scenario is around 59% higher than centralized scenario. Around the same proportional value can be seen in revenues. However, this proportion is not applied to total OPEX 1G2G, which value reached 86% higher due to the consideration of two 1G sugarcane biorefineries allied with the high OPEX of pyrolysis facility, especially about bioslurry transportation and storage.

Anhydrous ethanol corresponds to 45% of total revenues; sugar corresponds to 35% for centralized scenario and 32% for decentralized scenario. Surplus Electricity is responsible for 22% and 17% for centralized and decentralized scenario, respectively. Green naphtha corresponds to 2.5% and 1.7% for centralized and decentralized concept. Finally, biojet fuel presented the most deviation considering both scenarios, ranging from 5.5% to 3.8% for centralized and decentralized scenarios.

Table 28. Main input parameters for economic assessment.

Parameters	Centralized	Decentralized
CAPEX 1G (R\$ mi)	533	1522
CAPEX 2G (R\$ mi)	1970	2465
Total CAPEX (R\$ mi)	2503	3987
Sugarcane (R\$/TC)	76.08	76.08
Straw (R\$/T)	121.37	121.37
Sugarcane (MTC/year)	4.00	8.00
Straw (Mt/year)	0.18	0.36
Anhydrous ethanol price to the producer (R\$/L)	1.70	1.70
Sugar price to the producer (R\$/kg)	1.00	1.00
Electricity price to the producer (R\$/MWh)	193.95	193.95
Green naphtha price to the producer (R\$/L)	2.04	2.04
Biojet fuel price to the producer (R\$/L)	2.02	2.02
Anhydrous ethanol production (millions L/year)	215	338
Sugar production (millions of kg/year)	206	411
Surplus electricity (MWh/ano)	926400	1123200
Green naphtha production (millions L/year)	9.99	10.66
Biojet fuel production (millions L/year)	22.12	23.79

Revenue from anhydrous ethanol (R\$ mi/year)	364	574
Revenue from sugar (R\$ mi/year)	206	412
Revenue from electricity (R\$ mi/year)	180	218
Revenue from green naphtha (R\$ mi/year)	20	22
Revenue from biojet fuel (R\$ mi/year)	45	49
Total revenue (R\$ mi/year)	815	1274
OPEX 1G (only biorefinery) (R\$ mi/year)	87	143
OPEX 2G (only biorefinery) (R\$ mi/year)	94	137
Bioslurry transportation (average 25 km) (R\$/t)	0	54
Manpower (R\$ mi/year)	15	30
Sugarcane cost (R\$ mi/year)	304	609
Straw cost (R\$ mi/year)	22	44
Total OPEX 1G2G (R\$ mi/year)	523	963

With the main input data shown in Table 28, it is possible to calculate economic performance as shown in summary in Table 29.

Table 29. Main economic indicators.

Main economic indicators	Centralized	Decentralized
NPV (R\$ mi)	-864	-2147
MARR* (a.a.)	12.00%	12.00%
IRR (a.a.)	6.80%	3.30%
Payback (year)	9.90	16.18

Minimum Acceptable Rate of Return (MARR)

Minimum selling price (MSP) of biojet fuel green naphtha were calculated using both scenarios as basis. MSP is calculated based on an IRR equal to 12%. Therefore, the minimum selling price for green naphtha and biojet fuel should be equal to 8.50 R\$/L for centralized scenario, while this value should reach 16.20 R\$/L for decentralized scenario. Concerning December of 2016 as a reference, green naphtha and biojet fuel should be sold 4.2 and 16.0 times higher in order to guarantee the MSP equal to 12% for centralized and decentralized scenarios, respectively.

## 6 General conclusion

The most relevant input and output data retrieved from this work were presented in chapters I, II and III. Chapters I and II showed the literature review and simulation and experimental of fast pyrolysis process, respectively, followed by specific conclusions. Each one

detailed the information which is necessary for the understanding of chapter III. While chapter II approaches upstream hierarchies of fast pyrolysis process, chapter III approaches downstream hierarchies of gasification processes.

This work brings important results related to the integration of the 1G sugarcane biorefinery with the 2G thermochemical route. Basically, the 1G sugarcane biorefinery provides surplus sugarcane bagasse and straw (LCB) for 2G thermochemical route. This mixture passes through the drying process which removes moisture content. Fast pyrolysis hierarchy is fed by this dried LCB in order to produce bioslurry. The bioslurry is conducted to the gasifier to produce producer gas fuel production. Gas cleaning and conditioning hierarchy are set to adequate the producer gas into the downstream hierarchies in order to produce green naphtha and biojet fuel by Fischer-Tropsch synthesis. The gas not converted is conducted to the Combined Heat and Power hierarchy to produce steam and electricity to ensure steam and electricity demands to the overall integration 1G2G biorefinery. Due to bioslurry characteristics because of handling, storage, and transport form, two different scenarios were evaluated: centralized and decentralized. Additionally, fast pyrolysis experiment process was also carried out in order to provide information for the simulation processes. Ultimately, economic investigation using the main financial indicators was also carried out.

Gasification hierarchy uses Entrained flow gasifier to produce a free tar producer gas with a specific  $H_2/CO$  molar ratio while ASU unit is responsible to offer the gasification agent for this process and CHP offers the steam required for this process. Both scenarios have similar output data due to similar bioslurry mass flow from fast pyrolysis hierarchy. The gasifier reached  $1240\text{ }^\circ\text{C}$  and  $H_2/CO$  molar ratio equal to 1.01 which are in accordance with literature.

Producer gas from gasification hierarchy was cleaned and conditioned for the next FT hierarchy. A set of technologies was used to deliver syngas to Fischer-Tropsch hierarchy. To achieve syngas quality for FT process, a necessary recycle from FT hierarchy was developed to adequate syngas into FT requirements, especially regarding particulate matter, nitrogen and chlorine.

After the cleaning step, the syngas  $H_2/CO$  molar ratio is 1.1 and it is not ready for FT synthesis which requires value around 1.7. Therefore, the WGS reactor in FT hierarchy was set to adequate this molar ratio for the FT reactor. A mixture of liquid fuels, wax and off gas are produced from FT reactor. A fraction of off gas is conducted to recycle and the other to gas turbine while green naphtha, biojet fuel and wax are conducted to the distillation column. Light gas from this distillation column is conducted to gas turbine hierarchy and wax is separated to

be converted by the hydrocracking reactor to increase the amount of green naphtha and biojet fuel. Biojet fuel produced in this work is in accordance with regulatory bodies for biojet fuel commercial considering the contents of sulfur, nitrogen, halogen, minimum carbon and hydrogen content, minimum Lower Heating Value and others.

Light gas and off gas are conducted to the gas turbine hierarchy to produce electricity. HRSG is set downstream gas turbine in order to adequate heat integration and flue gas is conducted to the flue gas stack for disposal. The power produced in this hierarchy is 161 MW and 174 MW for centralized and decentralizes scenarios, respectively.

Steam produced in the gas turbine hierarchy is conducted to the steam turbine hierarchy. Three steam levels are produced throughout the 1G2G integration: 2.5 bar/131 °C, 22 bar/350 °C and 90 bar/530 °C. This hierarchy is also responsible to provide the steam demand for 1G sugarcane biorefinery (22 bar and 2.5 bar).

Steam and electricity integration are keys to provide steam and electricity for the 1G2G integration. Steam integration is only performed for the centralized scenario. In this case, power required to 1G sugarcane biorefinery is 26 MW while steam mass flow at 22 bar and 2.5 bar are 23854 kg/h and 274616 kg/h, respectively. Regarding electricity production, decentralized scenario has a surplus of 234 MW whereas centralized scenario has a surplus of 193 MW, which both are sold to the grid.

Economic issues and its indicators are key elements considered for investors. CAPEX and OPEX of pyrolysis hierarchy are considered the highest and they are responsible for around 60% of total 1G2G integration CAPEX due to mainly by fast pyrolysis reactor and product recovery and bioslurry mixing, besides storage and transport regarding with decentralized scenario. Pyrolysis hierarchy is followed by Steam Turbine Hierarchy CAPEX and OPEX around 12% due to the different levels of steam turbines, cooling tower system and steam integration.

Total CAPEX for centralized concept is 2503 MR\$ considering 1G2G biorefinery. Considering this amount, around 78% goes to 2G thermochemical route whereas 22% is for 1G sugarcane biorefinery. In the case of decentralized concept, CAPEX is 3987 MR\$ and around 61% if for 2G thermochemical route and 39% for 1G sugarcane biorefinery.

OPEX for only 1G sugarcane biorefinery and 2G thermochemical route in centralized scenario is 87 MR\$/year and 94 MR\$/year, respectively. OPEX for only 1G sugarcane biorefinery and 2G thermochemical route in decentralized scenario is 143 MR\$/year and 137 MR\$/year, respectively. Thus, although CAPEX is very different from scenarios,

OPEX showed similar results. This difference can be explained by two 1G sugarcane biorefineries in decentralized scenarios.

CAPEX and OPEX were considered input data to calculate economic indicators. Additionally, centralized scenario has the highest IRR equal to 6.80%. Considering MARR equal to 12%, these values are not attractive for any commercial strategy. Therefore, in order to guarantee MARR equal to 12%, the selling biojet fuel price should be raised by a factor of 4.2 for centralized scenario, and by a factor of 16.0 in decentralized scenario.

Once biojet fuel is considered a renewable fuel, there are some options to add value and overcome this high value, especially considering MARR value when calculating biojet fuel price. First, the technology developed in this work may suffer from medium and long future improvement, therefore, elevating the yield of both liquid fuels, besides minimizing CAPEX and OPEX through the scenarios and the integration into 1G sugarcane biorefinery, mainly considering the fast pyrolysis hierarchy. Second, subsidies due to renewable biofuels in order to mitigate fossil fuel carbon footprint. In general, renewable carbon footprint regulation bodies may help to solve this economic issue by adding economic advantages by using green naphtha or biojet fuel instead of fossil fuels.

Biojet fuel has been considered the most impacting product for aviation industries and companies with the potential to replace the conventional jet fuels. To date, there are no simulation and experiments data of fast pyrolysis process to produce bioslurry from LCB integrating the 1G sugarcane biorefinery and the 2G thermochemical route. Although the collection of simulation and experimental data obtained in this work might be improved, these results of this work might be used further assessment considering sugarcane biorefinery and thermochemical route. This thesis, and subsequent work to quantify the environmental impacts may help to optimize integrated process and the development of these technologies within new configurations.

### 6.1 *Further work suggestions*

- Life Cycle Analysis of the integration 1G2G
- Evaluation of different configuration regarding scenarios and technologies
- tertiary and quaternary reactions for modeling the fast pyrolysis process
- Updated values of process and equipment for CAPEX and OPEX evaluation
- Different process and catalysts for biojet fuel production

## 7 Memorial

Gómez, EO; **Neves, RC**; Medeiros, EM; Rezende, MCAF. *Energy and Exergy Analysis on Gasification Processes: A Preliminary Approach*. In: Katia Tannous. (Org.). *Innovative Solutions in Fluid-Particle Systems and Renewable Energy Management*. 1ed.: IGI Global, 2015, v. 1, p. 199-240. DOI: 10.4018/978-1-4666-8711-0.ch007.

Rosa, AP; **Neves, RC**; Chernicharo, CA. *Aproveitamento energético dos subprodutos, lodo e biogás, a partir do tratamento anaeróbico de efluentes pelo uso de processos termoquímicos*. *Revista Engenharia na Agricultura* (ISSN: 2175-6813). 2018.

**Neves, RC**; Vissotto, JP; Sanchez, EMS; Sanchez, C. G. . *Reformation of biomass producer gas by plasma torch*. *Revista Ciência e Tecnologia*, v. 19, p. 31-42, 2016. ISSN: 2236-6733.

**Neves, RC**; Funke, A; Gómez, EO; Bonomi, A; Dahmen, N; Filho, RM. *Process simulation of fast pyrolysis to produce bioslurry from lignocellulosic biomass residues combining first and second-generation biofuels*. 6th International Symposium on Energy from Biomass and Waste, 2016, Veneza.

Moreira, R; **Neves, RC**; Schmitt, CC; Breunig, M; Tambani, PC; Ushima, AH; Funke, A; Raffelt, K. *Characterization of Brazilian Sugarcane Bagasse and Sugarcane Straw Based on European Methodologies to Evaluate the Potential for Energy Conversion*. In: european biomass conference and exhibition proceedings. ISSN 2282-5819, 2017, Stockholm. DOI: 10.5071/25thEUBCE2017-1DV.1.6.

Medeiros, EM; **Neves, RC**; Gómez, EO; Rezende, MCAF; Klein, BC; Junqueira, TL; Silva, RJ; Filho, RM; Bonomi, A. *Preliminary assessment by the Virtual Sugarcane Biorefinery (VSB) framework of syngas production and power generation from a first-generation sugarcane plant lignocellulosic biomass*. In: 5th International Conference on Engineering for Waste and Biomass Valorisation, 2014, Rio de Janeiro.

**Neves, RC**; Silva, RJ; Medeiros, EM; Klein, BC; Santos, LO; Fre, RA; Rezende, MCAF; Gómez, EO; Filho, RM; Bonomi, A. *Comparative study of two standalone thermochemical routes for the production of electricity from lignocellulosic material of sugarcane*. 2015. 37th symposium on biotechnology for fuels and chemicals

Silva, RJ; **Neves, RC**; Rezende, MCAF; Junqueira, TL; Cavalett, O; Watanabe, M; Gómez, EO; Filho, RM; Bonomi, A. *Comparative technical, economic and environmental assessment of biomass-to-ethanol conversion technologies: biochemical and thermochemical*

*routes integrated in a sugarcane biorefinery*. 2015. 37th symposium on biotechnology for fuels and chemicals

*A vision on Biomass-to-Liquids (BTL) thermochemical routes in integrated sugarcane biorefineries for biojet fuel production*. **Renato Cruz Neves**, Bruno Colling Klein, Ricardo Justino da Silva, Mylene Cristina Alves Ferreira Rezende, Axel Funke, Edgardo Olivarez-Gómez, Antonio Bonomi, Rubens Maciel-Filho. Renewable and Sustainable Energy Reviews. Minor revisions needed

*Simulation and experiment of fast pyrolysis process of lignocellulosic biomass from First-Generation sugarcane biorefinery*. **Renato Cruz Neves**, Axel Funke, Pablo Andrés Silva Ortiz, Edgardo Olivares Gómez, Nicolaus Dahmen, Rubens Maciel Filho. To be submitted again after considerations

*From agriculture residue to upgraded product: The thermochemical conversion of sugarcane bagasse for fuel and chemical products*. Caroline Carriel Schmitt, Renata Moreira, **Renato Cruz Neves**, Daniel Richter Axel Funke, Klaus Raffelt, Jan-Dierk Grunwaldt, Nicolaus Dahmen. Under review at Fuel Processing Technology

*Characterization of Brazilian sugarcane bagasse and sugarcane straw based on European methodologies to evaluate the potential for energy conversion*. Renata Moreira, **Renato Cruz Neves**, Caroline Carriel Schmitt, Mackeridhe Breunig, Paula Tambani, Ademar Ushima, Axel Funke, Klaus Raffelt. To be submitted soon at Biomass and Bioenergy.

## References

- ABDOULMOUMINE, N. et al. A review on biomass gasification syngas cleanup. **Applied Energy**, v. 155, p. 294–307, out. 2015.
- ABU EL-RUB, Z.; BRAMER, E. A.; BREM, G. Experimental comparison of biomass chars with other catalysts for tar reduction. **Fuel**, v. 87, n. 10–11, p. 2243–2252, ago. 2008.
- AHMED, I. I.; GUPTA, A. K. Sugarcane bagasse gasification: Global reaction mechanism of syngas evolution. **Applied Energy**, v. 91, n. 1, p. 75–81, mar. 2012.
- AL ARNI, S.; BOSIO, B.; ARATO, E. Syngas from sugarcane pyrolysis: An experimental study for fuel cell applications. **Renewable Energy**, v. 35, n. 1, p. 29–35, jan. 2010.
- ALVES, C. M. et al. Techno-economic assessment of biorefinery technologies for aviation biofuels supply chains in Brazil. **Biofuels, Bioproducts and Biorefining**, v. 11, n. 1, p. 67–91, jan. 2017.
- ANDERSON, R.; FRIEDEL, R.; STORCH, H. Fischer-Tropsch reaction mechanism involving stepwise growth of carbon chain. **The Journal of Chemical Physics**, p. 313–319, 1951.
- ANIS, S.; ZAINAL, Z. A. Tar reduction in biomass producer gas via mechanical, catalytic and thermal methods: A review. **Renewable and Sustainable Energy Reviews**, v. 15, n. 5, p. 2355–2377, jun. 2011.
- ANP. **Anuário estatístico do petróleo**. Rio de Janeiro: [s.n.].
- ANP. **Anuário estatístico do petróleo, gás natural e biocombustíveis**. Rio de Janeiro: [s.n.].
- ANP. **Anuário estatístico brasileiro do petróleo, gás natural e biocombustíveis**. Riio de Janeiro: [s.n.].
- APFELBACHER, A.; CONRAD, S.; SCHULZKE, T. Ablative fast pyrolysis-Potential for cost effective conversion of agricultural residues. **Environmental Progress & Sustainable Energy**, v. 33, n. 3, p. 669–675, out. 2014.
- ARAMIDEH, S. et al. Numerical simulation of biomass fast pyrolysis in an auger reactor. **Fuel**, v. 156, p. 234–242, set. 2015.
- ARDILA, Y. C. **Gaseificação da Biomassa para a Produção de Gás de Síntese e Posterior Fermentação para Bioetanol: Modelagem e Simulação do Processo**. [s.l.] Universidade Estadual de Campinas, 2015.

ARGYLE, M.; BARTHOLOMEW, C. Heterogeneous Catalyst Deactivation and Regeneration: A Review. **Catalysts**, v. 5, n. 1, p. 145–269, 2015.

ASADULLAH, M. et al. Production of bio-oil from fixed bed pyrolysis of bagasse. **Fuel**, v. 86, n. 16, p. 2514–2520, nov. 2007.

ASADULLAH, M. Biomass gasification gas cleaning for downstream applications: A comparative critical review. **Renewable and Sustainable Energy Reviews**, v. 40, p. 118–132, dez. 2014.

ASPEN TECHNOLOGY. **Aspen physical property system, Physical property methods**. [s.l: s.n.].

ASPEN TECHNOLOGY. **Aspen Physical Property System**. Burlington, MA: [s.n.].

ASTM. **Designation: D1655 – 11a: Standard specification for aviation turbine fuels**. [s.l: s.n.].

ASTM. **Standard Specification for Aviation Turbine Fuel Containing Synthesized Hydrocarbons. D7566-17**. [s.l: s.n.].

ATAG. **Air transport action group**. [s.l: s.n.]. Disponível em: <<http://www.atag.org/component/downloads/downloads/72.html>>.

ATSONIOS, K. et al. Alternative thermochemical routes for aviation biofuels via alcohols synthesis: Process modeling, techno-economic assessment and comparison. **Applied Energy**, v. 138, p. 346–366, jan. 2015.

BABU, B. V. Biomass pyrolysis: a state-of-the-art review. **Biofuels, Bioproducts and Biorefining**, v. 2, n. 5, p. 393–414, set. 2008.

BACH, Q.-V.; SKREIBERG, Ø. Upgrading biomass fuels via wet torrefaction: A review and comparison with dry torrefaction. **Renewable and Sustainable Energy Reviews**, v. 54, p. 665–677, fev. 2016.

BAEYENS, J. et al. Challenges and opportunities in improving the production of bio-ethanol. **Progress in Energy and Combustion Science**, v. 47, p. 60–88, abr. 2015.

BAINS, P.; PSARRAS, P.; WILCOX, J. CO<sub>2</sub> capture from the industry sector. **Progress in Energy and Combustion Science**, v. 63, p. 146–172, nov. 2017.

BALAN, V.; CHIARAMONTI, D.; KUMAR, S. Review of US and EU initiatives toward development, demonstration, and commercialization of lignocellulosic biofuels. **Biofuels, Bioproducts and Biorefining**, v. 7, n. 6, p. 732–759, nov. 2013.

BALIBAN, R. C. et al. Hardwood Biomass to Gasoline, Diesel, and Jet Fuel: 1.

Process Synthesis and Global Optimization of a Thermochemical Refinery. **Energy & Fuels**, v. 27, n. 8, p. 4302–4324, 15 ago. 2013.

BAO, B.; EL-HALWAGI, M. M.; ELBASHIR, N. O. Simulation, integration, and economic analysis of gas-to-liquid processes. **Fuel Processing Technology**, v. 91, n. 7, p. 703–713, jul. 2010.

BARTHOLOMEW, C. RECENT TECHNOLOGICAL DEVELOPMENTS IN FISCHER-TROPSCH CATALYSIS. **Catalysis Letters**, v. 7, p. 303–316, 1990.

BARTHOLOMEW, C. Mechanisms of catalyst deactivation. **Applied Catalysis A: General**, v. 212, p. 17–60, 2001.

BASU, P. **Biomass gasification and pyrolysis - Practical design**. [s.l.] Elsevier, 2010.

BHATTACHARYA, P. et al. Wood/plastic copyrolysis in an auger reactor: Chemical and physical analysis of the products. **Fuel**, v. 88, n. 7, p. 1251–1260, jul. 2009.

BIOFUELSDIGEST. **The Pyromaniac, Class of 2015: The top 10 Pyrolysis projects in renewable fuels**. Disponível em: <<http://www.biofuelsdigest.com/bdigest/2015/08/03/the-pyromaniac-class-of-2015-the-top-10-pyrolysis-projects-in-renewable-fuels/>>. Acesso em: 3 ago. 2015.

BIOWARE. **Sobre a Bioware**. Disponível em: <<http://www.biofuelsdigest.com/bdigest/2015/08/03/the-pyromaniac-class-of-2015-the-top-10-pyrolysis-projects-in-renewable-fuels/>>. Acesso em: 5 abr. 2015.

BITYURIN, V. A.; FILIMONOVA, E. A.; NAIDIS, G. V. Simulation of Naphthalene Conversion in Biogas Initiated by Pulsed Corona Discharges. **IEEE Transactions on Plasma Science**, v. 37, n. 6, p. 911–919, jun. 2009.

BLAKEY, S.; RYE, L.; WILSON, C. **Aviation gas turbine alternative fuels: a review**. Proceedings of the Combustion Institute. **Anais...2011**

BOERRIGTER, H. et al. **Gas Cleaning for Integrated Biomass Gasification (BG)**. [s.l.: s.n.]. Disponível em: <<https://www.ecn.nl/publicaties/PdfFetch.aspx?nr=ECN-C--04-056>>.

BOERRIGTER, H.; RACUH, R. Syngas production in utilisation. Em H. Knoef, Handbook biomass gasification. In: KNOEF, H. (Ed.). **Handbook biomass gasificatio**. [s.l.] Biomass Technology Group (BTG), 2005. p. 211–230.

BOERRIGTER, H.; UIL, D.; CALIS, H. **Green diesel from biomass by Fischer-Tropsch synthesis: new insights in gas cleaning and process design**.

<https://www.ecn.nl/fileadmin/ecn/units/bio/Overig/pdf/Fischer-Tropsch03.pdf>: [s.n].  
Disponível em: <<https://www.ecn.nl/fileadmin/ecn/units/bio/Overig/pdf/Fischer-Tropsch03.pdf>>.

BONOMI, A., CAVALETT, O., DA CUNHA, M. P., & LIMA, M. A. **Virtual Biorefinery**. Cham: Springer International Publishing, 2016.

BONOMI, A. et al. (EDS.). **Virtual Biorefinery**. Cham: Springer International Publishing, 2016a.

BONOMI, A. et al. The Virtual Sugarcane Biorefinery Concept. In: [s.l: s.n.]. p. 5–11.

BOROSON, M. L. et al. Product yields and kinetics from the vapor phase cracking of wood pyrolysis tars. **AIChE Journal**, v. 35, n. 1, p. 120–128, 1989.

BOUCHY, C. et al. Fischer-Tropsch Waxes Upgrading via Hydrocracking and Selective Hydroisomerization. **Oil & Gas Science and Technology - Revue de l'IFP**, v. 64, n. 1, p. 91–112, 7 jan. 2009.

BOULOS, M.; FAUCHAIS, P.; PFENDER, R. **Thermal plasma: fundamentals and applications**. [s.l.] Plenum Press, 1994.

BRIDGWATER, A. Principles and practice of biomass fast pyrolysis processes for liquids. **Journal of Analytical and Applied Pyrolysis**, v. 51, p. 3–22, 1999.

BRIDGWATER, A. Review of fast pyrolysis of biomass and product upgrading. **Biomass and Bioenergy**, v. 38, p. 68–94, mar. 2012a.

BRIDGWATER, A. V. Review of fast pyrolysis of biomass and product upgrading. **Biomass and Bioenergy**, v. 38, p. 68–94, mar. 2012b.

BRIDGWATER, A. V. The technical and economic feasibility of biomass gasification for power generation. **Fuel**, v. 74, p. 631–653, 1995.

BULUSHEV, D. A.; ROSS, J. R. H. Catalysis for conversion of biomass to fuels via pyrolysis and gasification: A review. **Catalysis Today**, v. 171, n. 1, p. 1–13, ago. 2011.

BURAGOHAIN, B.; MAHANTA, P.; MOHOLKAR, V. S. Biomass gasification for decentralized power generation: The Indian perspective. **Renewable and Sustainable Energy Reviews**, v. 14, n. 1, p. 73–92, jan. 2010.

CAI, J. et al. Review of physicochemical properties and analytical characterization of lignocellulosic biomass. **Renewable and Sustainable Energy Reviews**, v. 76, p. 309–322, set. 2017.

CALEMMA, V. et al. Middle distillates from hydrocracking of FT waxes:

Composition, characteristics and emission properties. **Catalysis Today**, v. 149, n. 1–2, p. 40–46, jan. 2010.

CAMPOY, M. et al. Air–steam gasification of biomass in a fluidised bed: Process optimisation by enriched air. **Fuel Processing Technology**, v. 90, n. 5, p. 677–685, maio 2009.

CARRIER, M. et al. Impact of the lignocellulosic material on fast pyrolysis yields and product quality. **Bioresource Technology**, v. 150, p. 129–138, dez. 2013.

CAVALETT, O. et al. The Agricultural Production Model. In: [s.l: s.n.]. p. 13–51.

CHANDEL, A. K. et al. Techno-Economic Analysis of Second-Generation Ethanol in Brazil: Competitive, Complementary Aspects with First-Generation Ethanol. In: DA SILVA, S. S.; CHANDEL, A. K. (Eds.). . **Biofuels in Brazil**. Cham: Springer International Publishing, 2014. p. 1–29.

CHANG, J. Next generation integrated electrostatic gas cleaning systems. **Journal of Electrostatics**, v. 57, p. 273–291, 2003.

CHARON, N. et al. Multi-technique characterization of fast pyrolysis oils. **Journal of Analytical and Applied Pyrolysis**, v. 116, p. 18–26, nov. 2015.

CHERUBINI, F. et al. Linearity between temperature peak and bioenergy CO<sub>2</sub> emission rates. **Nature Climate Change**, v. 4, n. 11, p. 983–987, 5 nov. 2014.

CHIANG, K.-Y. et al. Reducing tar yield in gasification of paper-reject sludge by using a hot-gas cleaning system. **Energy**, v. 50, p. 47–53, fev. 2013.

CHINCHEN, G. C. et al. Synthesis of Methanol. **Applied Catalysis**, v. 36, p. 1–65, jan. 1988.

CHIODINI, A. et al. Enhancements in Biomass-to-Liquid processes: Gasification aiming at high hydrogen/carbon monoxide ratios for direct Fischer-Tropsch synthesis applications. **Biomass and Bioenergy**, v. 106, p. 104–114, nov. 2017.

CHO, I. J. et al. Enhancement of synthesis gas production using gasification-plasma hybrid system. **International Journal of Hydrogen Energy**, v. 40, n. 4, p. 1709–1716, jan. 2015.

CHOI, Y.; STENGER, H. G. Water gas shift reaction kinetics and reactor modeling for fuel cell grade hydrogen. **Journal of Power Sources**, v. 124, n. 2, p. 432–439, nov. 2003.

CHU, S.; MAJUMDAR, A. Opportunities and challenges for a sustainable energy future. **Nature**, v. 488, n. 7411, p. 294–303, 16 ago. 2012.

COLL, R. et al. Steam reforming model compounds of biomass gasification tars: conversion at different operating conditions and tendency towards coke formation. **Fuel**

**Processing Technology**, v. 74, n. 1, p. 19–31, nov. 2001.

CONAB. **Acompanhamento da safra brasileira de cana-de-açúcar**. [s.l.: s.n.]. Disponível em: <[http://www.conab.gov.br/OlalaCMS/uploads/arquivos/17\\_12\\_19\\_09\\_49\\_08\\_cana\\_dezembro.pdf](http://www.conab.gov.br/OlalaCMS/uploads/arquivos/17_12_19_09_49_08_cana_dezembro.pdf)>.

CORTEZ, L. A. B. et al. **Roadmap for sustainable aviation biofuels for Brazil — A Flightpath to Aviation Biofuels in Brazil**. [s.l.] Editora Edgard Blücher, 2014.

D.W. GREEN, R. H. P. **Perry's Chemical Engineer's Handbook, Eighth Edition, McGraw-Hill**. [s.l.: s.n.].

DAHMEN, N. et al. The bioliq® bioslurry gasification process for the production of biosynfuels, organic chemicals, and energy. **Energy, Sustainability and Society**, v. 2, n. 1, p. 1–44, 2012.

DAHMEN, N. et al. The bioliq process for producing synthetic transportation fuels. **Wiley Interdisciplinary Reviews: Energy and Environment**, v. 6, n. 3, p. e236, maio 2017.

DAI, J.; CUI, H.; GRACE, J. R. Biomass feeding for thermochemical reactors. **Progress in Energy and Combustion Science**, v. 38, n. 5, p. 716–736, out. 2012.

DALAI, A. K.; DAVIS, B. H. Fischer–Tropsch synthesis: A review of water effects on the performances of unsupported and supported Co catalysts. **Applied Catalysis A: General**, v. 348, n. 1, p. 1–15, set. 2008.

DAMARTZIS, T.; MICHAÏLOS, S.; ZABANIOTOU, A. Energetic assessment of a combined heat and power integrated biomass gasification-internal combustion engine system by using Aspen Plus?? **Fuel Processing Technology**, v. 95, p. 37–44, 2012.

DE SOUZA-SANTOS, M. L. Very High-Pressure Fuel-Slurry Integrated Gasifier/Gas Turbine (FSIG/GT) Power Generation Applied to Biomass. **Energy and Fuels**, v. 29, n. 12, p. 8066–8073, 2015.

DE SOUZA-SANTOS, M. L. Proposals for power generation based on processes consuming biomass-glycerol slurries. **Energy**, v. 120, p. 959–974, fev. 2017.

DE SOUZA NOEL SIMAS BARBOSA, L.; HYTÖNEN, E.; VAINIKKA, P. Carbon mass balance in sugarcane biorefineries in Brazil for evaluating carbon capture and utilization opportunities. **Biomass and Bioenergy**, v. 105, p. 351–363, out. 2017.

DEMIRBAS, A. Political, economic and environmental impacts of biofuels: A review. **Applied Energy**, v. 86, p. S108–S117, nov. 2009.

DEMIRBAS, A.; ARIN, G. An Overview of Biomass Pyrolysis. **Energy Sources**,

v. 24, n. 5, p. 471–482, maio 2002.

DEMOPLANTS. **Projects - Bioenergy task 34**. Disponível em: <<http://demoplants21.bioenergy2020.eu/projects/displaymap/twhWVt>>. Acesso em: 28 mar. 2017.

DHYANI, V.; BHASKAR, T. A comprehensive review on the pyrolysis of lignocellulosic biomass. **Renewable Energy**, abr. 2017.

DIAS, M. O. DE S. et al. Integrated versus stand-alone second generation ethanol production from sugarcane bagasse and trash. **Bioresource Technology**, v. 103, n. 1, p. 152–161, 2012a.

DIAS, M. O. DE S. et al. Sugarcane processing for ethanol and sugar in Brazil. **Environmental Development**, v. 15, p. 1–17, 2014.

DIAS, M. O. S. et al. Improving second generation ethanol production through optimization of first generation production process from sugarcane. **Energy**, v. 43, n. 1, p. 246–252, jul. 2012b.

DO, T. X.; LIM, Y. IL; YEO, H. Techno-economic analysis of biooil production process from palm empty fruit bunches. **Energy Conversion and Management**, v. 80, p. 525–534, 2014.

DRY, M. The Fischer–Tropsch process: 1950–2000. **Catalysis Today**, v. 71, p. 237–241, 2002.

DUTTA, A. et al. Conceptual Process Design and Techno-Economic Assessment of Ex Situ Catalytic Fast Pyrolysis of Biomass: A Fixed Bed Reactor Implementation Scenario for Future Feasibility. **Topics in Catalysis**, v. 59, n. 1, p. 2–18, jan. 2016.

ELIOTT, R. M. et al. Tar Reforming under a Microwave Plasma Torch. **Energy & Fuels**, v. 27, n. 2, p. 1174–1181, 21 fev. 2013.

ESCOBAR, J. C. et al. Biofuels: Environment, technology and food security. **Renewable and Sustainable Energy Reviews**, v. 13, n. 6–7, p. 1275–1287, ago. 2009.

FAHIM, M.; AL-SAHHAF, T.; ELKILANI, A. Introdução. In: FAHIM, M.; AL-SAHHAF, T.; ELKILANI, A. (Eds.). **Introdução ao Refino de Petróleo**. [s.l.] Elsevier, 2012. p. 1–11.

FAPESP. **Flightpath to aviation biofuels in Brazil: action plan**. [s.l.: s.n.]. Disponível em: <<http://www.fapesp.br/publicacoes/flightpath-to-aviation-biofuels-in-brazil-action-plan.pdf>>.

FERDOUS, D. et al. Pyrolysis of lignins: Experimental and kinetics studies.

**Energy and Fuels**, v. 16, n. 6, p. 1405–1412, 2002.

FIGUEROA, J. E. J. et al. Evaluation of pyrolysis and steam gasification processes of sugarcane bagasse in a fixed bed reactor. **Chemical Engineering Transactions**, v. 32, p. 925–930, 2013.

FONSECA, F. G. **Moisture content as a design and operational parameter for fast pyrolysis**. [s.l.] Instituto Superior Técnico & Karlsruhe Institute of Technology, 2015.

FOURCAULT, A.; MARIAS, F.; MICHON, U. Modelling of thermal removal of tars in a high temperature stage fed by a plasma torch. **Biomass and Bioenergy**, v. 34, n. 9, p. 1363–1374, set. 2010.

FUNKE, A. et al. Fast pyrolysis char - Assessment of alternative uses within the bioliq® concept. **Bioresource Technology**, v. 200, p. 905–913, 2016a.

FUNKE, A. et al. Fast Pyrolysis of Biomass Residues in a Twin-screw Mixing Reactor. **Journal of Visualized Experiments**, n. 115, 9 set. 2016b.

FUNKE, A. et al. Dimensional Analysis of Auger-Type Fast Pyrolysis Reactors. **Energy Technology**, v. 5, n. 1, p. 119–129, jan. 2017a.

FUNKE, A. et al. Experimental comparison of two bench scale units for fast and intermediate pyrolysis. **Journal of Analytical and Applied Pyrolysis**, v. 124, p. 504–514, mar. 2017b.

FUNKE, A. et al. Modelling and improvement of heat transfer coefficient in auger type reactors for fast pyrolysis application. **Chemical Engineering and Processing - Process Intensification**, maio 2018.

GARCÍA-PÉREZ, M.; CHAALA, A.; ROY, C. Vacuum pyrolysis of sugarcane bagasse. **Journal of Analytical and Applied Pyrolysis**, v. 65, p. 111–136, 2002.

GOHARDANI, A. S. et al. Green space propulsion: Opportunities and prospects. **Progress in Aerospace Sciences**, v. 71, p. 128–149, nov. 2014.

GÓMEZ-BAREA, A.; LECKNER, B. Modeling of biomass gasification in fluidized bed. **Progress in Energy and Combustion Science**, v. 36, n. 4, p. 444–509, ago. 2010.

GRAMMELIS, P. **Solid Biofuels for Energy: A Lower Greenhouse Gas Alternative**. [s.l.] Springer Science & Business Media, 2010.

GUPTA, K. K.; REHMAN, A.; SARVIYA, R. M. Bio-fuels for the gas turbine: A review. **Renewable and Sustainable Energy Reviews**, v. 14, n. 9, p. 2946–2955, dez. 2010.

GUTIÉRREZ-ANTONIO, C. et al. A review on the production processes of

renewable jet fuel. **Renewable and Sustainable Energy Reviews**, v. 79, p. 709–729, nov. 2017.

HALLAC, B. B. et al. An optimized simulation model for iron-based Fischer–Tropsch catalyst design: Transfer limitations as functions of operating and design conditions. **Chemical Engineering Journal**, v. 263, p. 268–279, mar. 2015.

HAN, J.; KIM, H. The reduction and control technology of tar during biomass gasification/pyrolysis: An overview. **Renewable and Sustainable Energy Reviews**, v. 12, n. 2, p. 397–416, fev. 2008.

HANAOKA, T. et al. Jet fuel synthesis from Fischer–Tropsch product under mild hydrocracking conditions using Pt-loaded catalysts. **Chemical Engineering Journal**, v. 263, p. 178–185, mar. 2015.

HARA, M.; NAKAJIMA, K.; KAMATA, K. Recent progress in the development of solid catalysts for biomass conversion into high value-added chemicals. **Science and Technology of Advanced Materials**, v. 16, n. 3, p. 034903, 20 jun. 2015.

HARI, K.; YAAKOB, Z.; BINITHA, N. N. Aviation biofuel from renewable resources: Routes, opportunities and challenges. **Renewable and Sustainable Energy Reviews**, v. 42, p. 1234–1244, fev. 2015.

HARO, P. et al. Potential routes for thermochemical biorefineries. **Biofuels, Bioproducts and Biorefining**, v. 7, n. 5, p. 551–572, set. 2013.

HASLER, P.; BUEHLER, R.; NUSSBAUMER, T. **Evaluation of gas cleaning technologies for biomass gasification**. Biomass for Energy and Industry, 10th European Conference and Technology Exhibition. **Anais...** Würzburg: 1998

HASLER, P.; NUSSBAUMER, T. Gas cleaning for IC engine applications from fixed bed biomass gasification. **Biomass and Bioenergy**, v. 16, p. 385–395, 1999.

HASSAN, E. M. et al. The Potential Use of Whole-tree Biomass for Bio-oil Fuels. **Energy Sources, Part A: Recovery, Utilization, and Environmental Effects**, v. 31, n. 20, p. 1829–1839, 20 ago. 2009.

HE, W.; PARK, C. S.; NORBECK, J. M. Rheological Study of Comingled Biomass and Coal Slurries with Hydrothermal Pretreatment †. **Energy & Fuels**, v. 23, n. 10, p. 4763–4767, 15 out. 2009.

HEIDENREICH, S.; FOSCOLO, P. U. New concepts in biomass gasification. **Progress in Energy and Combustion Science**, v. 46, p. 72–95, fev. 2015.

HENRICH, E. et al. Fast pyrolysis of lignocellulosics in a twin screw mixer reactor.

**Fuel Processing Technology**, v. 143, p. 151–161, mar. 2016.

HENRICH, E.; DAHMEN, N.; DINJUS, E. Cost estimate for biosynfuel production via biosyncrude gasification. **Biofuels, Bioproducts and Biorefining**, v. 3, n. 1, p. 28–41, jan. 2009.

HENRICH, E.; WEIRICH, E. Pressurized entrained flow gasifier for biomass. **Environmental Engineering Science**, v. 21, 2004.

HRYCAK, B.; JASIŃSKI, M.; MIZERACZYK, J. Spectroscopic investigations of microwave microplasmas in various gases at atmospheric pressure. **The European Physical Journal D**, v. 60, n. 3, p. 609–619, 20 dez. 2010.

HU, S. **Life Cycle Analysis of the Production of Aviation Fuels Using the CE-CERT Process**. [s.l.] University of California, 2012.

HUANG, H.; YUAN, X. Recent progress in the direct liquefaction of typical biomass. **Progress in Energy and Combustion Science**, v. 49, p. 59–80, ago. 2015.

HUGOT, E. **Handbook of Cane Sugar Engineering**. 3. ed. [s.l.] Elsevier Science, 1986.

ICAO. **Global Framework for Aviation Alternative Fuels**. Disponível em: <<https://www.icao.int/environmental-protection/GFAAF/Pages/default.aspx>>. Acesso em: 25 set. 2017.

IEA. **Energy Statistics Manual**. Paris, France: [s.n.]. Disponível em: <[https://www.iea.org/publications/freepublications/publication/statistics\\_manual.pdf](https://www.iea.org/publications/freepublications/publication/statistics_manual.pdf)>.

IGLESIA, E. Design, synthesis, and use of cobalt-based Fischer-Tropsch synthesis catalysts. **Applied Catalysis A: General**, v. 161, p. 59–78, 1997.

IGLESIAS GONZALEZ, M.; KRAUSHAAR-CZARNETZKI, B.; SCHAUB, G. Process comparison of biomass-to-liquid (BtL) routes Fischer–Tropsch synthesis and methanol to gasoline. **Biomass Conversion and Biorefinery**, v. 1, n. 4, p. 229–243, 2 dez. 2011.

IM-ORB, K.; SIMASATITKUL, L.; ARPORNWICHANOP, A. Analysis of synthesis gas production with a flexible H<sub>2</sub>/CO ratio from rice straw gasification. **Fuel**, v. 164, p. 361–373, 2016a.

IM-ORB, K.; SIMASATITKUL, L.; ARPORNWICHANOP, A. Techno-economic analysis of the biomass gasification and Fischer–Tropsch integrated process with off-gas recirculation. **Energy**, v. 94, p. 483–496, jan. 2016b.

INDEXMUNDI. **World Jet Fuel Production by Year**. Disponível em: <<https://www.indexmundi.com/energy/?product=jet-fuel&graph=production>>. Acesso em: 1

abr. 2017.

INGRAM, L. et al. Pyrolysis of Wood and Bark in an Auger Reactor: Physical Properties and Chemical Analysis of the Produced Bio-oils. **Energy & Fuels**, v. 22, n. 1, p. 614–625, jan. 2008.

IPCC. **National Greenhouse Gas Inventories**. [s.l.] IPCC Guidelines, 2006.

ISAHAK, W. N. R. W. et al. A review on bio-oil production from biomass by using pyrolysis method. **Renewable and Sustainable Energy Reviews**, v. 16, n. 8, p. 5910–5923, out. 2012.

JAHIRUL, M. et al. Biofuels Production through Biomass Pyrolysis —A Technological Review. **Energies**, v. 5, n. 12, p. 4952–5001, 23 nov. 2012.

JONES, S. et al. **Production of gasoline and diesel from biomass via fast pyrolysis, hydrotreating and hydrocracking: a design case**Energy. Springfield, VA: [s.n.].

JUNQUEIRA, T. L. et al. Use of VSB to Plan Research Programs and Public Policies. In: [s.l: s.n.]. p. 257–282.

JUNQUEIRA, T. L. et al. Techno-economic analysis and climate change impacts of sugarcane biorefineries considering different time horizons. **Biotechnology for Biofuels**, v. 10, n. 1, p. 50, 14 dez. 2017.

KALTSCHMITT, M.; NEULING, U. (EDS.). **Biokerosene**. Berlin, Heidelberg: Springer Berlin Heidelberg, 2018.

KAN, T.; STREZOV, V.; EVANS, T. J. Lignocellulosic biomass pyrolysis: A review of product properties and effects of pyrolysis parameters. **Renewable and Sustainable Energy Reviews**, v. 57, p. 1126–1140, maio 2016.

KIM, K. et al. Long-term operation of biomass-to-liquid systems coupled to gasification and Fischer–Tropsch processes for biofuel production. **Bioresource Technology**, v. 127, p. 391–399, jan. 2013.

KINGSTON, T. A.; HEINDEL, T. J. Granular mixing optimization and the influence of operating conditions in a double screw mixer. **Powder Technology**, v. 266, p. 144–155, nov. 2014.

KIRUBAKARAN, V. et al. A review on gasification of biomass. **Renewable and Sustainable Energy Reviews**, v. 13, n. 1, p. 179–186, jan. 2009.

KLEIN, B. C. et al. Techno-economic and environmental assessment of renewable jet fuel production in integrated Brazilian sugarcane biorefineries. **Applied Energy**, v. 209, p. 290–305, jan. 2018.

KLERK, A. DE. Fischer–Tropsch fuels refinery design. **Energy & Environmental Science**, v. 4, n. 4, p. 1177, 2011.

KNOEF, H. **Handbook of biomass gasification**. [s.l.] BTG Biomass Technology Group, 2005.

KUMABE, K. et al. Production of hydrocarbons in Fischer–Tropsch synthesis with Fe-based catalyst: Investigations of primary kerosene yield and carbon mass balance. **Fuel**, v. 89, n. 8, p. 2088–2095, ago. 2010.

KUMAR, A.; JONES, D. D.; HANNA, M. A. Thermochemical Biomass Gasification: A Review of the Current Status of the Technology. **Energies**, v. 2, n. 3, p. 556–581, 21 jul. 2009.

LA VILLETTA, M.; COSTA, M.; MASSAROTTI, N. Modelling approaches to biomass gasification: A review with emphasis on the stoichiometric method. **Renewable and Sustainable Energy Reviews**, v. 74, p. 71–88, jul. 2017.

LAN, W. et al. Progress in techniques of biomass conversion into syngas. **Journal of the Energy Institute**, v. 88, n. 2, p. 151–156, maio 2015.

LANG, C. et al. Water gas shift catalysts for hydrogen production from biomass steam gasification. **Fuel Processing Technology**, v. 156, p. 246–252, fev. 2017.

LARSON, E.; JIN, H.; CELIK, F. **Gasification-Based Fuels and Electricity Production from Biomass, without and with Carbon Capture and Storage**. [s.l.: s.n.]. Disponível em: <<https://acee.princeton.edu/wp-content/uploads/2016/10/LarsonJinCelik-Biofuels-October-2005.pdf>>.

LEE, D. S. et al. Aviation and global climate change in the 21st century. **Atmospheric Environment**, v. 43, n. 22–23, p. 3520–3537, jul. 2009.

LEE, D. S. et al. Transport impacts on atmosphere and climate: Aviation. **Atmospheric Environment**, v. 44, n. 37, p. 4678–4734, dez. 2010.

LI, X. T. et al. Biomass gasification in a circulating fluidized bed. **Biomass and Bioenergy**, v. 26, n. 2, p. 171–193, fev. 2004.

LIEW, W. H.; HASSIM, M. H.; NG, D. K. S. Review of evolution, technology and sustainability assessments of biofuel production. **Journal of Cleaner Production**, v. 71, p. 11–29, maio 2014.

LIM, M. T.; ALIMUDDIN, Z. Bubbling fluidized bed biomass gasification—Performance, process findings and energy analysis. **Renewable Energy**, v. 33, n. 10, p. 2339–2343, out. 2008.

LIU, G.; YAN, B.; CHEN, G. Technical review on jet fuel production. **Renewable and Sustainable Energy Reviews**, v. 25, p. 59–70, set. 2013.

LOWRY, H. **Chemistry of coal utilization**. [s.l.] John Wiley & Sons, 1945.

LUQUE, R. et al. Design and development of catalysts for Biomass-To-Liquid-Fischer–Tropsch (BTL-FT) processes for biofuels production. **Energy Environ. Sci.**, v. 5, n. 1, p. 5186–5202, 2012.

MARIAS, F. et al. Design of a High Temperature Reactor Fed by a Plasma Torch for Tar Conversion: Comparison Between CFD Modelling and Experimental Results. **Waste and Biomass Valorization**, v. 6, n. 1, p. 97–108, 19 fev. 2015.

MATVEEV, I.; SERBIN, S.; LUX, S. Efficiency of a Hybrid-Type Plasma-Assisted Fuel Reformation System. **IEEE Transactions on Plasma Science**, v. 36, p. 2940–2946, 2008.

MCCALL, M. et al. **Production of aviation fuel from renewable feedstocks**, 2009.

MENG, X. et al. Biomass gasification in a 100 kWth steam-oxygen blown circulating fluidized bed gasifier: Effects of operational conditions on product gas distribution and tar formation. **Biomass and Bioenergy**, v. 35, n. 7, p. 2910–2924, jul. 2011.

MERICHEM. **LO-CAT**. Disponível em: <<http://www.merichem.com/company/overview/technical-lit/tech-papers/gas-sweetening>>. Acesso em: 18 jan. 2018.

MESA-PÉREZ, J. M. et al. Fast oxidative pyrolysis of sugar cane straw in a fluidized bed reactor. **Applied Thermal Engineering**, v. 56, n. 1–2, p. 167–175, jul. 2013.

MILLER, R. S.; BELLAN, J. A Generalized Biomass Pyrolysis Model Based on Superimposed Cellulose, Hemicellulose and Lignin Kinetics. **Combustion Science and Technology**, v. 126, n. 1–6, p. 97–137, jul. 1997.

MILNE, T.; EVANS, R.; ABATZOGLOU, N. **Biomass gasifier “tars”: their nature, formation, and conversion**. [s.l: s.n.].

MME. **Ministério de Minas e Energia**. Disponível em: <Ministério de Minas e Energia>. Acesso em: 15 nov. 2018.

MOHAN, D.; PITTMAN, C. U.; STEELE, P. H. Pyrolysis of Wood/Biomass for Bio-oil: A Critical Review. **Energy & Fuels**, v. 20, n. 3, p. 848–889, maio 2006.

MOK, W.; ANTAL, M. Effects of pressure on biomass pyrolysis. II. Heat of reaction of cellulose pyrolysis. **Thermochimica Acta**, v. 68, p. 165–186, 1983.

MORAES, M. A. F. D. et al. Jet biofuels in Brazil: Sustainability challenges. **Renewable and Sustainable Energy Reviews**, v. 40, p. 716–726, dez. 2014.

MORAIS, E. R. et al. Biorefinery Alternatives. In: **The Virtual Sugarcane Biorefinery Concept**. [s.l.: s.n.]. p. 53–132.

MORGANO, MT. et al. Screw pyrolysis with integrated sequential hot gas filtration. **Journal of Analytical and Applied Pyrolysis**, v. 113, p. 216–224, maio 2015.

MORRIS, K.; ALLEN, R. W. K. Fabric filters. In: **Gas Cleaning in Demanding Applications**. Dordrecht: Springer Netherlands, 1997. p. 70–95.

MOSAYEBI, A.; HAGHTALAB, A. The comprehensive kinetic modeling of the Fischer–Tropsch synthesis over Co@Ru/ $\gamma$ -Al<sub>2</sub>O<sub>3</sub> core–shell structure catalyst. **Chemical Engineering Journal**, v. 259, p. 191–204, jan. 2015.

NAIR, S. A. et al. A high-temperature pulsed corona plasma system for fuel gas cleaning. **Journal of Electrostatics**, v. 61, n. 2, p. 117–127, jun. 2004.

NEUMANN, J. et al. Production and characterization of a new quality pyrolysis oil, char and syngas from digestate – Introducing the thermo-catalytic reforming process. **Journal of Analytical and Applied Pyrolysis**, v. 113, p. 137–142, maio 2015.

NEUMANN, J. et al. Upgraded biofuel from residue biomass by Thermo-Catalytic Reforming and hydrodeoxygenation. **Biomass and Bioenergy**, v. 89, p. 91–97, jun. 2016.

NEVES, R. **Reforma de gás de gaseificação por meio de tocha de plasma: ensaios preliminares**. [s.l.] UNICAMP, 2013.

NICOLEIT, T.; DAHMEN, N.; SAUER, J. Production and Storage of Gasifiable Slurries Based on Flash-Pyrolyzed Straw. **Energy Technology**, v. 4, n. 1, p. 221–229, 2016.

NIGAM, P. S.; SINGH, A. Production of liquid biofuels from renewable resources. **Progress in Energy and Combustion Science**, v. 37, n. 1, p. 52–68, fev. 2011.

NOURELDIN, M. M. B. et al. Benchmarking, insights, and potential for improvement of Fischer-Tropsch-based biomass-to-liquid technology. **Clean Technologies and Environmental Policy**, v. 16, n. 1, p. 37–44, 2014.

OLIVEIRA, C. M. et al. Process integration of a multiperiod sugarcane biorefinery. **Applied Energy**, nov. 2017.

ONEFILE, A. **Why airlines keep pushing biofuels: They have no choice**.

Disponível

em:

<<http://go.galegroup.com/ps/i.do?id=GALE%7CA422700971&v=2.1&u=capes&it=r&p=AO NE&sw=w&asid=481fbfb0f415230a1c7afc0afd84da8c>>. Acesso em: 9 set. 2015.

ORTIZ, P.; JR., S. Compared exergy analysis of sugarcane bagasse sequential hydrolysis and fermentation and simultaneous saccharification and fermentation. **International Journal of Exergy**, v. 19, n. 4, p. 459, 2016.

ORTIZ, P.; JÚNIOR, S. Exergy analysis of pretreatment processes of bioethanol production based on sugarcane bagasse. **Energy**, v. 76, p. 130–138, nov. 2014.

ÖZKARA-AYDINOĞLU, Ş. et al.  $\alpha$ -olefin selectivity of Fe–Cu–K catalysts in Fischer–Tropsch synthesis: Effects of catalyst composition and process conditions. **Chemical Engineering Journal**, v. 181–182, p. 581–589, fev. 2012.

PALMA, V. et al. Innovative structured catalytic systems for methane steam reforming intensification. **Chemical Engineering and Processing: Process Intensification**, v. 120, p. 207–215, out. 2017.

PANWAR, N. L.; KOTHARI, R.; TYAGI, V. V. Thermo chemical conversion of biomass – Eco friendly energy routes. **Renewable and Sustainable Energy Reviews**, v. 16, n. 4, p. 1801–1816, maio 2012.

PAPADIKIS, K.; GU, S.; BRIDGWATER, A. V. CFD modelling of the fast pyrolysis of biomass in fluidised bed reactors: Modelling the impact of biomass shrinkage. **Chemical Engineering Journal**, v. 149, n. 1–3, p. 417–427, 1 jul. 2009.

PEREIRA, L. G.; MACLEAN, H. L.; SAVILLE, B. A. Financial analyses of potential biojet fuel production technologies. **Biofuels, Bioproducts and Biorefining**, v. 11, n. 4, p. 665–681, jul. 2017.

PETERS, J. F. et al. A kinetic reaction model for biomass pyrolysis processes in Aspen Plus. **Applied Energy**, v. 188, p. 595–603, fev. 2017.

PETERS, M.; TIMMERHAUS, K.; WEST, R. **Plant design and economics for chemical engineering**. 5. ed. Boston: McGraw-Hill Education, 2003.

PFITZER, C. et al. Fast Pyrolysis of Wheat Straw in the Bioliq Pilot Plant. **Energy & Fuels**, v. 30, n. 10, p. 8047–8054, 20 out. 2016.

PHILLIPS, S. et al. **Thermochemical Ethanol via Indirect Gasification and Mixed Alcohol Synthesis of Lignocellulosic Biomass**. Golden, Colorado: [s.n.].

PLIS, P.; WILK, R. K. Theoretical and experimental investigation of biomass gasification process in a fixed bed gasifier. **Energy**, v. 36, n. 6, p. 3838–3845, jun. 2011.

PONDINI, M.; EBERT, M. **Process synthesis and design of low temperature Fischer-Tropsch crude production from biomass derived syngas**. [s.l.] Chalmers University of Technology, 2013.

PUSKAS, I.; HURLBUT, R. . Comments about the causes of deviations from the Anderson–Schulz–Flory distribution of the Fischer–Tropsch reaction products. **Catalysis Today**, v. 84, n. 1–2, p. 99–109, ago. 2003.

PYNE. **IEA Bioenergy task 34**. Disponível em: <<http://www.pyne.co.uk>>. Acesso em: 10 mar. 2017.

RADLEIN, D.; QUIGNARD, A. A Short Historical Review of Fast Pyrolysis of Biomass. **Oil & Gas Science and Technology – Revue d'IFP Energies nouvelles**, v. 68, n. 4, p. 765–783, 23 jul. 2013.

RAFFELT, K. et al. The BTL2 Process of Biomass Utilization Entrained-Flow Gasification of Pyrolyzed Biomass Slurries. **Applied Biochemistry and Biotechnology**, v. 129, n. 1–3, p. 153–164, 2006.

RAMOS, A. et al. ATUAL ESTÁGIO DE DESENVOLVIMENTO DA TECNOLOGIA GTL E PERSPECTIVAS PARA O BRASIL. **Química Nova**, v. 34, 2001.

RANZI, E. et al. Chemical kinetics of biomass pyrolysis. **Energy and Fuels**, v. 22, n. 6, p. 4292–4300, 2008.

REIJNEN, K.; VAN BRAKEL, J. Gas Cleaning at High Temperatures and 13gh Pressures: A Review. **Powder Technology**, v. 40, n. 51–111, 1984.

RICCA, A. et al. Innovative catalyst design for methane steam reforming intensification. **Fuel**, v. 198, p. 175–182, jun. 2017.

RICHARDSON, Y.; BLIN, J.; JULBE, A. A short overview on purification and conditioning of syngas produced by biomass gasification: Catalytic strategies, process intensification and new concepts. **Progress in Energy and Combustion Science**, v. 38, n. 6, p. 765–781, dez. 2012.

RIEDEL, T. et al. Comparative study of Fischer–Tropsch synthesis with H<sub>2</sub>/CO and H<sub>2</sub>/CO<sub>2</sub> syngas using Fe- and Co-based catalysts. **Applied Catalysis A: General**, v. 186, p. 201–213, 1999.

RINGER, M.; PUTSCHE, V.; SCAHILL, J. **Large-Scale Pyrolysis Oil Production: A Technology Assessment and Economic Analysis**NREL/TP-510-37779. Golden: [s.n.].

ROEDIG, M.; KLOSE, W. **Modelling of Coal Pyrolysis Using a Twin Screw Reactor**. Proceedings of the 4th Ulcos seminar. **Anais...**2008

ROJO, C. et al. Impact of alternative jet fuels on aircraft-induced aerosols. **Fuel**, v. 144, p. 335–341, mar. 2015.

ROSTRUP-NIELSEN, J. Syngas in perspective. **Catalysis Today**, v. 71, p. 243–247, 2002.

SAGAR, A. D.; KARTHA, S. Bioenergy and Sustainable Development? **Annual Review of Environment and Resources**, v. 32, n. 1, p. 131–167, nov. 2007.

SAINNA, M.; MK, A. Catalyst and Catalysis for Fischer-Tropsch Synthesis: A Comparative Analysis of Iron and Cobalt Catalysts on SBA-15. **Journal of Thermodynamics & Catalysis**, v. 7, n. 2, 2016.

SAITOVITCH, H.; SILVA, P. INTERAÇÕES HIPERFINAS EM CATALISADORES METÁLICOS. **Química Nova**, v. 28, p. 529–534, 2005.

SAMAL, S. Thermal plasma technology: The prospective future in material processing. **Journal of Cleaner Production**, v. 142, p. 3131–3150, jan. 2017.

SÁNCHEZ, C. **Tecnologias de gaseificação de biomassa**. 1. ed. [s.l.: s.n.].

SANCHEZ, E. Alcatrão ou bio-óleo: caracterização, amostragem e utilização. In: SÁNCHEZ, C. (Ed.). **Tecnologia da gaseificação de biomassa**. [s.l.: s.n.]. p. 257–262.

SANDSTRÖM, L. et al. Pyrolysis of Nordic biomass types in a cyclone pilot plant — Mass balances and yields. **Fuel Processing Technology**, v. 152, p. 274–284, nov. 2016.

SANTOS, C. I. et al. Integrated 1st and 2nd generation sugarcane bio-refinery for jet fuel production in Brazil: Techno-economic and greenhouse gas emissions assessment. **Renewable Energy**, maio 2017.

SCHOLZE, B.; MEIER, D. Characterization of the water-insoluble fraction from pyrolysis oil (pyrolytic lignin). Part I. PY–GC/MS, FTIR, and functional groups. **Journal of Analytical and Applied Pyrolysis**, v. 60, n. 1, p. 41–54, jun. 2001.

SCHULZ, H. Short history and present trends of Fischer–Tropsch synthesis. **Applied Catalysis A: General**, v. 186, p. 3–12, 1999.

SCHULZ, H.; CLAEYS, M. Kinetic modelling of Fischer–Tropsch product distributions. **Applied Catalysis A: General**, v. 186, p. 91–107, 1999.

SEGGIANI, M. et al. Cogasification of sewage sludge in an updraft gasifier. **Fuel**, v. 93, p. 486–491, mar. 2012.

SEIXAS, B. **Confirmado! Espírito Santo vai sediar fábrica de bio-óleo**. Disponível em: <<https://www.gazetaonline.com.br/noticias/economia/2018/02/confirmado-espirito-santo-vai-sediar-fabrica-de-bio-oleo-1014120943.html>>.

SELVATICO, D.; LANZINI, A.; SANTARELLI, M. Low Temperature Fischer-Tropsch fuels from syngas: Kinetic modeling and process simulation of different plant

configurations. **Fuel**, v. 186, p. 544–560, dez. 2016.

SENAPATI, P. K.; BEHERA, S. Experimental investigation on an entrained flow type biomass gasification system using coconut coir dust as powdery biomass feedstock. **Bioresource Technology**, v. 117, p. 99–106, ago. 2012.

SHARMA, S. D. et al. A critical review of syngas cleaning technologies — fundamental limitations and practical problems. **Powder Technology**, v. 180, n. 1–2, p. 115–121, jan. 2008.

SHEMFE, M. B.; GU, S.; RANGANATHAN, P. Techno-economic performance analysis of biofuel production and miniature electric power generation from biomass fast pyrolysis and bio-oil upgrading. **Fuel**, v. 143, p. 361–372, mar. 2015.

SHETH, P. N.; BABU, B. V. Experimental studies on producer gas generation from wood waste in a downdraft biomass gasifier. **Bioresource Technology**, v. 100, n. 12, p. 3127–3133, jun. 2009.

SIEMENS, A. **Modern gas turbines with high fuel flexibility**. Kuala Lumpur: [s.n.]. Disponível em: <<http://m.energy.siemens.com/hq/pool/hq/energy-topics/pdfs/en/gas-turbines-power-plants/ModernGasTurbineswithHighFuelFlexibility.pdf>>.

SIKARWAR, S. et al. Progress in biofuel production from gasification. **Progress in Energy and Combustion Science**, v. 61, p. 189–248, 2017.

SIMELL, P. et al. Clean syngas from biomass—process development and concept assessment. **Biomass Conversion and Biorefinery**, v. 4, n. 4, p. 357–370, 1 dez. 2014.

SKYNRG. **Rationale for sustainable aviation fuel (SAF)**. Disponível em: <<http://skynrg.com/sustainability/rationale-sustainable-aviation-fuel/>>. Acesso em: 27 set. 2017.

SPATH, P.; DAYTON, D. **Preliminary Screening —Technical and Economic Assessment of Synthesis Gas to Fuels and Chemicals with Emphasis on the Potential for Biomass-Derived Synga**. Golden, Colorado: [s.n.].

STEYNBERG, A. Introduction to Fischer-Tropsch technology. In: **Fischer-Tropsch technology**. [s.l.] Elsevier Science & Technology Books, 2004. p. 1–63.

STEYNBERG, A.; DRY, M. **Fischer-Tropsch technology**. Elsevier S ed. [s.l.: s.n.].

SUDIRO, M.; BERTUCCO, A. Production of synthetic gasoline and diesel fuel by alternative processes using natural gas and coal: Process simulation and optimization. **Energy**, v. 34, n. 12, p. 2206–2214, dez. 2009.

SUNDE, K.; BREKKE, A.; SOLBERG, B. Environmental impacts and costs of woody Biomass-to-Liquid (BTL) production and use — A review. **Forest Policy and Economics**, v. 13, n. 8, p. 591–602, out. 2011.

SUTTON, D.; KELLEHER, B.; ROSS, J. Review of literature on catalysts for biomass gasification. **Fuel Processing Technology**, v. 73, p. 155–173, 2001.

SWAIN, P. K.; DAS, L. M.; NAIK, S. N. Biomass to liquid: A prospective challenge to research and development in 21st century. **Renewable and Sustainable Energy Reviews**, v. 15, n. 9, p. 4917–4933, dez. 2011.

SWANSON, R. M. et al. Techno-economic analysis of biomass-to-liquids production based on gasification. **Fuel**, v. 89, n. SUPPL. 1, p. S11–S19, 2010.

SZARGUT, J.; MORRIS, D.; STEWARD, F. **Exergy analysis of thermal, chemical and metallurgical processes**. 1 edition ed. [s.l.] Hemisphere, 1988.

TAKESHITA, T.; YAMAJI, K. Important roles of Fischer–Tropsch synfuels in the global energy future. **Energy Policy**, v. 36, n. 8, p. 2773–2784, ago. 2008.

TAO, K. et al. Plasma enhanced catalytic reforming of biomass tar model compound to syngas. **Fuel**, v. 104, p. 53–57, fev. 2013.

TEIXEIRA, F.; PRIMO, K.; LORA, E. Impacto ambiental do uso energético da biomassa e tecnologias para o controle de emissões. In: CORTEZ, L.; LORA, E.; GÓMEZ, E. (Eds.). **Biomassa para energia**. Editora Un ed. [s.l.: s.n.]. p. 645–670.

TIJMENSEN, M. et al. Exploration of the possibilities for production of Fischer Tropsch liquids and power via biomass gasification. **Biomass and Bioenergy**, v. 23, p. 129–152, 2002.

TRIPPE, F. et al. Techno-economic analysis of fast pyrolysis as a process step within biomass-to-liquid fuel production. **Waste and Biomass Valorization**, v. 1, n. 4, p. 415–430, 2010.

TRIPPE, F. et al. Techno-economic assessment of gasification as a process step within biomass-to-liquid (BtL) fuel and chemicals production. **Fuel Processing Technology**, v. 92, n. 11, p. 2169–2184, nov. 2011.

TRIPPE, F. et al. Comprehensive techno-economic assessment of dimethyl ether (DME) synthesis and Fischer-Tropsch synthesis as alternative process steps within biomass-to-liquid production. **Fuel Processing Technology**, v. 106, p. 577–586, 2013.

TSAI, W. T.; LEE, M. K.; CHANG, Y. M. Fast pyrolysis of rice straw, sugarcane bagasse and coconut shell in an induction-heating reactor. **Journal of Analytical and Applied**

**Pyrolysis**, v. 76, n. 1–2, p. 230–237, jun. 2006.

TURK, B. et al. **Novel technologies for gaseous contaminants control**. [s.l.: s.n.].

UHM, H. S. et al. High-Efficiency Gasification of Low-Grade Coal by Microwave Steam Plasma. **Energy & Fuels**, v. 28, n. 7, p. 4402–4408, 17 jul. 2014.

VAN DER DRIFT, A. et al. **Bio-syngas: key intermediate for large scale production of green fuels and chemicals**. [s.l.: s.n.].

VAN DER DRIFT, A.; BOERRIGTER, H.; CODA, B. Entrained flow gasification of biomass. **ECN - Energy Centre of the Netherlands**, n. April, p. 58, 2004.

VAN DER DRIFT, A.; VAN DOORN, J.; VERMEULEN, J. Ten residual biomass fuels for circulating fluidized-bed gasification. **Biomass and Bioenergy**, v. 20, p. 45–56, 2001.

VAN OOST, G. et al. Pyrolysis/gasification of biomass for synthetic fuel production using a hybrid gas–water stabilized plasma torch. **Vacuum**, v. 83, n. 1, p. 209–212, set. 2008.

VECINO MANTILLA, S. et al. Comparative study of bio-oil production from sugarcane bagasse and palm empty fruit bunch: Yield optimization and bio-oil characterization. **Journal of Analytical and Applied Pyrolysis**, v. 108, p. 284–294, jul. 2014.

VENDERBOSCH, R.; PRINS, W. Fast pyrolysis technology development. **Biofuels, Bioproducts and Biorefining**, v. 4, n. 2, p. 178–208, mar. 2010.

WANG, Y. et al. Kinetics modelling of Fischer–Tropsch synthesis over an industrial Fe–Cu–K catalyst. **Fuel**, v. 82, p. 195–213, 2003.

WARNECKE, R. Gasification of biomass: comparison of fixed bed and fluidized bed gasifier. **Biomass & Bioenergy**, v. 18, p. 489–497, 2000.

WATANABE, M. D. B. et al. Sustainability Assessment Methodologies. In: [s.l.: s.n.], p. 155–188.

WEILAND, F. et al. Pressurized Oxygen Blown Entrained-Flow Gasification of Wood Powder. **Energy & Fuels**, v. 27, n. 2, p. 932–941, 21 fev. 2013.

WISE, M.; MURATORI, M.; KYLE, P. Biojet fuels and emissions mitigation in aviation: An integrated assessment modeling analysis. **Transportation Research Part D: Transport and Environment**, v. 52, p. 244–253, maio 2017.

WOOLCOCK, P. J.; BROWN, R. C. A review of cleaning technologies for biomass-derived syngas. **Biomass and Bioenergy**, v. 52, p. 54–84, maio 2013.

WOOLEY, R. J.; PUTSCHE, V. **Development of an ASPEN PLUS Physical Property Database for Biofuels Components** Victoria. Golden: [s.n.].

WRIGHT, M. M. et al. **Techno-Economic Analysis of Biomass Fast Pyrolysis to Transportation Fuels**. Golden, Colorado: [s.n.].

YANIK, J. et al. Fast pyrolysis of agricultural wastes: Characterization of pyrolysis products. **Fuel Processing Technology**, v. 88, n. 10, p. 942–947, out. 2007.

YOON, S. J.; LEE, G. J. Syngas Production from Coal through Microwave Plasma Gasification: Influence of Oxygen, Steam, and Coal Particle Size. **Energy & Fuels**, v. 26, n. 1, p. 524–529, 19 jan. 2012.

YU, J. et al. Surrogate Definition and Chemical Kinetic Modeling for Two Different Jet Aviation Fuels. **Energy & Fuels**, p. acs.energyfuels.5b02414, 26 jan. 2016.

ZHANG, W. et al. Gas cleaning strategies for biomass gasification product gas. **International Journal of Low-Carbon Technologies**, v. 7, n. 2, p. 69–74, jun. 2012.

ZHANG, Y. et al. Production of jet and diesel biofuels from renewable lignocellulosic biomass. **Applied Energy**, v. 150, p. 128–137, jul. 2015.

**Appendix – CAPEX and OPEX**

This appendix presents all CAPEX and OPEX tables simulated in this work.

CAPEX for biomass handling and feeding hierarchy															
Scenario	Equipment	Value	Unit	Equipment	Base year	Year wished	Correction CEPCI	Corrected value	R\$/€ or R\$/US\$	Corrected value (R\$)	Simulation	Coefficient	Value (R\$)	Installed value (R\$)	Reference
Centralized	Chopper	111125	kg/h	420400	2007	2016	1.0310	433442	3.352	1452792	310119	0.75	3136829	7246075	(SWANSON et al., 2010)
	Chopper conveyor	111125	kg/h	61400	2007	2016	1.0310	63305	3.352	212182	310119	0.75	458138	1058299	(SWANSON et al., 2010)
	Chopper screen with recycle conveyor	111125	kg/h	20800	2007	2016	1.0310	21445	3.352	71879	310119	0.75	155200	358512	(SWANSON et al., 2010)
	Rotary dryer	111125	kg/h	6337000	2007	2016	1.0310	6533599	3.352	21899006	310119	0.75	47283743	109225447	(SWANSON et al., 2010)
	Grinder	111125	kg/h	668400	2007	2016	1.0310	689136	3.352	2309815	310119	0.75	4987290	11520639	(SWANSON et al., 2010)
	Grinder conveyor	111125	kg/h	61400	2007	2016	1.0310	63305	3.352	212182	310119	0.75	458138	1058299	(SWANSON et al., 2010)
	Grinder screen with recycle conveyor	111125	kg/h	20800	2007	2016	1.0310	21445	3.352	71879	310119	0.75	155200	358512	(SWANSON et al., 2010)
	Flue gas stack	325065	kg/h	51581	2002	2016	1.3693	70631	3.352	236736	339767	1	247442	571592	(SWANSON et al., 2010)
Total													56881981	131397375	
Decentralized	Chopper	111125	kg/h	420400	2007	2016	1.0310	433442	3.352	1452792	167257	0.75	1974162	4560314	(SWANSON et al., 2010)
	Chopper conveyor	111125	kg/h	61400	2007	2016	1.0310	63305	3.352	212182	167257	0.75	288329	666040	(SWANSON et al., 2010)
	Chopper screen with recycle conveyor	111125	kg/h	20800	2007	2016	1.0310	21445	3.352	71879	167257	0.75	97675	225629	(SWANSON et al., 2010)
	Rotary dryer	111125	kg/h	6337000	2007	2016	1.0310	6533599	3.352	21899006	167257	0.75	29758004	68740989	(SWANSON et al., 2010)
	Grinder	111125	kg/h	668400	2007	2016	1.0310	689136	3.352	2309815	167257	0.75	3138749	7250509	(SWANSON et al., 2010)
	Grinder conveyor	111125	kg/h	61400	2007	2016	1.0310	63305	3.352	212182	167257	0.75	288329	666040	(SWANSON et al., 2010)
	Grinder screen with recycle conveyor	111125	kg/h	20800	2007	2016	1.0310	21445	3.352	71879	167257	0.75	97675	225629	(SWANSON et al., 2010)
	Flue gas stack	325065	kg/h	51581	2002	2016	1.3693	70631	3.352	236736	183104	1	133349	308037	(SWANSON et al., 2010)
Total													35642923	82643189	
Two decentralized plants													71285846	165286377	

OPEX for biomass handling and feeding hierarchy				
Scenario	Unit	Value	Value (R\$)/year	Reference
Centralized	4	% of CAPEX	2275279	Consideration
Decentralized	4	% of CAPEX	1425717	Consideration
Two decentralized plants	4	% of CAPEX	2851434	Consideration

CAPEX for pyrolysis hierarchy																
Scenario	Equipment	Value	Unit	Equipment	Base year	Year wished	Correction CEPCI	Corrected value	R\$/€ or R\$/US\$	Corrected value (R\$)	Simulation	Coefficient	Value (R\$)	Installed value (R\$)	Reference	
Centralized	Pyrolysis reactor	25000	kg/h	40480000	2008	2016	0.9414	38109169.27	3.528	134436157	131508	0.7	429758629	992742433	(HENRICH; DAHMEN; DINJUS, 2009; TRIPPE et al., 2010) (TRIPPE et al., 2010)	
	Additional units (heat carrier loop, product recovery, and bioslurry mixing)	13.5	%	Pyrolysis reactor										134020228		
	Total													1126762662		
Decentralized	Pyrolysis reactor	25000	kg/h	40480000	2008	2016	0.9414	38109169.27	3.528	134436157	70550	0.7	277911167	641974795	(HENRICH; DAHMEN; DINJUS, 2009; TRIPPE et al., 2010) (TRIPPE et al., 2010)	
	Additional units (heat carrier loop, product recovery, and bioslurry mixing)	13.5	%	Pyrolysis reactor										86666597		
	Total													728641392		
Two decentralized plants														1457282784		

OPEX for pyrolysis hierarchy					
Scenario		Value	Unit	Value (R\$)/year	Reference
Centralized	Pyrolysis reactor and additional units	4.23	% of CAPEX	47662061	(PETERS; TIMMERHAUS; WEST, 2003; TRIPPE et al., 2010)
	Total			47662061	
Decentralized	Storage & transport	1.5	% of CAPEX	10929621	(PETERS; TIMMERHAUS; WEST, 2003; TRIPPE et al., 2010)
	Pyrolysis reactor and additional units	4.23	% of CAPEX	30821531	
	Total			41751152	
Two decentralized plants				83502304	

OPEX	Average distance (km)	Bioslurry mass flow (t)	Transportation cost (€/t)	Transportation cost (R\$/t)	Reference
Bioslurry transportation (decentralized scenario)	25	70.55	15.38	54.27	(Henrich et al 2009)

CAPEX for gasification hierarchy																
Scenario	Equipment	Value	Unit	Installed equipment	Equipment	Base year	Year wished	Correction CEPCI	Corrected value	R\$/€ or R\$/US\$	Corrected value (R\$)	Simulation	Coefficient	Value (R\$)	Installed value (R\$)	Reference
Centralized	Bioslurry blending tank	672	m <sup>3</sup>	282384	122244	2010	2016	0.9835	120225	3.528	424111	70.70	0.57	117502	271429	(TRIPPE et al., 2011)
	Bioslurry blending tank agitators	3600	m <sup>3</sup> /h	206091	89217	2010	2016	0.9835	87743	3.528	309527	378.74	0.49	102683	237198	(TRIPPE et al., 2011)
	bioslurry blending tank pumps	42	m <sup>3</sup> /h	44717	19358	2010	2016	0.9835	19038	3.528	67160	4.42	0.33	31944	73790	(TRIPPE et al., 2011)
	Entrained flow gasifier	808	MW	26239109	11358922	2010	2016	0.9835	11171256	3.528	39408383	493.10	0.8	26546470	61322345	(TRIPPE et al., 2011)
	Slag dewatering, depressurizer, crusher	13	t/h	3495027	1512999	2010	2016	0.9835	1488002	3.528	5249163	3.75	0.7	2197806	5076933	(TRIPPE et al., 2011)
	Slag handling tank	150	m <sup>3</sup>	146096	63245	2010	2016	0.9835	62200	3.528	219421	43.25	0.57	107993	249464	(TRIPPE et al., 2011)

	Slag conveyer	13	t/h	80052	34655	2010	2016	0.9835	34082	3.528	120230	3.75	0.7	50340	116285	(TRIPPE et al., 2011)
	Slag separation screen	13	t/h	200129	86636	2010	2016	0.9835	85205	3.528	300573	3.75	0.7	125849	290711	(TRIPPE et al., 2011)
	Slag conveyer	13	t/h	80052	34655	2010	2016	0.9835	34082	3.528	120230	3.75	0.7	50340	116285	(TRIPPE et al., 2011)
	Storage bin	500	m <sup>3</sup>	237477	102804	2010	2016	0.9835	101105	3.528	356665	144.15	0.57	175541	405500	(TRIPPE et al., 2011)
	Unloading equipment	50	t/h	226623	98105	2010	2016	0.9835	96484	3.528	340364	14.42	0.69	144293	333316	(TRIPPE et al., 2011)
	Gasification foundation	1			2753288	2010	2016	0.9835	2707800	3.528	9552194	0.61	0.7	6760348	15616404	(TRIPPE et al., 2011)
	Air Separation Unit (oxygen flow)	79958	kg/h	9935138	4300926	2002	2016	1.3693	5889311	3.528	20775481	75517.00	0.69	19972115	46135585	(SWANSON et al., 2010)
	Total													56383222	130245244	
Decentralized	Bioslurry receive and unload	1250000	kg/h	1693376	733063	2010	2016	0.9835	720952	3.528	2543273	141100.00	0.69	564545	1304099	(TRIPPE et al., 2011)
	Bioslurry tank without agitator	5040	m <sup>3</sup>	1160749	502489	2010	2016	0.9835	494187	3.528	1743323	568.92	0.57	502770	1161399	(TRIPPE et al., 2011)
	Centrifugal bioslurry pumps	504	m <sup>3</sup> /h	41557	17990	2010	2016	0.9835	17693	3.528	62414	56.89	0.33	30384	70187	(TRIPPE et al., 2011)
	Bioslurry blending tank	672	m <sup>3</sup>	282384	122244	2010	2016	0.9835	120225	3.528	424111	75.86	0.57	122313	282542	(TRIPPE et al., 2011)
	Bioslurry blending tank agitators	3600	m <sup>3</sup> /h	206091	89217	2010	2016	0.9835	87743	3.528	309527	406.37	0.49	106287	245523	(TRIPPE et al., 2011)
	bioslurry blending tank pumps	42	m <sup>3</sup> /h	44717	19358	2010	2016	0.9835	19038	3.528	67160	4.74	0.33	32695	75524	(TRIPPE et al., 2011)
	Handling and feed foundation	1		792550	343095	2010	2016	0.9835	337427	3.528	1190327	0.11	1	134364	310381	(TRIPPE et al., 2011)
	Entrained flow gasifier	808	MW	26239109	11358922	2010	2016	0.9835	11171256	3.528	39408383	530.50	0.8	28145518	65016148	(TRIPPE et al., 2011)
	Slag dewatering, depressurizer, crusher	13	t/h	3495027	1512999	2010	2016	0.9835	1488002	3.528	5249163	3.98	0.7	2292982	5296788	(TRIPPE et al., 2011)
	Slag handling tank	150	m <sup>3</sup>	146096	63245	2010	2016	0.9835	62200	3.528	219421	45.95	0.57	111786	258226	(TRIPPE et al., 2011)
	Slag conveyer	13	t/h	80052	34655	2010	2016	0.9835	34082	3.528	120230	3.98	0.7	52520	121321	(TRIPPE et al., 2011)
	Slag separation screen	13	t/h	200129	86636	2010	2016	0.9835	85205	3.528	300573	3.98	0.7	131299	303300	(TRIPPE et al., 2011)
	Slag conveyer	13	t/h	80052	34655	2010	2016	0.9835	34082	3.528	120230	3.98	0.7	52520	121321	(TRIPPE et al., 2011)
	Storage bin	500	m <sup>3</sup>	237477	102804	2010	2016	0.9835	101105	3.528	356665	153.15	0.57	181707	419743	(TRIPPE et al., 2011)
	Unloading equipment	50	t/h	226623	98105	2010	2016	0.9835	96484	3.528	340364	15.32	0.69	150450	347540	(TRIPPE et al., 2011)
	Gasification foundation	1			2753288	2010	2016	0.9835	2707800	3.528	9552194	1.00	0.7	9552194	22065569	(TRIPPE et al., 2011)
	Air Separation Unit (to gasifier)	79958	kg/h	9935138	4300926	2002	2016	1.3693	5889311	3.528	20775481	80988.00	0.69	20959623	48416728	(SWANSON et al., 2010)
	Total													63123956	145816339	

OPEX for gasification hierarchy					
Scenario		Unit	Value	Value (R\$)/year	Reference
Centralized	Bioslurry operation	4	% of CAPEX	23297	(PETERS; TIMMERHAUS; WEST, 2003; TRIPPE et al., 2010)
	Air Separation Unit (to gasifier)	5	% of CAPEX	2306779	(PETERS; TIMMERHAUS; WEST, 2003; TRIPPE et al., 2010)
	Slag recovery and handling	2	% of CAPEX	131770	(PETERS; TIMMERHAUS; WEST, 2003; TRIPPE et al., 2010)
	Gasifier reactor	5	% of CAPEX	3066117	(PETERS; TIMMERHAUS; WEST, 2003; TRIPPE et al., 2010)
	Steam gasification equipment	5	% of CAPEX	3066117	(PETERS; TIMMERHAUS; WEST, 2003; TRIPPE et al., 2010)
	Total				8594080
Decentralized	Bioslurry operation	4	% of CAPEX	101427	(PETERS; TIMMERHAUS; WEST, 2003; TRIPPE et al., 2010)
	Air Separation Unit (to gasifier)	5	% of CAPEX	2420836	(PETERS; TIMMERHAUS; WEST, 2003; TRIPPE et al., 2010)
	Slag recovery and handling	2	% of CAPEX	137365	(PETERS; TIMMERHAUS; WEST, 2003; TRIPPE et al., 2010)
	Gasifier reactor	5	% of CAPEX	3250807	(PETERS; TIMMERHAUS; WEST, 2003; TRIPPE et al., 2010)
	Steam gasification equipment	5	% of CAPEX	3250807	(PETERS; TIMMERHAUS; WEST, 2003; TRIPPE et al., 2010)
	Total				9161243

CAPEX for Gas cleaning and conditioning																
Scenario	Equipment	Value	Unit	Installed equipment	Equipment	Base year	Year wished	Correction CEPCI	Corrected value	R\$/€ or R\$/US\$	Corrected value (R\$)	Simulation	Coefficient	Value (R\$)	Installed value (R\$)	Reference
Centralized	Ceramic filter	400	m³/h	227377	98432	2008	2016	0.9414	92667	3.528	326896	14073	0.7	3952276	9129758	(TRIPPE et al., 2011)
	Direct quench	122083	kg/h		377600	2007	2016	1.0310	389315	3.352	1304886	320298	0.75	2689962	6213811	(SWANSO N et al., 2010)
	Amine system	91583	kg/h		6789129	2007	2016	1.0310	6999755	3.352	23461445	179512	0.75	38865346	89778948	(PHILLIPS et al., 2007)
	LOCAT absorber	64292	kg/h		23800	2007	2016	1.0310	24538	3.352	82247	68184	0.75	85953	198553	(SWANSO N et al., 2010)
	LOCAT oxidizer vessel	64292	kg/h		1000000	2007	2016	1.0310	1031024	3.352	3455737	68184	0.75	3611491	8342544	(SWANSO N et al., 2010)
	Zinc oxide guard bed	148750	kg/h		122000.00	2007	2016	1.0310	125785	3.352	421600	262173	0.75	644909	1489741	(SWANSO N et al., 2010)
	Total															115153355
Decentralized	Ceramic filter	400	m³/h	227377	98432	2008	2016	0.9414	92667	3.528	326896	14944	0.7	4121849	9521472	(TRIPPE et al., 2011)
	Direct quench	122083	kg/h		377600	2007	2016	1.0310	389315	3.352	1304886	340112	0.75	2813824	6499932	(SWANSO N et al., 2010)
	Amine system	91583	kg/h		6789129	2007	2016	1.0310	6999755	3.352	23461445	191984	0.75	40873441	94417648	(PHILLIPS et al., 2007)
	LOCAT absorber	64292	kg/h		23800	2007	2016	1.0310	24538	3.352	82247	71854	0.75	89400	206515	(SWANSO N et al., 2010)
	LOCAT oxidizer vessel	64292	kg/h		1000000	2007	2016	1.0310	1031024	3.352	3455737	71854	0.75	3756323	8677105	(SWANSO N et al., 2010)
	Zinc oxide guard bed	148750	kg/h		122000	2007	2016	1.03102	125785	3.352	421600	283656	0.75	684151	1580388	(SWANSO N et al., 2010)
	Total															120903061

OPEX for for Gas cleaning and conditioning												
Scenario		Unit	Value	Base year	Year wished	Correction CEPCI	Corrected value	R\$/€ or R\$/US\$	Corrected value (R\$)	Simulation	Value (R\$)/year	Reference
Centralized	Ceramic filter	5	% of CAPEX								456488	(TRIPPE et al., 2011)
	Direct quench	2	% of CAPEX								124276	(TRIPPE et al., 2011)
	Amine makeup	0.4944	\$/kg	2007	2016	1.031	0.510	3.352	1.709	9600	16402	(SWANSON et al., 2010)
	LOCAT chemicals	0.176	\$/kg	2007	2016	1.031	0.181	3.352	0.608	N/A		
	Zinc oxide guard bed	0.0001	\$/kg	2007	2016	1.031	0.000	3.352	0.000	1258430400	555373	(SWANSON et al., 2010)
	Total											1152539
Decentralized	Ceramic filter	5	% of CAPEX								476074	(TRIPPE et al., 2011)
	Direct quench	2	% of CAPEX								129999	(TRIPPE et al., 2011)
	Amine makeup	0.4944	\$/kg	2007	2016	1.031	0.510	3.352	1.709	10080	17222	(SWANSON et al., 2010)
	LOCAT chemicals	0.176	\$/kg	2007	2016	1.031	0.181	3.352	0.608	N/A		
	Zinc oxide guard bed	0.0001	\$/kg	2007	2016	1.031	0.000	3.352	0.000	1361548800	600881	(SWANSON et al., 2010)
	Total											1224176

CAPEX for Fischer-Tropsch hierarchy																
Scenario	Equipment	Value	Unit	Installed equipment	Equipment	Base year	Year wished	Correction CEPCI	Corrected value	R\$/€ or R\$/US\$	Corrected value (R\$)	Simulation	Coefficient	Value (R\$)	Installed value (R\$)	Reference
Centralized	Water Gas Shift reactor	210000	kg/h	1165951	504741	2010	2016	0.9835	496402	3.528	1751136	143968	0.80	1294664	2990675	(TRIPPE et al., 2011)
	FT reactor	178042	kg/h	34365342	9545928	2007	2016	1.0310	9842081	3.352	32988217	344619	0.60	49028588	113256039	(LARSON; JIN; CELIK, 2005)
	Off-gas separation	207083	kg/h		72000	2007	2016	1.0310	74234	3.352	248813	344619	0.60	337746	780192	(SWANSON et al., 2010)
	Water separation	1132	kg/h		39200	2007	2016	1.0310	40416	3.352	135465	344619	0.60	4187188	9672404	(SWANSON et al., 2010)
	Distillation column	60958	kg/h		217742	2007	2016	1.0310	224497	3.352	752459	5185	0.60	171519	396209	(SWANSON et al., 2010)
	Pressure Swing Adsorber	2792	kg/h		366000	2007	2016	1.0310	377355	3.352	1264800	475	0.60	437039	1009559	(SWANSON et al., 2010)
	Wax hydrocracking	13933	kg/h		7927152	2007	2016	1.0310	8173084	3.352	27394153	1401	0.70	5486887	12674710	(LARSON; JIN; CELIK, 2005)
	Gasoline storage tank (used for green naphtha)	3625	kg/h		646300	2007	2016	1.0310	666351	3.352	2233443	1400	0.70	1147490	2650702	(SWANSON et al., 2010)
	Gasoline storage tank (used for green biojet fuel)	3625	kg/h		646300	2007	2016	1.0310	666351	3.352	2233443	3089	0.70	1996787	4612578	(SWANSON et al., 2010)
	Total															148043068
Decentralized	Water Gas Shift reactor	210000	kg/h	1165951	504741	2010	2016	0.9835	496402	3.528	1751136	157220	0.80	1389155	3208947	(TRIPPE et al., 2011)
	FT reactor	178042	kg/h	34365342	9545928	2007	2016	1.0310	9842081	3.352	32988217	373896	0.60	51486853	118934631	(LARSON; JIN; CELIK, 2005)
	Off-gas separation	207083	kg/h		72000	2007	2016	1.0310	74234	3.352	248813	373896	0.60	354680	819311	(SWANSON et al., 2010)
	Water separation	1132	kg/h		39200	2007	2016	1.0310	40416	3.352	135465	373896	0.60	4397131	10157372	(SWANSON et al., 2010)
	Distillation column	60958	kg/h		217742	2007	2016	1.0310	224497	3.352	752459	5568	0.60	179012	413518	(SWANSON et al., 2010)
	Pressure Swing Adsorber	2792	kg/h		366000	2007	2016	1.0310	377355	3.352	1264800	514	0.60	458228	1058506	(SWANSON et al., 2010)
	Wax hydrocracking	13933	kg/h		7927152	2007	2016	1.0310	8173084	3.352	27394153	1506	0.70	5771608	13332415	(LARSON; JIN; CELIK, 2005)
	Gasoline storage tank (used for green naphtha)	3625	kg/h		646300	2007	2016	1.0310	666351	3.352	2233443	1496	0.70	1202019	2776664	(SWANSON et al., 2010)
	Gasoline storage tank (used for green biojet fuel)	3625	kg/h		646300	2007	2016	1.0310	666351	3.352	2233443	3322	0.70	2101063	4853454	(SWANSON et al., 2010)
	Total															155554819



CAPEX for Gas Turbine hierarchy																	
Scenario	Equipment	Value	Unit	Installed equipment	Equipment	Base year	Year wished	Correction CEPCI	Corrected value	R\$/€ or R\$/US\$	Corrected value (R\$)	Simulation	Coefficient	Value (R\$)	Installed value (R\$)	Reference	
Centralized	Gas turbine	86.7	MW (el)	10100000	4372294	2011	2016	0.9249	4043831	3.528	14265257	162	0.75	22793080	52652015	(LARSON; JIN; CELIK, 2005; TRIPPE et al., 2013)	
	Heat Recovery Steam Generator (HRSG)	201	MW (th)	12400000	5367965	2011	2016	0.9249	4964703	3.528	17513781	181	1.00	15761968	36410145		(LARSON; JIN; CELIK, 2005; TRIPPE et al., 2013)
	Flue gas stack Total	325065.7271	kg/h		51581	2002	2016	1.3693	70631	3.352	236736	1131404	1.00	823969	1903368		
Decentralized	Gas turbine	86.7	MW (el)	10100000	4372294	2011	2016	0.9249	4043831	3.528	14265257	174	0.75	24069199	55599850	(LARSON; JIN; CELIK, 2005; TRIPPE et al., 2013)	
	Heat Recovery Steam Generator (HRSG)	201	MW (th)	12400000	5367965	2011	2016	0.9249	4964703	3.528	17513781	195	1.00	16950029	39154568		(LARSON; JIN; CELIK, 2005; TRIPPE et al., 2013)
	Flue gas stack Total	325065.7271	kg/h		51581	2002	2016	1.3693	70631	3.352	236736	1216196	1.00	885720	2046014		
															90965528	96800432	

OPEX for Gas Turbine hierarchy				
Scenario	Unit	Value	Value (R\$)/year	Reference
Centralized	4.5	% of CAPEX	4093449	(TRIPPE et al., 2011)
Decentralized	4.5	% of CAPEX	4356019	(TRIPPE et al., 2011)

CAPEX for Steam Turbine hierarchy																
Scenario	Equipment	Value	Unit	Installed equipment	Equipment	Base year	Year wished	Correction CEPCI	Corrected value	R\$/€ or R\$/US\$	Corrected value (R\$)	Simulation	Coefficient	Value (R\$)	Installed value (R\$)	Reference
Centralized	Steam turbine	8.95	MW (el)		3133000	1990	2016	1.5148	4745934	3.352	15907197	104	0.60	69492778	160528318	(SWANSON et al., 2010) (LARSON; JIN; CELIK, 2005; TRIPPE et al., 2013) Consideration based on Swanson et al. (SWANSON et al., 2010)
	Steam cycle	98.6	MW (el)	16100000	6969697	2010	2016	0.9835	6854548	3.528	24180507	104	0.67	25138675	58070338	
	Water pump and deaerator	733485	kg/h		158540	2002	2016	1.3693	217091	3.352	727635	642582	0.60	672103	1552558	
	Total															
Decentralized - Gasification facility	Steam turbine	8.95	MW (el)		3133000	1990	2016	1.5148	4745934	3.352	15907197	132	0.60	79777977	184287126	(SWANSON et al., 2010) (LARSON; JIN; CELIK, 2005; TRIPPE et al., 2013) Consideration based on Swanson et al. (SWANSON et al., 2010)
	Steam cycle	98.6	MW (el)	16100000	6969697	2010	2016	0.9835	6854548	3.528	24180507	132	0.67	29327774	67747159	
	Water pump and deaerator	733485	kg/h		158540	2002	2016	1.3693	217091	3.352	727635	593426	0.60	640765	1480166	
	Total															
Decentralized - Pyrolysis facility	Steam turbine	8.95	MW (el)		3133000	1990	2016	1.5148	4745934	3.352	15907197	13	0.60	19684878	45472068	(SWANSON et al., 2010) (LARSON; JIN; CELIK, 2005; TRIPPE et al., 2013) Consideration based on Swanson et al.
	Steam cycle	98.6	MW (el)	16100000	6969697	2010	2016	0.9835	6854548	3.352	24180507	13	0.67	6146454	14198308	
	Water pump and deaerator	733485	kg/h		158540	2002	2016	1.3693	217091	3.352	727635	83394	0.60	197406	456007	

Total	60126384	al. (SWANSO N et al., 2010)
-------	----------	--------------------------------------

OPEX for Steam Turbine hierarchy				
Scenario	Unit	Value	Value (R\$)/year	Reference
Centralized	4.5	% of CAPEX	9906805	(TRIPPE et al., 2011)
Decentralized - Gasification facility	4.5	% of CAPEX	11408150	(TRIPPE et al., 2011)
Decentralized - Pyrolysis facility	4.5	% of CAPEX	2705687	(TRIPPE et al., 2011)

CAPEX for steam and electricity integration																	
Scenario	Equipment	Value	Unit	Installed equipment	Equipment	Base year	Year wished	Correction CEPCI	Corrected value	R\$/€ or R\$/US\$	Corrected value (R\$)	Simulation	Coefficient	Value (R\$)	Installed value (R\$)	Reference	
Centralized	Cooling tower system	10.20	kW (th)		267316	2002	2016	1.3693	366039	3.352	1226873	65	0.33	2257735	5215368	(SWANS ON et al., 2010)	
	Water treatment unit	127200	kg/h	459541	198935	2010	2016	0.9835	195649	3.528	690182	164292	0.70	825571	1907068		(TRIPPE et al., 2011)
	Total														7122437		
Decentralized - Gasification facility	Cooling tower system	10.20	kW (th)		267316	2002	2016	1.3693	366039	3.352	1226873	46.588	0.33	2025385	4678640	(SWANS ON et al., 2010)	
	Water treatment unit	127200	kg/h	459541	198935	2010	2016	0.9835	195649	3.528	690182	172304	0.70	853551	1971703	(TRIPPE et al., 2011)	
	Total														6650343		
Decentralized - Pyrolysis facility	Cooling tower system	10.20	kW (th)		267316	2002	2016	1.3693	366039	3.352	1226873	7.6	0.33	1112612	2570133	(SWANS ON et al., 2010)	
	Water treatment unit	127200	kg/h	459541	198935	2010	2016	0.9835	195649	3.528	690182	4170	0.70	63084	145724	(TRIPPE et al., 2011)	
	Total														2715857		

OPEX for for steam and electricity integration															
Scenario		Value	Unit	Value	Base year	Year wished	Correction CEPCI	Corrected value	R\$/€ or R\$/US\$	Corrected value (R\$)	Simulation	Value (R\$)/hour	Value (R\$)/year	Reference	
Centralized	Cooling water	20.82	L	0.010	2010	2016	0.9835	0.0098	3.352	0.033	164292	260	1248587	(SWANSON et al., 2010)	
	Steam cycle	24.23	L	0.010	2010	2016	0.9835	0.0098	3.352	0.033	642582	874	4196756	(SWANSON et al., 2010)	
	Water disposal	4.92	L	0.010	2010	2016	0.9835	0.0098	3.352	0.033	128853	863	4143013	(SWANSON et al., 2010)	
	Other (Electricity integration, among others) Total	4		% of CAPEX										284897	Consideration based on Trippe et al. (TRIPPE et al., 2011)
Decentralized - Gasification facility	Cooling water	20.82	L	0.010	2010	2016	0.9835	0.0098	3.352	0.033	172304	273	1309477	(SWANSON et al., 2010)	
	Steam integration	24.23	L	0.010	2010	2016	0.9835	0.0098	3.352	0.033	593426	807	3875714	(SWANSON et al., 2010)	
	Water disposal	4.92	L	0.010	2010	2016	0.9835	0.0098	3.352	0.033	9914	66	318765	(SWANSON et al., 2010)	
	Other (Electricity integration, among others) Total	4		% of CAPEX										266014	Consideration based on Trippe et al. (TRIPPE et al., 2011)
Decentralized - Pyrolysis facility	Cooling water	20.82	L	0.010	2010	2016	0.9835	0.0098	3.352	0.033	4170	7	31691	(SWANSON et al., 2010)	
	Steam integration	24.23	L	0.010	2010	2016	0.9835	0.0098	3.352	0.033	83394	113	544653	(SWANSON et al., 2010)	
	Water disposal	4.92	L	0.010	2010	2016	0.9835	0.0098	3.352	0.033	127066	851	4085556	(SWANSON et al., 2010)	
	Other (Electricity integration, among others) Total	4		% of CAPEX										108634	Consideration based on Trippe et al. (TRIPPE et al., 2011)
														4770534	

**Appendix – Fischer-Tropsch hierarchy**

Process or parameters	Variable	Unit	Centralized	Decentralized
			Value	Value
WGS cycle	Temperature	°C	200	200
	Pressure	bar	24.88	24.88
	Mass flow of syngas to WGC reactor	kg/h	61521	67880
	Steam to WGS reactor	°C	350	350
		bar	25	25
	Steam mole flow to WGS reactor	kmol/h	4576	4958
	CO mole flow to WGS reactor	kmol/h	1129	1244
	Steam/CO molar ratio in WGS reactor		4.05	3.99
Syngas to FT reactor	Temperature	°C	199	199
	Pressure	bar	24.88	24.88
	CH4	kg/h	6.79E+03	7.30E+03
	CO2	kg/h	1.31E+05	1.44E+05
	H2O	kg/h	6.45E+04	6.97E+04
	N2	kg/h	8.38E+03	8.96E+03
	O2	kg/h	2.05E-07	2.29E-07
	H2	kg/h	1.30E+04	1.39E+04
	CO	kg/h	1.06E+05	1.14E+05
	NH3	kg/h	9.46E-02	1.02E-01
	HCL	kg/h	6.65E-04	7.12E-04
	C2H6	kg/h	4.74E+03	5.10E+03
	C3H8	kg/h	3.50E+03	3.76E+03
	C4H10	kg/h	2.57E+03	2.76E+03
	C5H12	kg/h	1.78E+03	1.92E+03
	METHANOL	kg/h	4.85E+01	5.23E+01
	HCN	kg/h	5.41E-01	6.02E-01
	C6H14	kg/h	1.07E+03	1.15E+03
	C7H16	kg/h	5.21E+02	5.63E+02
	C8H18	kg/h	1.99E+02	2.15E+02
	C9H20	kg/h	6.71E+01	7.26E+01
	C10H22	kg/h	2.14E+01	2.32E+01
	C11H24	kg/h	6.76E+00	7.32E+00
	C12H26	kg/h	2.11E+00	2.28E+00
	C13H28	kg/h	6.92E-01	7.51E-01
	C14H30	kg/h	2.43E-01	2.63E-01
	C15H32	kg/h	7.92E-02	8.60E-02
	C16H34	kg/h	2.81E-02	3.05E-02
	C17H36	kg/h	8.48E-03	9.20E-03
	C18H38	kg/h	3.02E-03	3.27E-03
C19H40	kg/h	1.06E-03	1.15E-03	
C20H42	kg/h	3.26E-04	3.54E-04	
C21H44	kg/h	1.22E-04	1.33E-04	

	C22H46	kg/h	5.04E-05	5.48E-05
	C23H48	kg/h	1.55E-05	1.68E-05
	C24H50	kg/h	5.50E-06	5.99E-06
	C25H52	kg/h	2.15E-06	2.34E-06
	C26H54	kg/h	7.61E-07	8.26E-07
	C27H56	kg/h	2.29E-07	2.49E-07
	C28H58	kg/h	1.14E-07	1.24E-07
	C29H60	kg/h	5.23E-08	5.70E-08
	C30H62	kg/h	2.06E-08	2.24E-08
	C31H64	kg/h	4.78E-08	5.21E-08
	C32H66	kg/h	4.08E-09	4.45E-09
	C33H68	kg/h	9.72E-09	1.06E-08
	C34H70	kg/h	3.13E-08	3.41E-08
	C35H72	kg/h	2.10E-09	0.00E+00
	C8H16	kg/h	1.91E+01	2.07E+01
	C9H18	kg/h	9.73E+00	1.05E+01
	C10H20	kg/h	8.74E+00	9.45E+00
	C11H22	kg/h	1.35E-01	1.46E-01
	C12H24	kg/h	9.29E-01	1.01E+00
	C13H26	kg/h	1.34E-02	1.45E-02
	C14H28	kg/h	1.87E-03	2.02E-03
	C15H30	kg/h	3.71E-03	4.03E-03
	C16H32	kg/h	8.62E-04	9.35E-04
	Total mass flow	kg/h	3.45E+05	3.73E+05
Syncrude after FT reactor	Temperature	°C	180	180
	Pressure	bar	24.8	24.8
	CH4	kg/h	1.13E+04	1.21E+04
	CO2	kg/h	1.31E+05	1.44E+05
	H2O	kg/h	8.77E+04	9.45E+04
	N2	kg/h	8.38E+03	8.96E+03
	O2	kg/h	2.05E-07	2.29E-07
	H2	kg/h	6.61E+03	7.10E+03
	CO	kg/h	6.93E+04	7.45E+04
	NH3	kg/h	9.46E-02	1.02E-01
	HCL	kg/h	6.65E-04	7.12E-04
	C2H6	kg/h	7.92E+03	8.52E+03
	C3H8	kg/h	5.88E+03	6.32E+03
	C4H10	kg/h	4.39E+03	4.72E+03
	C5H12	kg/h	3.20E+03	3.44E+03
	METHANOL	kg/h	8.49E+02	9.13E+02
	HCN	kg/h	5.41E-01	6.02E-01
	C6H14	kg/h	2.18E+03	2.34E+03
	C7H16	kg/h	1.40E+03	1.51E+03
	C8H18	kg/h	8.96E+02	9.64E+02
	C9H20	kg/h	6.24E+02	6.71E+02
	C10H22	kg/h	4.68E+02	5.03E+02

	C11H24	kg/h	3.66E+02	3.93E+02
	C12H26	kg/h	2.91E+02	3.13E+02
	C13H28	kg/h	2.34E+02	2.52E+02
	C14H30	kg/h	1.89E+02	2.03E+02
	C15H32	kg/h	1.53E+02	1.64E+02
	C16H34	kg/h	1.24E+02	1.33E+02
	C17H36	kg/h	1.01E+02	1.08E+02
	C18H38	kg/h	8.16E+01	8.77E+01
	C19H40	kg/h	6.63E+01	7.13E+01
	C20H42	kg/h	5.39E+01	5.79E+01
	C21H44	kg/h	4.38E+01	4.71E+01
	C22H46	kg/h	3.56E+01	3.83E+01
	C23H48	kg/h	2.90E+01	3.12E+01
	C24H50	kg/h	2.36E+01	2.53E+01
	C25H52	kg/h	1.92E+01	2.06E+01
	C26H54	kg/h	1.56E+01	1.68E+01
	C27H56	kg/h	1.27E+01	1.37E+01
	C28H58	kg/h	1.04E+01	1.11E+01
	C29H60	kg/h	8.43E+00	9.06E+00
	C30H62	kg/h	6.86E+00	7.37E+00
	C31H64	kg/h	5.59E+00	6.00E+00
	C32H66	kg/h	4.55E+00	4.89E+00
	C33H68	kg/h	3.70E+00	3.98E+00
	C34H70	kg/h	3.02E+00	3.24E+00
	C35H72	kg/h	2.46E+00	2.64E+00
	C8H16	kg/h	1.03E+02	1.11E+02
	C9H18	kg/h	6.30E+01	6.78E+01
	C10H20	kg/h	4.25E+01	4.57E+01
	C11H22	kg/h	2.15E+01	2.32E+01
	C12H24	kg/h	1.45E+01	1.56E+01
	C13H26	kg/h	8.62E+00	9.26E+00
	C14H28	kg/h	5.46E+00	5.87E+00
	C15H30	kg/h	3.46E+00	3.72E+00
	C16H32	kg/h	2.20E+00	2.36E+00
	Total mass flow	kg/h	3.45E+05	3.73E+05
Off-gas	Temperature	°C	35	35
	Pressure	bar	24.8	24.8
	CH4	kg/h	1.13E+04	1.21E+04
	CO2	kg/h	1.31E+05	1.43E+05
	H2O	kg/h	4.49E+02	4.85E+02
	N2	kg/h	8.37E+03	8.96E+03
	O2	kg/h	2.05E-07	2.29E-07
	H2	kg/h	6.61E+03	7.10E+03
	CO	kg/h	6.93E+04	7.45E+04
	NH3	kg/h	1.24E-02	1.35E-02
	HCL	kg/h	6.61E-04	7.08E-04

---

C2H6	kg/h	7.90E+03	8.49E+03
C3H8	kg/h	5.83E+03	6.27E+03
C4H10	kg/h	4.28E+03	4.61E+03
C5H12	kg/h	2.97E+03	3.20E+03
METHANOL	kg/h	8.08E+01	8.71E+01
HCN	kg/h	5.16E-01	5.74E-01
C6H14	kg/h	1.78E+03	1.92E+03
C7H16	kg/h	8.68E+02	9.38E+02
C8H18	kg/h	3.31E+02	3.58E+02
C9H20	kg/h	1.12E+02	1.21E+02
C10H22	kg/h	3.57E+01	3.87E+01
C11H24	kg/h	1.13E+01	1.22E+01
C12H26	kg/h	3.51E+00	3.80E+00
C13H28	kg/h	1.15E+00	1.25E+00
C14H30	kg/h	4.05E-01	4.39E-01
C15H32	kg/h	1.32E-01	1.43E-01
C16H34	kg/h	4.68E-02	5.08E-02
C17H36	kg/h	1.41E-02	1.53E-02
C18H38	kg/h	5.03E-03	5.46E-03
C19H40	kg/h	1.76E-03	1.92E-03
C20H42	kg/h	5.43E-04	5.91E-04
C21H44	kg/h	2.04E-04	2.21E-04
C22H46	kg/h	8.40E-05	9.13E-05
C23H48	kg/h	2.58E-05	2.81E-05
C24H50	kg/h	9.17E-06	9.98E-06
C25H52	kg/h	3.58E-06	3.90E-06
C26H54	kg/h	1.27E-06	1.38E-06
C27H56	kg/h	3.83E-07	4.17E-07
C28H58	kg/h	1.90E-07	2.07E-07
C29H60	kg/h	8.74E-08	9.53E-08
C30H62	kg/h	3.44E-08	3.75E-08
C31H64	kg/h	7.99E-08	8.71E-08
C32H66	kg/h	6.82E-09	7.43E-09
C33H68	kg/h	1.62E-08	1.77E-08
C34H70	kg/h	5.23E-08	5.71E-08
C35H72	kg/h	3.51E-09	3.83E-09
C8H16	kg/h	3.19E+01	3.45E+01
C9H18	kg/h	1.62E+01	1.75E+01
C10H20	kg/h	1.46E+01	1.57E+01
C11H22	kg/h	2.25E-01	2.44E-01
C12H24	kg/h	1.55E+00	1.68E+00
C13H26	kg/h	2.23E-02	2.42E-02
C14H28	kg/h	3.11E-03	3.37E-03
C15H30	kg/h	6.19E-03	6.71E-03
C16H32	kg/h	1.44E-03	1.56E-03
Total mass flow	kg/h	2.51E+05	2.73E+05

---

Recycle to Gas Cleaning and conditioning hierarchy	Temperature	°C	35	35
		Pressure	bar	24.8
	Recycle ratio		0.6	0.6
	CH4	kg/h	6.77E+03	7.28E+03
	CO2	kg/h	7.87E+04	8.60E+04
	H2O	kg/h	2.69E+02	2.91E+02
	N2	kg/h	5.02E+03	5.38E+03
	O2	kg/h	1.23E-07	1.38E-07
	H2	kg/h	3.95E+03	4.25E+03
	CO	kg/h	4.16E+04	4.47E+04
	NH3	kg/h	7.46E-03	8.09E-03
	HCL	kg/h	3.97E-04	4.25E-04
	C2H6	kg/h	4.74E+03	5.10E+03
	C3H8	kg/h	3.50E+03	3.76E+03
	C4H10	kg/h	2.57E+03	2.76E+03
	C5H12	kg/h	1.78E+03	1.92E+03
	METHANOL	kg/h	4.85E+01	5.23E+01
	HCN	kg/h	3.10E-01	3.45E-01
	C6H14	kg/h	1.07E+03	1.15E+03
	C7H16	kg/h	5.21E+02	5.63E+02
	C8H18	kg/h	1.99E+02	2.15E+02
	C9H20	kg/h	6.71E+01	7.26E+01
	C10H22	kg/h	2.14E+01	2.32E+01
	C11H24	kg/h	6.76E+00	7.32E+00
	C12H26	kg/h	2.11E+00	2.28E+00
	C13H28	kg/h	6.92E-01	7.51E-01
	C14H30	kg/h	2.43E-01	2.63E-01
	C15H32	kg/h	7.92E-02	8.60E-02
	C16H34	kg/h	2.81E-02	3.05E-02
	C17H36	kg/h	8.48E-03	9.20E-03
	C18H38	kg/h	3.02E-03	3.27E-03
	C19H40	kg/h	1.06E-03	1.15E-03
	C20H42	kg/h	3.26E-04	3.54E-04
	C21H44	kg/h	1.22E-04	1.33E-04
	C22H46	kg/h	5.04E-05	5.48E-05
	C23H48	kg/h	1.55E-05	1.68E-05
	C24H50	kg/h	5.50E-06	5.99E-06
	C25H52	kg/h	2.15E-06	2.34E-06
	C26H54	kg/h	7.61E-07	8.26E-07
	C27H56	kg/h	2.29E-07	2.49E-07
	C28H58	kg/h	1.14E-07	1.24E-07
	C29H60	kg/h	5.23E-08	5.70E-08
	C30H62	kg/h	2.06E-08	2.24E-08
	C31H64	kg/h	4.78E-08	5.21E-08
	C32H66	kg/h	4.08E-09	4.45E-09
	C33H68	kg/h	9.72E-09	1.06E-08

	C34H70	kg/h	3.13E-08	3.41E-08
	C35H72	kg/h	2.10E-09	2.29E-09
	C8H16	kg/h	1.91E+01	2.07E+01
	C9H18	kg/h	9.73E+00	1.05E+01
	C10H20	kg/h	8.74E+00	9.45E+00
	C11H22	kg/h	1.35E-01	1.46E-01
	C12H24	kg/h	9.29E-01	1.01E+00
	C13H26	kg/h	1.34E-02	1.45E-02
	C14H28	kg/h	1.87E-03	2.02E-03
	C15H30	kg/h	3.71E-03	4.03E-03
	C16H32	kg/h	8.62E-04	9.35E-04
	Total mass flow	kg/h	1.51E+05	1.64E+05
Wax to hydrocracking	Temperature	°C	350	350
	Pressure	bar	35	35
	CH4	kg/h	2.53E-22	2.74E-22
	CO2	kg/h	2.11E-18	2.34E-18
	H2O	kg/h	4.34E-13	4.75E-13
	N2	kg/h	0.00E+00	0.00E+00
	O2	kg/h	0.00E+00	0.00E+00
	H2	kg/h	0.00E+00	0.00E+00
	CO	kg/h	4.85E-24	2.45E-20
	NH3	kg/h	1.68E-22	1.84E-22
	HCL	kg/h	1.13E-25	0.00E+00
	C2H6	kg/h	3.33E-18	1.22E-25
	C3H8	kg/h	3.00E-15	3.60E-18
	C4H10	kg/h	2.01E-12	2.18E-12
	C5H12	kg/h	9.83E-10	1.07E-09
	METHANOL	kg/h	2.17E-12	2.37E-12
	HCN	kg/h	9.41E-16	1.06E-15
	C6H14	kg/h	3.40E-07	3.72E-07
	C7H16	kg/h	8.41E-05	9.24E-05
	C8H18	kg/h	4.54E-02	5.03E-02
	C9H20	kg/h	2.54E+00	2.76E+00
	C10H22	kg/h	2.22E+01	2.42E+01
	C11H24	kg/h	1.14E+02	1.24E+02
	C12H26	kg/h	1.99E+02	2.14E+02
	C13H28	kg/h	1.87E+02	2.01E+02
	C14H30	kg/h	1.56E+02	1.67E+02
	C15H32	kg/h	1.28E+02	1.37E+02
	C16H34	kg/h	1.04E+02	1.12E+02
	C17H36	kg/h	8.46E+01	9.08E+01
	C18H38	kg/h	6.88E+01	7.39E+01
	C19H40	kg/h	5.59E+01	6.01E+01
	C20H42	kg/h	4.55E+01	4.88E+01
	C21H44	kg/h	3.70E+01	3.97E+01
	C22H46	kg/h	3.01E+01	3.23E+01

	C23H48	kg/h	2.45E+01	2.63E+01
	C24H50	kg/h	1.99E+01	2.14E+01
	C25H52	kg/h	1.62E+01	1.74E+01
	C26H54	kg/h	1.32E+01	1.42E+01
	C27H56	kg/h	1.07E+01	1.15E+01
	C28H58	kg/h	8.74E+00	9.39E+00
	C29H60	kg/h	7.12E+00	7.64E+00
	C30H62	kg/h	5.79E+00	6.22E+00
	C31H64	kg/h	4.72E+00	5.07E+00
	C32H66	kg/h	3.84E+00	4.13E+00
	C33H68	kg/h	3.13E+00	3.36E+00
	C34H70	kg/h	2.55E+00	2.74E+00
	C35H72	kg/h	2.07E+00	2.23E+00
	C8H16	kg/h	3.07E-02	3.36E-02
	C9H18	kg/h	8.72E-02	9.47E-02
	C10H20	kg/h	1.25E-03	1.38E-03
	C11H22	kg/h	1.21E+01	1.30E+01
	C12H24	kg/h	1.40E+00	1.52E+00
	C13H26	kg/h	7.09E+00	7.62E+00
	C14H28	kg/h	4.55E+00	4.89E+00
	C15H30	kg/h	2.89E+00	3.10E+00
	C16H32	kg/h	1.84E+00	1.98E+00
	Total mass flow	kg/h	1.39E+03	1.49E+03
Hydrogen from PSA to hydrocracking unit	Temperature	°C	35	35
	Pressure	bar	24.88	24.88
	CH4	kg/h	1.49E-01	1.60E-01
	CO2	kg/h	1.74E+00	1.89E+00
	N2	kg/h	1.11E-01	1.18E-01
	O2	kg/h	2.71E-12	3.03E-12
	H2	kg/h	1.16E+01	1.25E+01
	CO	kg/h	9.17E-01	9.84E-01
	NH3	kg/h	1.65E-07	1.78E-07
	C2H6	kg/h	1.05E-01	1.12E-01
	C3H8	kg/h	7.71E-02	8.28E-02
	C4H10	kg/h	5.67E-02	6.08E-02
	C5H12	kg/h	3.93E-02	4.22E-02
	Total mass flow	kg/h	1.48E+01	1.59E+01
Off-gas to Gas Turbine hierarchy	Temperature	°C	35	35
	Pressure	bar	24.88	24.88
	CH4	kg/h	4.52E+03	4.86E+03
	CO2	kg/h	5.27E+04	5.76E+04
	H2O	kg/h	1.91E+02	2.07E+02
	N2	kg/h	3.35E+03	3.59E+03
	O2	kg/h	8.18E-08	9.17E-08
	H2	kg/h	2.64E+03	2.84E+03
	CO	kg/h	2.77E+04	2.98E+04

---

NH3	kg/h	5.04E-03	5.47E-03
HCL	kg/h	2.66E-04	2.85E-04
C2H6	kg/h	3.18E+03	3.42E+03
C3H8	kg/h	2.38E+03	2.55E+03
C4H10	kg/h	1.80E+03	1.93E+03
C5H12	kg/h	1.31E+03	1.41E+03
METHANOL	kg/h	3.58E+01	3.86E+01
HCN	kg/h	2.22E-01	2.47E-01
C6H14	kg/h	8.13E+02	8.76E+02
C7H16	kg/h	4.04E+02	4.37E+02
C8H18	kg/h	1.51E+02	1.64E+02
C9H20	kg/h	4.47E+01	4.84E+01
C10H22	kg/h	1.43E+01	1.55E+01
C11H24	kg/h	4.50E+00	4.88E+00
C12H26	kg/h	1.40E+00	1.52E+00
C13H28	kg/h	4.61E-01	5.00E-01
C14H30	kg/h	1.62E-01	1.76E-01
C15H32	kg/h	5.28E-02	5.73E-02
C16H34	kg/h	1.87E-02	2.03E-02
C17H36	kg/h	5.65E-03	6.14E-03
C18H38	kg/h	2.01E-03	2.18E-03
C19H40	kg/h	7.05E-04	7.66E-04
C20H42	kg/h	2.17E-04	2.36E-04
C21H44	kg/h	8.14E-05	8.85E-05
C22H46	kg/h	3.36E-05	3.65E-05
C23H48	kg/h	1.03E-05	1.12E-05
C24H50	kg/h	3.67E-06	3.99E-06
C25H52	kg/h	1.43E-06	1.56E-06
C26H54	kg/h	5.07E-07	5.52E-07
C27H56	kg/h	1.53E-07	1.67E-07
C28H58	kg/h	7.60E-08	8.28E-08
C29H60	kg/h	3.50E-08	3.81E-08
C30H62	kg/h	1.38E-08	1.50E-08
C31H64	kg/h	3.20E-08	3.48E-08
C32H66	kg/h	2.73E-09	2.97E-09
C33H68	kg/h	6.50E-09	7.09E-09
C34H70	kg/h	2.09E-08	2.28E-08
C35H72	kg/h	1.40E-09	1.53E-09
C8H16	kg/h	1.33E+01	1.44E+01
C9H18	kg/h	6.48E+00	7.02E+00
C10H20	kg/h	6.68E+00	7.22E+00
C11H22	kg/h	9.01E-02	9.76E-02
C12H24	kg/h	6.19E-01	6.71E-01
C13H26	kg/h	8.91E-03	9.66E-03
C14H28	kg/h	1.24E-03	1.35E-03
C15H30	kg/h	2.47E-03	2.69E-03

---

Green Naphtha	C16H32	kg/h	5.75E-04	6.24E-04
	Total mass flow	kg/h	1.01E+05	1.10E+05
	Temperature	°C	25	25
	Pressure	bar	1.013	1.013
	CH4	kg/h	2.77E-02	2.93E-02
	CO2	kg/h	3.38E+00	3.64E+00
	H2O	kg/h	5.11E+00	5.45E+00
	N2	kg/h	3.37E-03	3.56E-03
	O2	kg/h	0.00E+00	0.00E+00
	H2	kg/h	1.02E-03	1.08E-03
	CO	kg/h	3.02E-02	3.19E-02
	NH3	kg/h	4.03E-06	4.30E-06
	HCL	kg/h	4.09E-08	4.32E-08
	C2H6	kg/h	5.63E-01	5.96E-01
	C3H8	kg/h	4.06E+00	4.30E+00
	C4H10	kg/h	2.52E+01	2.67E+01
	C5H12	kg/h	1.08E+02	1.14E+02
	METHANOL	kg/h	3.65E+00	3.89E+00
	HCN	kg/h	8.67E-03	9.53E-03
	C6H14	kg/h	2.97E+02	3.17E+02
	C7H16	kg/h	4.71E+02	5.04E+02
	C8H18	kg/h	4.43E+02	4.74E+02
	C9H20	kg/h	3.33E-05	3.44E-05
	C10H22	kg/h	9.70E-14	1.00E-13
	C11H24	kg/h	0.00E+00	7.03E-20
	C12H26	kg/h	5.61E-21	4.50E-20
	C13H28	kg/h	4.32E-23	0.00E+00
	C14H30	kg/h	0.00E+00	0.00E+00
	C15H32	kg/h	0.00E+00	0.00E+00
	C16H34	kg/h	0.00E+00	0.00E+00
	C17H36	kg/h	0.00E+00	0.00E+00
	C18H38	kg/h	0.00E+00	0.00E+00
C19H40	kg/h	5.43E-22	0.00E+00	
C20H42	kg/h	2.11E-24	5.44E-24	
C21H44	kg/h	0.00E+00	0.00E+00	
C22H46	kg/h	0.00E+00	0.00E+00	
C23H48	kg/h	0.00E+00	0.00E+00	
C24H50	kg/h	2.49E-19	0.00E+00	
C25H52	kg/h	3.33E-19	0.00E+00	
C26H54	kg/h	0.00E+00	3.93E-19	
C27H56	kg/h	8.18E-20	1.72E-19	
C28H58	kg/h	0.00E+00	2.68E-19	
C29H60	kg/h	2.21E-19	2.56E-19	
C30H62	kg/h	0.00E+00	0.00E+00	
C31H64	kg/h	2.39E-19	3.07E-19	
C32H66	kg/h	0.00E+00	0.00E+00	

	C33H68	kg/h	0.00E+00	0.00E+00
	C34H70	kg/h	0.00E+00	1.76E-20
	C35H72	kg/h	1.44E-19	9.60E-19
	C8H16	kg/h	1.79E+01	1.87E+01
	C9H18	kg/h	1.17E-02	1.21E-02
	C10H20	kg/h	2.20E+01	2.36E+01
	C11H22	kg/h	1.34E-18	9.40E-19
	C12H24	kg/h	4.18E-15	4.34E-15
	C13H26	kg/h	0.00E+00	0.00E+00
	C14H28	kg/h	0.00E+00	0.00E+00
	C15H30	kg/h	0.00E+00	5.78E-20
	C16H32	kg/h	1.01E-19	0.00E+00
	Total mass flow	kg/h	1.40E+03	1.50E+03
Biojet fuel	Temperature	°C	25.0299	25.0299
	Pressure	bar	1.013	1.013
	CH4	kg/h	3.30E-10	3.55E-10
	CO2	kg/h	1.74E+00	1.89E+00
	H2O	kg/h	2.79E-05	3.03E-05
	N2	kg/h	8.87E-12	9.53E-12
	O2	kg/h	0.00E+00	0.00E+00
	H2	kg/h	1.16E+01	1.25E+01
	CO	kg/h	9.17E-01	9.84E-01
	NH3	kg/h	1.65E-07	1.78E-07
	HCL	kg/h	4.13E-15	4.44E-15
	C2H6	kg/h	1.05E-01	1.12E-01
	C3H8	kg/h	7.71E-02	8.28E-02
	C4H10	kg/h	5.68E-02	6.10E-02
	C5H12	kg/h	4.37E-02	4.69E-02
	METHANOL	kg/h	4.79E-05	5.20E-05
	HCN	kg/h	5.30E-08	5.93E-08
	C6H14	kg/h	1.12E-01	1.21E-01
	C7H16	kg/h	2.25E+00	2.45E+00
	C8H18	kg/h	4.08E+02	4.40E+02
	C9H20	kg/h	7.58E+02	8.15E+02
	C10H22	kg/h	6.12E+02	6.58E+02
	C11H24	kg/h	4.05E+02	4.34E+02
	C12H26	kg/h	2.23E+02	2.40E+02
	C13H28	kg/h	1.56E+02	1.68E+02
	C14H30	kg/h	1.22E+02	1.31E+02
	C15H32	kg/h	9.79E+01	1.05E+02
	C16H34	kg/h	7.91E+01	8.52E+01
	C17H36	kg/h	1.60E+01	1.72E+01
	C18H38	kg/h	1.29E+01	1.39E+01
	C19H40	kg/h	1.04E+01	1.12E+01
	C20H42	kg/h	8.42E+00	9.08E+00
	C21H44	kg/h	6.83E+00	7.37E+00

	C22H46	kg/h	5.55E+00	5.99E+00
	C23H48	kg/h	4.51E+00	4.87E+00
	C24H50	kg/h	3.67E+00	3.96E+00
	C25H52	kg/h	2.98E+00	3.22E+00
	C26H54	kg/h	2.43E+00	2.62E+00
	C27H56	kg/h	1.98E+00	2.13E+00
	C28H58	kg/h	1.61E+00	1.74E+00
	C29H60	kg/h	1.31E+00	1.41E+00
	C30H62	kg/h	1.07E+00	1.15E+00
	C31H64	kg/h	8.68E-01	9.37E-01
	C32H66	kg/h	7.07E-01	7.63E-01
	C33H68	kg/h	5.76E-01	6.21E-01
	C34H70	kg/h	4.69E-01	5.06E-01
	C35H72	kg/h	3.82E-01	4.12E-01
	C8H16	kg/h	5.30E+01	5.74E+01
	C9H18	kg/h	4.67E+01	5.02E+01
	C10H20	kg/h	4.24E+00	4.63E+00
	C11H22	kg/h	9.25E+00	9.90E+00
	C12H24	kg/h	1.16E+01	1.24E+01
	C13H26	kg/h	1.50E+00	1.62E+00
	C14H28	kg/h	9.01E-01	9.71E-01
	C15H30	kg/h	5.71E-01	6.16E-01
	C16H32	kg/h	3.53E-01	3.81E-01
	Total mass flow	kg/h	3.09E+03	3.32E+03
To treatment from decanter	Temperature	°C	25.0299	25.0299
	Pressure	bar	1.013	1.013
	CH4	kg/h	1.45E-01	1.56E-01
	CO2	kg/h	2.22E+01	2.42E+01
	H2O	kg/h	8.72E+04	9.40E+04
	N2	kg/h	1.09E-02	1.16E-02
	O2	kg/h	6.07E-12	6.79E-12
	H2	kg/h	2.97E-02	3.18E-02
	CO	kg/h	9.44E-02	1.01E-01
	NH3	kg/h	8.21E-02	8.88E-02
	HCL	kg/h	1.87E-06	2.00E-06
	C2H6	kg/h	1.22E-01	1.31E-01
	C3H8	kg/h	1.17E-02	1.25E-02
	C4H10	kg/h	9.40E-04	1.01E-03
	C5H12	kg/h	3.54E-05	3.79E-05
	METHANOL	kg/h	7.61E+02	8.18E+02
	HCN	kg/h	4.50E-04	4.99E-04
	C6H14	kg/h	7.98E-07	8.56E-07
	C7H16	kg/h	1.07E-08	1.14E-08
	C8H18	kg/h	6.83E-11	7.35E-11
	C9H20	kg/h	3.60E-13	3.87E-13
	C10H22	kg/h	1.28E-15	1.38E-15

	C11H24	kg/h	3.65E-16	3.94E-16
	C12H26	kg/h	2.96E-16	3.20E-16
	C13H28	kg/h	2.40E-16	2.59E-16
	C14H30	kg/h	1.94E-16	2.10E-16
	C15H32	kg/h	1.57E-16	1.70E-16
	C16H34	kg/h	1.28E-16	1.38E-16
	C17H36	kg/h	1.04E-16	1.12E-16
	C18H38	kg/h	8.41E-17	9.07E-17
	C19H40	kg/h	6.83E-17	7.37E-17
	C20H42	kg/h	5.55E-17	5.99E-17
	C21H44	kg/h	4.51E-17	4.87E-17
	C22H46	kg/h	3.67E-17	3.96E-17
	C23H48	kg/h	2.99E-17	3.22E-17
	C24H50	kg/h	2.43E-17	2.62E-17
	C25H52	kg/h	1.98E-17	2.13E-17
	C26H54	kg/h	1.61E-17	1.74E-17
	C27H56	kg/h	1.31E-17	1.41E-17
	C28H58	kg/h	1.07E-17	1.15E-17
	C29H60	kg/h	8.68E-18	9.36E-18
	C30H62	kg/h	7.07E-18	7.62E-18
	C31H64	kg/h	5.75E-18	6.21E-18
	C32H66	kg/h	4.69E-18	5.05E-18
	C33H68	kg/h	3.82E-18	4.12E-18
	C34H70	kg/h	3.11E-18	3.35E-18
	C35H72	kg/h	2.53E-18	2.73E-18
	C8H16	kg/h	3.65E-10	3.93E-10
	C9H18	kg/h	8.61E-10	9.26E-10
	C10H20	kg/h	8.12E-01	8.75E-01
	C11H22	kg/h	6.41E-07	6.90E-07
	C12H24	kg/h	1.33E-17	1.44E-17
	C13H26	kg/h	8.85E-18	9.55E-18
	C14H28	kg/h	4.75E-15	5.11E-15
	C15H30	kg/h	3.56E-18	3.84E-18
	C16H32	kg/h	2.26E-18	2.44E-18
	Total mass flow	kg/h	8.80E+04	9.49E+04
Steam produced	Temperature	°C	130	130
	Pressure	bar	2.5	2.5
	Mass flow	kg/h	1.27E+05	1.37E+05
Electricity needed	Power required	kW	97	106